31986

National Library of Canada
Bibliothèque nationale du Canada

CANADIAN THESES ON MICROFICHE

THÈSES CANADIENNES SUR MICROFICHE

NAME OF AUTHOR/*NOM DE L'AUTEUR* DAVID W. HILL

TITLE OF THESIS/*TITRE DE LA THÈSE* The Influence of Temperature and Load on Moisture Transfer in Freezing Soil.

UNIVERSITY/*UNIVERSITÉ* University of Alberta.

DEGREE FOR WHICH THESIS WAS PRESENTED/ *GRADE POUR LEQUEL CETTE THÈSE FUT PRÉSENTÉE* M.Sc.

YEAR THIS DEGREE CONFERRED/*ANNÉE D'OBTENTION DE CE GRADE* 1977

NAME OF SUPERVISOR/*NOM DU DIRECTEUR DE THÈSE* Dr N.R. Morgenstern.

Permission is hereby granted to the NATIONAL LIBRARY OF CANADA to microfilm this thesis and to lend or sell copies of the film.

The author reserves other publication rights, and neither the thesis nor extensive extracts from it may be printed or otherwise reproduced without the author's written permission.

L'autorisation est, par la présente, accordée à la BIBLIOTHÈQUE NATIONALE DU CANADA de microfilmer cette thèse et de prêter ou de vendre des exemplaires du film.

L'auteur se réserve les autres droits de publication; ni la thèse ni de longs extraits de celle-ci ne doivent être imprimés ou autrement reproduits sans l'autorisation écrite de l'auteur.

DATED/*DATÉ* 20th April SIGNED/*SIGNÉ* David Hill

PERMANENT ADDRESS/*RÉSIDENCE FIXÉ* Box 746 4810 - 93 st., Edmonton, T5J 2L4
Alta.

NL-91 (3-74)

National Library of Canada

Cataloguing Branch
Canadian Theses Division

Ottawa, Canada
K1A 0N4

Bibliothèque nationale du Canada

Direction du catalogage
Division des thèses canadiennes

NOTICE

The quality of this microfiche is heavily dependent upon the quality of the original thesis submitted for microfilming. Every effort has been made to ensure the highest quality of reproduction possible.

If pages are missing, contact the university which granted the degree.

Some pages may have indistinct print especially if the original pages were typed with a poor typewriter ribbon or if the university sent us a poor photocopy.

Previously copyrighted materials (journal articles, published tests, etc.) are not filmed.

Reproduction in full or in part of this film is governed by the Canadian Copyright Act, R.S.C. 1970, c. C-30. Please read the authorization forms which accompany this thesis.

THIS DISSERTATION
HAS BEEN MICROFILMED
EXACTLY AS RECEIVED

AVIS

La qualité de cette microfiche dépend grandement de la qualité de la thèse soumise au microfilmage. Nous avons tout fait pour assurer une qualité supérieure de reproduction.

S'il manque des pages, veuillez communiquer avec l'université qui a conféré le grade.

La qualité d'impression de certaines pages peut laisser à désirer, surtout si les pages originales ont été dactylographiées à l'aide d'un ruban usé ou si l'université nous a fait parvenir une photocopie de mauvaise qualité.

Les documents qui font déjà l'objet d'un droit d'auteur (articles de revue, examens publiés, etc.) ne sont pas microfilmés.

La reproduction, même partielle, de ce microfilm est soumise à la Loi canadienne sur le droit d'auteur, SRC 1970, c. C-30. Veuillez prendre connaissance des formules d'autorisation qui accompagnent cette thèse.

LA THÈSE A ÉTÉ
MICROFILMÉE TELLE QUE
NOUS L'AVONS REÇUE

NL-339 (3/77)

THE UNIVERSITY OF ALBERTA

THE INFLUENCE OF TEMPERATURE AND LOAD ON MOISTURE TRANSFER IN FREEZING SOILS

by

© DAVID W. HILL

A THESIS

SUBMITTED TO THE FACULTY OF GRADUATE STUDIES AND RESEARCH

IN PARTIAL FULFILMENT OF THE REQUIREMENTS FOR THE DEGREE

OF MASTER OF SCIENCE

DEPARTMENT OF CIVIL ENGINEERING

EDMONTON, ALBERTA

SPRING, 1977

THE UNIVERSITY OF ALBERTA

FACULTY OF GRADUATE STUDIES AND RESEARCH

The undersigned certify that they have read, and recommend to the Faculty of Graduate Studies and Research, for acceptance, a thesis entitled. "The Influence of Temperature and Load on Moisture Transfer in Freezing Soils". submitted by David W. Hill in partial fulfilment of the requirements for the degree of Master of Science in Civil Engineering.

....
Supervisor
N.R. Morgenstern

S. Thomson
....
S. Thomson

....
B. Gilpin

Date March 28th '77

TO MY MOTHER

ABSTRACT

An experimental study was carried out to obtain the moisture migration characteristics of Devon Silt under varying conditions of applied load and freezing rate. All testing was carried out under open system drainage conditions.

Short term and long term experiments were carried out and it was found that for the majority of cases short term testing could be used to predict long term freezing behaviour. The limitations of this observation are not completely understood however guidelines as to duration of testing to obtain the true moisture migration characteristics are given.

The experimental program showed that the moisture migration characteristics were affected by both the applied load and the rate of heat removal. The effects of the heat energy removal rate indicated that the concept of an energy balance should be considered in the development of a theory predicting moisture migration rates in freezing soils.

ACKNOWLEDGEMENTS

The author would like to thank Dr. N.R.Morgenstern for suggesting the thesis topic and for the invaluable help and guidance given during all stages of this study.

The author also thanks Messrs. O.Wood, A.Muir and J.Cyre for their assistance in both the experimental program and the thesis preparation.

Gratitude is also extended to to the many graduate collegues especially Messrs. R.W.Tweedie and J.S.Weaver for their assistance during apparatus set up.

The author also wishes to thank Ms. S.Kowal and Ms. S.Searle for their help in the final preparation of this thesis.

Finally the author wishes to thank Messrs. K.D.Flock and L.V.Medeiros for their help with the computing work carried out during the the experimental program.

TABLE OF CONTENTS

PAGE

Abstract v

Acknowledgements vi

Table of Contents vii

List of Tables ix

List of Figures x

List of Photographic Plates xi

CHAPTER 1 INTRODUCTION 1

1.1 Permafrost and Associated Geotechical Problems 1

1.2 Scope of the Thesis 3

CHAPTER 2 LITERATURE REVIEW 4

2.1.1 Freezing Behaviour 4

2.1.2 Mechanism of Frost Heaving 6

2.1.3 Water Pressures During Freezing . 13

2.1.4 Effects of Applied Load 16

2.1.5 Effects of Heat Energy Removal Rate 19

2.1.6 Magnitude of Heave 20

2.2.1 Basic concepts of Frost Heaving . 23

2.2.2 Energy Budget 23

2.2.3 Potential Gradient 25

CHAPTER 3 TEST PROCEDURE AND DESCRIPTION OF EQUIPMENT

3.1 Materials 28

3.2 Testing Program and Procedure ... 28

3.3 Description of Equipment 32

CHAPTER PAGE

CHAPTER 4 TEST RESULTS 44
4.1 Test Program 44
4.2 Results of Series NDS 49
4.3 Results of Series NDS-B 57
4.4 Results of Series NDS-C 60
4.5 Results of Series NDS-D 62
4.6 Conclusions From Observations ... 63
4.7 Limitations of Experimental Data 71
CHAPTER 5 ANALYSIS OF TEST DATA 74
5.1 Temperature Data Analysis 74
5.2 Pore Pressures Developed at the Frost Front 81
CHAPTER 6 CONCLUSIONS AND RECOMMENDATIONS 88
6.1 Conclusions 88
6.2 Equipment Performance and Procedure 89
6.3 Recommendations 92
List of References 94
APPENDIX A EXPERIMENTAL RESULTS 101
APPENDIX B PROGRAM LISTING AND SAMPLE OUTPUT 133

LIST OF TABLES

TABLE PAGE

2.1 Shut-off Pressures of Soils 15

3.1 Properties of Devon Silt 29

4.1 Results of Series NDS 51

4.2 Results of Series NDS-B 58

4.3 Results of Series NDS-C 61

4.4 Results of Series NDS-D 61

5.1 Suction developed at the Frost Front 84

LIST OF FIGURES

FIGURE PAGE

2.1 Theoretical Relationship Between Soil Water Potential and Freezing Point Depression 15

2.2 Schematic Representation of Relationship between Heaving Rate, Heaving pressure and Particle Size Resulting from Ice Lens Growth 21

2.3 Relationship between Heaving Pressures and Average Diameter of Fractions 21

3.1 'Grain Size' Curve of Devon Silt 30

3.2 Schematic diagram of Experimental Set-Up 33

3.3 to 3.7 Drawings for Experimental Apparatus 34

3.8 Volume Change Indicator 42

4.1 Sample Experimental Results NDS 7 47

4.2 Void Ratio Versus Applied Load 50

4.3 Thermal Data NDS 1-NDS 6 53

4.4 Thermal Data NDS 7-NDS 12 53

4.5 B Test Results NDS 6 55

4.6 B Test Results NDS 6 55

4.7 to 4.15 Total Heave and Segregational Heave Data .. 65

4.16 Efficiency Verus Square Root of Step Temperature . 72

5.1 to 5.4 Temperature Data Analysis 78

5.5 Suction Developed at the Frost Front 84

5.6 Schematic Diagram of Pore Pressure Distribution in the Soil Sample 86

LIST OF PHOTOGRAPHIC PLATES

PLATE PAGE

1 Horizontal and Vertical Ice Lenses 56

CHAPTER 1

INTRODUCTION

1.1 Permafrost and Associated Geotechnical Problems

With the rapid development of the industries associated with the recovery of natural resources found extensively in the Canadian North, an understanding of the behaviour of frozen, freezing and thawing ground is necessary to permit the safe design of the many and varied structures which this expansion demands.

Recent research has widened our understanding of the mechanics of cold region geotechnics enabling the design engineer to predict the behaviour of soils, frozen and thawing, accurately both in terms of strength and deformation. For problems involving thawed soil the conventional principles of temperate zone soil mechanics are applicable. Work by Nixon and Morgenstern (1973) encompassed the problems of thawing ground and the development of a method of determining the magnitude of pore pressures generated during thaw and the prediction of thaw settlements was presented. This was a comprehensive theory which considered the two controlling dynamic factors of pore pressure dissipation and a moving thaw boundary.

The characteristics of thawed soil were investigated by Roggensack (1976) and its behaviour is now well understood.

Freezing problems however are not as well comprehended. The effects of freezing a frost susceptible soil are most clearly exhibited in a heaving of the ground surface. The magnitude of this heaving varies as a function of several factors such as applied load, stress history and grain size distribution. Further investigation of the soil after freezing reveals the development of discrete ice lenses which may grow to appreciable thicknesses. A decription of these lenses was given by MacKay (1972) in a study of ground ice occurrence in the high Arctic.

The build-up of discrete ice layers is caused by the migration of water in the soil under the influence of a potential gradient created at or near the freezing interface. The prediction of the magnitude of this potential gradient has so far been impossible due to the complexity of the problem.

If the heaving of the ground surface is inhibited, substantial heaving pressures may be developed, or conversely if the overburden stress at the frost plane is high enough the growth of segregated ice is impeded.

Another problem associated with the build up of ice layers is the effects of any subsequent thaw. The localized increase in water content of the soil implies a decrease of strength on thawing if drainage is hinderd by some factor such as low permeability of the soil.

1.2 Scope of the Thesis

To date no comprehensive understanding of frost heave behaviour is known and consequently the effects of the many controlling variables in the problem must be investigated. The purpose of this study was to examine the freezing behaviour of a frost susceptible soil under varying conditions of applied load and temperature distribution, and to correlate behaviour with those parameters.

CHAPTER 2

LITERATURE REVIEW

2.1.1 Freezing Behaviour

It is known that most saturated soils under low stresses exhibit an affinity for water during freezing and the formation of lenses and layers of ice occurs. Coarse grained soils may expel water on freezing if drainage is permitted, (MacKay 1971, McRoberts 1972). In reviewing the geotechnical properties of freezing ground, Anderson and Morgenstern (1973) stated that ice lensing results when a soil has the ability to supply water to an active ice front for a sufficiently long time to grow an ice lens. Frost action is contingent on the existence of certain factors. These are a frost susceptible soil, an adequate moisture supply and a sufficiently low temperature to cause some of the water to freeze.

The effects of frost action are displayed mainly in the form of vertical displacement of the soil surface. Other problems also occur, e.g., the increased soil moisture content due to water migration during the freezing process is reflected in a decrease in soil strength after thaw occurs. Vertical displacement of subsurface objects such as boulders, piles and posts are also of major concern.

It is of importance at this point to define the behaviour that the author refers to as heaving. The volumetric increase of a soil sample on freezing is due to two components:

1) The volumetric increase of in situ pore water due to its phase change. This may be expressed mathematically as

$$\frac{dh}{dt} = 0.09n \frac{dx}{dt} \qquad 2.1$$

Where n = porosity of the soil

x = depth of frost penetration

t = time

h = heave due to freezing of insitu per water.

2) The volumetric increase due to moisture transfer and its subsequent phase change. This is given by

$$\frac{dh}{dt} = 1.09V \qquad 2.2$$

Where h = heave due to the formation of segregated ice

v = velocity of the water arriving at the frost front due to a potential gradient.

It is the latter which is of major importance in engineering considerations since the suppression of heaving due to freezing of insitu pore water implies the application of loads high enough to inhibit crystallization completely and these magnitudes are well beyond those of engineering interest.

Taber (1930) first showed the phenomenon of moisture migration in an experiment in which a soil with a pore fluid of benzene was frozen. The sample heaved on freezing and yet benzene itself exhibits no volumetric expansion on freezing. He concluded that the build-up of frozen benzene lenses and the resulting volume increase and heaving pressures were due to moisture transfer.

The affinity of a freezing soil for water is due to soil water suctions set up at or near the ice/water interface and it is these negative pore pressures that are of great interest. Theories have been postulated within the framework of capillary physics and thermodynamics, both of which give an insight into the mechanisms which cause these suctions and the resulting water movements. However none as yet completely describe the ice/water interface phenomena adequately.

2.1.2 Mechanism of Frost Heaving

Whenever a negative temperature gradient is imposed on a soil the volumetric heat is removed causing a drop in bulk temperature. When all the volumetric heat is removed and the bulk temperature is 0°C, nucleation of ice occurs with a subsequent release of latent heat. If supercooling of the pore water occurs nucleation will occur at some temperature lower than 0°C. The magnitude of the supercooling effect depends on several factors. Available evidence indicates that 2°C to 8°C of supercooling may be required in the laboratory but little or none in natural surroundings. In coarse-textured soils the freezing interface closely follows the 0°C isotherm in its downward course. In fine textured soils it may be as much as several degrees behind due to freezing point depression (Anderson and Morgenstern 1973)

It is now well established that soil particles are surrounded by an absorbed layer of water with different properties from that of the pore water (Anderson and Morgenstern, 1973). The thickness of this film is a function of temperature (Anderson, 1968). This water which does not freeze in a similar manner to the pore water is known as the unfrozen water content. To date the unfrozen water contents have been correlated to surface area, (Anderson, Tice and McKim, 1973), Atterberg limits, freezing point depression, clay mineralogy and activity ratio, (Dillon and Andersland 1966.)

The equilibrium of the unfrozen water content may be described by the Clausius-Clapeyron equation applicable to this situation

$$\frac{Dp}{Dt} = \frac{\Delta\bar{H}_{fs}}{T\Delta v} \qquad 2.3$$

Where Dp = change in pressure across the freezing front

Dt = change in temperature across the freezing front

$\Delta\bar{H}_{fs}$ = The diminished latent heat of freezing soil water

T = The freezing temperature of the soil

Δv = change in specific volume during phase change transformation.

The factors determing the solid/ liquid boundary on the phase diagram for ice in frozen soil involve the magnitude of the reduction in the freezing temperature T and the diminished latent heat of freezing soil water, $\Delta\bar{H}_{fs}$. Data are not available to fully resolve the question, but estimates indicate that of the two opposing effects the decrease in $\Delta\bar{H}_{fs}$ predominates, (Anderson and Morgerstern 1973)

The application of pressure tends to increase the thickness of the unfrozen water layer. Evidence that the thickness of the unfrozen water layer does increase with increasing pressure is provided in the observation of Hoekstra and Keune (1967) that the electrical conductance of a frozen clay water mixture increases dramatically with pressure.

As more heat is removed and after ice nucleation the freezing interface descends. As this occurs one of two things may happen. In one case the pore water may freeze in situ as growing ice crystals invade, fill the soil pores and engulf the soil grains. In this case the development of heaving forces results entirely from the expansion of in-situ water due to phase change. This is the mode of behaviour in the situation of freezing a coarse grained soil in a closed system configuration. Alternatively, segregated ice lenses may form in a plane of favorable temperature near but a little behind the zero degree isotherm. The ice lenses may thus enlarge by the addition of ice formed from upward migrating soil water. It is this upward flow of water and the potential and thermal gradients which control this migration that are of special interest. The frost front moves in accordance with the relative balance or unbalance between heat energy brought to and removed from the frost front. An advancing frost front results in the engulfment of soil particles by ice crystals or in situ freezing. If the rate of heat removal equals the rate of heat supplied, the frost front becomes immobile, i.e. a stationary frost front.

Once the freezing front becomes stationary and water in sufficient quantities is available to the front,the ice crystals grow by freezing the adjacent water. Due to the rigidity and perfection of the ice crystals, soil particles are rejected by the ice, resulting in the segregation of ice and soil particles (Anderson, 1968).

The heat balance at the frost front is a function of several modes of heat transport. Conduction of heat through the frozen zone is the sink of heat removal. Conduction of heat towards the frost front through the unfrozen zone and heat released by the porewater and by any water flowing into the sample are the major sources of heat energy. Heat released by the porewater is volumetric heat and latent heat of fusion. The latent heat of fusion is the major source of heat (Nixon 1973).

There are two commonly adopted explanations for the mechanism of ice lens growth. Consideration of capillary physics, where the soil pore is analogous to a fine capillary in which ice is nucleating yields the Kelvin equation.

$$P_i - P_w = \frac{2\sigma_{iw}}{r_{iw}} \qquad 2.4$$

Where P_i = pressure on the ice, overburden pressure

P_w = pressure in the porewater

σ_{iw} = pressure differential across the ice/water interface

r_{iw} = radius of the ice/water interface.

Many forms of this equation have been developed for various configurations e.g. unsaturated soils where the effects of air tensions must be considered. The formulation above is the basic equation for the pressure difference across an ice/ water interface for small ice crystals in their own melt.

Penner (1959) postulated a complete capillary model relating pore size and associated suctions. Assuming the size of the soil pore determines the size of the advancing ice crystal, the quantity r_{iw} in equation 2.4 may be interpreted as the radius of the pore. A part of the soil pore is occupied by absorbed water which probably places an additional size limitation on the ice crystal. As the frost front progresses, its propagation may be temporarily halted if the radius of the ice crystal is greater than that of the soil pore. However, heat is still being removed from the system and since the ice crystal cannot enter the pore space supercooling of the pore fluid ahead of the frost front will occur. The depression of the freezing point is given by the relation

$$T - T_o = \frac{V_o 2\sigma_{iw} T_o}{r_{iw} L} \qquad 2.5$$

Where T = freezing point in degrees Kelvin

T_o = normal freezing point

V_o = specific volume of water at the freezing temperature

σ_{iw} = stress difference across the ice/water interface

r_{iw} = radius of the ice water interface

L = latent heat of fusion of water.

As the porewater is further cooled it may be noted from equation 2.5 that the radius of the ice water interface must decrease to maintain equality of both sides. Supercooling will continue until the radius has become small enough to enter the soil pore. As the radius of curvature of the ice crystal diminishes, the Kelvin equation (equation 2.4) predicts that $P_i - P_w$ will increase, and since P_i is effectively the overburden pressure and hence not a variant, P_w must decrease. This decrease in the pore water pressure will generate the suction gradient which draws water to the freezing front. The freezing of this water results in the growth of ice lenses. This theory has several shortcomings and is not capable of describing all freezing conditions. Some of these are: 1) The capillary theory is based on a uniform pore size or particle size distribution. In nature, virtually all soils exhibit a non-uniform particle size distribution and consequently difficulties arise in assigning a typical radius for use in the theory, 2) The capillary theory is a static theory based on the premise that pore radius or grain size distribution is the unique parameter controlling the ice lensing capability of the soil. The theory does not account for any other factors affecting the freezing soil system e.g. temperature gradient or stress history and is incapable of accounting for any changes in these factors.

An alternative mechanism for moisture migration is known as the thermodynamic model. As discussed previously a soil particle has an equilibrum value of thickness of adsorbed water layer for a given set of conditions of temperature and pressure. Considering a soil particle at the frost front, some of the adsorbed water on the cold side of the particle may crystallize and leave the film. In order to maintain the equilibrium film thickness water molecules from the unfrozen void water are absorbed by the film. A process is thereby set up to move water molecules to the freezing front. This process would also imply the exclusion of the soil particles from the ice structure giving lenses of pure ice on freezing, as found in nature.

2.1.3. Water Pressures During Freezing

Knowledge of the pore water pressure distribution through the soil sample is of utmost importance in the solution of the frost heave problem. In the preceding chapter two mechanisims were discussed whereby a potential gradient may be set up on freezing. Investigation of this potential gradient by several authors has thrown some light on the problem. Williams (1967) in a series of experiments in which the pore pressure was measured as the frost front penetrated through the sample,showed that a negative pore pressure was developed at the frost front and concluded that this was responsible for the potential gradient causing moisture migration into the sample.

Calculations using the Kelvin equation yield values of pore press developed at the frost front and these are found to vary inversly with pore size (Penner 1958). Williams (1967) presented data showing that the value of pore radius obtained from air intrusion experiments could be used to predict pore pressures developed at the freezing front.

Sutherland and Gaskin (1973) showed that pore pressure at the freezing front could be reasonably predicted using grain size and capillary pore size, and their work lent support to Everett's (1965) proposal that in calculations the r_{iw} value to be used is associated with the effective size D_{10} rather than the mean particle size D_{50}. However, the authors concluded that predicted values of the drop in porewater pressures using values of pore size obtained by the air entry method grossly underestimated the actual measured values.

In the frozen zone the movement of water which occurs under the influence of suctions in the frozen zone is thought to be induced by the different energy levels of the unfrozen water and ice in the soil matrix. Harlan (1974) equated the Gibbs free energy difference between the two phases with the potential of the water in the soil in equilibrium with ice at a constant vapour pressure, temperature and pressure. Provided the ice crystals are not too small and have properties not unlike those of bulk ice at atmospheric pressure, the vapour pressure of the ice is independent of the amount of ice in the system and similarly the unfrozen water content is independent of total water contents. The development gives a relationship between temperature below 0°C i.e. freezing point depression and soil water potential as in Fig 2.1.

Harlan predicts a suction profile in the unfrozen water in the frozen zone and perhaps continuing into the unfrozen zone. The flow of moisture in the frozen zone has been demonstrated and documented by Hoekstra (1966). Due to the very low permeability of frozen soil the amount of flow

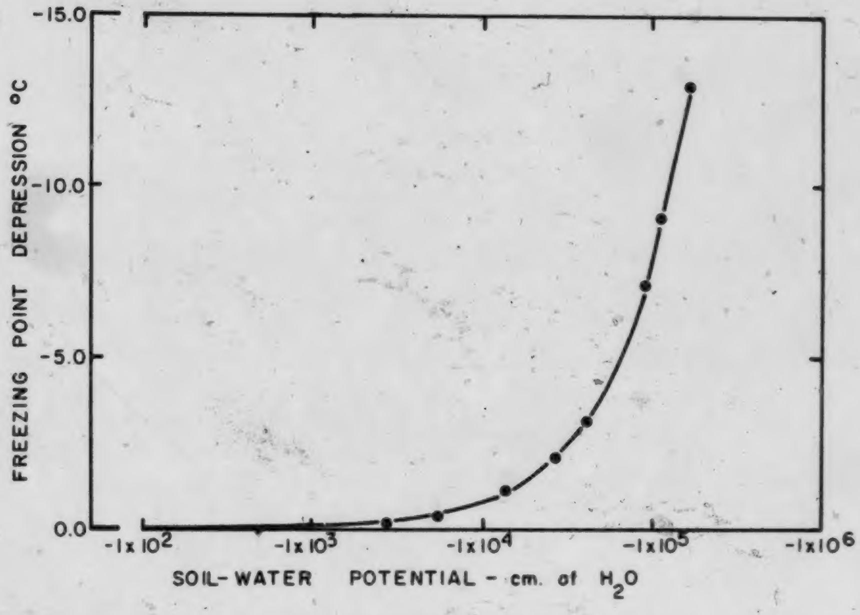

Fig. 2.1. Theoretical Relationship Between Soil Water Potential and Freezing Point Depression. (Harlan, 1974)

SOIL	TEST	%CLAY	SHUT-OFF PRESSURE kg/cm²	SOURCE
TRUAX DRUMLIN SOIL	LABORATORY, HEAVE RATE MEASURED	6	0.41	LINELL AND KAPLAR (1959)
LADD FIELD SILT	" " " "	4	0.52	" " " "
LORING SILTY GRAVEL	" " " "	5	0.58	" " " "
INDIANA SILT	" " " "	7.5	0.63	" " " "
EAST BOSTON TILL	" " " "	13.5	0.72	" " " "
DEVON SILT	LABORATORY, WATER FLOW MEASURED	17	1.25	ARVIDSON AND MORGENSTERN (1974)
MODIFIED DEVON SILT	" " " "	28	2.14	" " " "
LEDA CLAY	LABORATORY, (σ_i - u) DETERMINATION	47	3.99	WILLIAMS (1967 Fig. 9 pp.69)
SILT	" " "	6	0.07	" " " "

Table 2.1 Shut-off Pressures of Soils

induced by these tensions is negligible in engineering terms. However the mode of behaviour is of interest.

By examination of the above, the concept of a discrete interface advancing through a soil comes into doubt since not only is there formation of ice at the 0°C isotherm but also at some distance behind it at a position of favourable heat conditions. This greatly complicates the problem, however it is believed that for engineering applications the post 0°C isotherm freezing may be neglected and the simplifying assumption that all of the ice formation occurs at the interface be made. It is also assumed that any suctions generated originated at or near this interface.

2.1.4 Effects of Applied Load

The fact that increased load can depress the heave rate has been appreciated by workers in the field of frost action for some 40 years and there are several well documented case records which illustrate the phenomenon.

When an ice/water interface advances through a freezing soil it can be observed that water is either attracted to or expelled from the freezing front. It is found that for the same soil type attraction occurs when the applied load is low and that expulsion conditions exist when the applied load is higher. Moreover, there exists a unique stress, for a given soil type and stress history at which no flow into or out of the sample will occur. This stress is called the shut-off pressure.

Beskow (1935) was the first to document that increased pressure causes a decrease in heaving rate in a silty soil. Beskow manipulated the stress level by either changing the surface load, the pore water pressure or combinations of both and found that the heaving rate was identical if the difference between applied stress and the pore water pressure remained constant. The larger the difference between the two stresses the slower was the heaving rate.

Linell and Kaplar (1959) showed the existence of a shut- off pressure for a variety of soils. Their results are presented in Table 2.1

Other supporting laboratory evidence presented by Anderson (1973) is also summarized in Table 2.1. These tests showed that when the applied load was lower than the shut off pressure water was attracted to the freezing point and when the applied load exceeded the shut-off pressure, water was expelled.

Theoretical justification of the existence of the shut off pressure may be gained from a consideration of the capillary model. Equation 2.4 predicts that a pressure difference exists across the curved surface of the ice water interface due to the energy of the interface.

Two conditions are predicted by this equation. If the applied load on freezing is less than ($2\sigma_{iw}$) water migration occurs towards the interface and an ice lens grows. If however,the stress difference is greater than ($2\sigma_{iw}$) then ice will propagate through the soil pores and water may be expelled. This stress ($2\sigma_{iw}$) is, then, the shut off pressure.

Arvidson (1973) equated ($2\sigma_{iw}$) with the shut-off pressure and attempted to predict the value of shut-off pressure using typical values of σ_{iw} and r_{iw},however the agreement between predicted and observed was not good and showed the limitations of assuming values for parameters which cannot be accurately assessed.

Takashi (1974) in a series of experiments in which the rate of penetration of the frost front was kept constant,showed the different modes of behaviour of moisture migration due to changes in applied load. Values of shut-off pressure obtained ranged from 1.2 Kg/cm^2 for a silt to 3.5 Kg/cm^2 for a silty clay.

An example of a case record in which both total heave rate is known and where the freezing rates are given is presented by Aitken (1974) for a field test program conducted near Fairbanks, Alaska. These tests were conducted by monitoring the total heave experienced by a series of 24 foot square loaded platforms. Allowance for heave due to freezing of situ water in the total heave results gives the segregational heave rate with respect to applied load. Aitken showed that the segregational heave rate decreased almost linearly with increasing applied load.

2.1.5 Effects of Heat Energy Removal Rate

The effects of the rate of removal of heat from the frost front are uncertain. Beskow (1935) demonstrated that the heaving rate was not always influenced by the rate of frost penetration. In his experiments the temperature was varied between -3°C and -10°C above the sample without affecting the heave rate. The colder temperatures, although increasing the rate of frost penetration, did not increase the heaving rate. Penner (1959) however,showed experimentally that the rate of heave was a function of the rate of heat removal using cold side temperatures of -2°C to -6°C. The difficulty in assessing the overall effects of heat and moisture flow arise not only from the complexity of the mathematics but also from the lack of experimental measurements of heave rates, heat flow, moisture flow, temperature distributions and moisture tensions while ice lensing is in progress. In the absence of such information, the quantitative treatment of the combined heat and moisture flow appears very difficult.

Tagaki (1970) presented an analysis of ice lens formation. This work formulates in great detail the heat and moisture flow equations in a layer of unfrozen soil overlain by a layer of ice. This theory does not predict the cessation of the growth of this ice layer or the advance of an in-situ frost front beyond its initial position. Although extremely rigorous in presentation, the theory in its present form is not capable of predicting the magnitude of frost heaving likely to be experienced in the field.

2.1.6 Magnitude of Heave

The magnitude of the heaving observed during freezing is due to the combination of heave due to freezing of in-situ water and heave due to moisture transfer. For a stationary frost front the former of these is reduced to zero and hence only segregational heave occurs. With a stationary frost front the component affecting the magnitude of heave is a function of the magnitude of suction generated at the frost front. If the suction is decreased by some means the rate of water flow into the sample would be also be decreased hence lowering the magnitude of the rate of heave.

The effects of applied load and heat flux removal for a given soil have been reviewed previously, however the effects of a different soil type for conditions of constant applied load and heat flux removal must be considered.

The most obvious factor is that of particle size. Penner (1967b) summarized heaving behaviour in a schematic graph (Fig 2.2). In zone 1 the heaving behaviour is subdued since at this grain size range low values of suction would be generated and although the permeability of the material

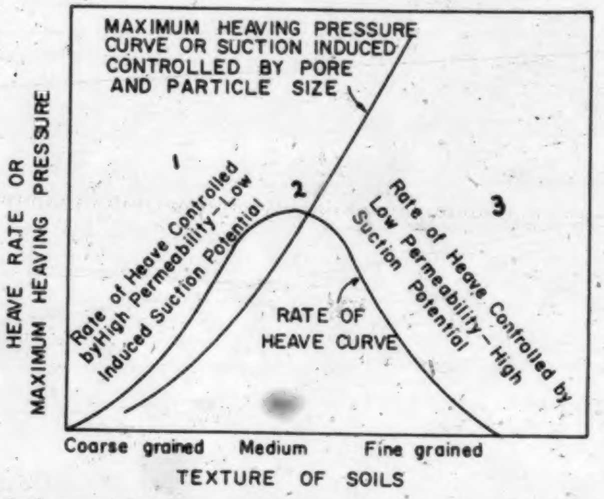
MAXIMUM HEAVING PRESSURE CURVE OR SUCTION INDUCED CONTROLLED BY PORE AND PARTICLE SIZE
HEAVE RATE OR MAXIMUM HEAVING PRESSURE
1
2
3
Rate of Heave Controlled by High Permeability–Low Induced Suction Potential
Rate of Heave Controlled by Low Permeability–High Suction Potential
RATE OF HEAVE CURVE
Coarse grained
Medium
Fine grained
TEXTURE OF SOILS

Fig. 2.2 Schematic Representation of Relationship Between Heaving Rate, Heaving Pressure and Particle Size Resulting from Ice Lens Growth. (Penner, 1967)

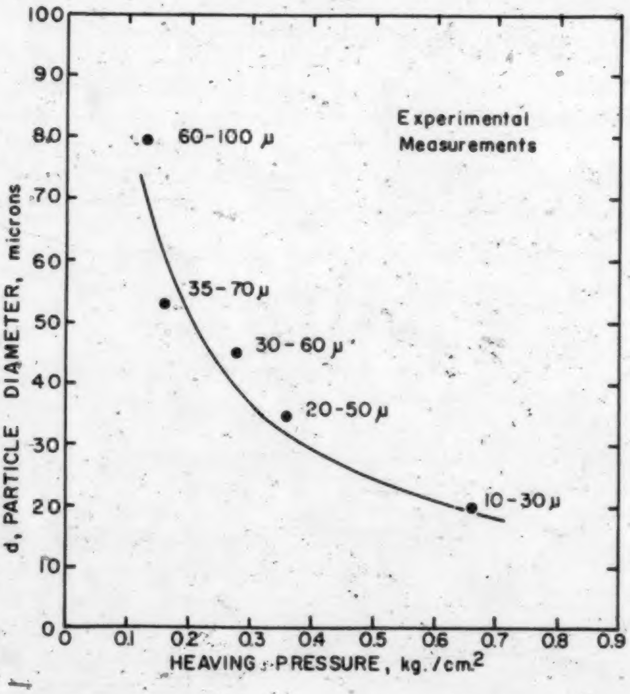

Fig. 2.3 Relationship Between Heaving Pressures and Average Diameter of Fractions. (Penner, 1967)

would permit high flow rates, the potential gradient would not be sufficient to draw in an appreciable amount of water. Zone 3, however, is the opposite case; i.e. high suctions would be generated but due to the combined effects of cavitation and low permeability water flow would be restricted. Zone 2 is the optimum for maximum heave due to ice segregation. A combination of moderate suctions and permeability render this particle size very frost susceptible.

The effects of grain size alone on the suction developed at the frost front was demonstrated very clearly by Penner (1967a) by the freezing of glass beads of varying diameters and measuring the associated suction gradient. A curve of load diameter versus water potential was obtained and is given in Fig 2.3.

Another factor governing the rate of heave is the availability of water. As stated previously, ice lensing results when a soil has the ability to supply water to an active ice front for a sufficiently long time to grow an ice lens, (Anderson and Morgenstern 1973). If that ability to supply water is removed the freezing process essentially becomes a closed system and the heaving behaviour is greatly subdued. McGaw (1972) correlated heaving rates with depth to the water table i.e. moisture availability, on four different soil types. The results showed that if water was made virtually unavailable by lowering the water table suffiently, heave could be virtually eliminated.

2.2.1 Basic Concepts of Frost Heaving

The development of a comprehensive theory of frost heaving must embrace the effects of the external factors of applied load and heat flux removal on the moisture migration behaviour. Consequently we must investigate the heat energy balance at the frost front and attempt to relate it in some way to the rate of moisture migration into the sample.

2.2.2 Energy Budget

The concept of an energy budget is a valuable framework on which to base any development of a frost heave theory. Although there is conflicting evidence on the subject, it is felt intuitively that the rate of heat removal must play some part in the rate of moisture migration. A combination of Beskow's (1935) results and those of Penner (1972) and Kaplar (1970), with the suction gradient increasing with heat flux removal up to a certain level, and then becoming constant at this magnitude may best describe the effects of rate of heat removal.

The transport of energy takes place under the influence of five factors; conduction, convection, radiation , mass transport and latent heat of fusion of the migrated water. Convection and radiation may be immediately neglected as being of no importance to this problem (Harlan, 1973). The effect of mass transport may also be omitted as the magnitude of heat energy involved in this term is very small since the temperature of the water flowing into the sample is very close to 0°C.

The heat energy balance for a stationary frost front may be expressed mathematically by:

Heat out by conduction - heat in by conduction - latent heat of fusion $\gg 0$

The heat out by conduction is given by

$$Q_1 = K_f \frac{dT}{dz_1} \qquad 2.6$$

Where K_f = The thermal conductivity of frozen soil

T = temperature

z_1 = distance in the axial direction the frozen zone

Similarly the heat conducted to the frost front by the unfrozen soil is given by

$$Q_2 = K_u \frac{dT}{dz_2} \qquad 2.7$$

Where K_u = the thermal conductivity of the unfrozen soil.

Z_2 = distance in the axial direction in the unfrozen zone

Assuming a stationary frost front, the heat brought to the frost front as latent heat of fusion may be expressed as

$$Q_3 = Lv \qquad 2.8$$

Where L = latent heat of fusion

v = velocity of the water arriving at the frost front.

The velocity of the water assuming at the frost front may be given as

$$v = ki \qquad 2.9$$

Where k = the coefficient of permeability

i = the hydraulic gradient through the soil.

Hence the sum of the heat transfer terms at the frost front may be expressed as

$$Q_1 - Q_2 - Q_3 \geqslant 0 \qquad 2.10$$

The inequality sign being included to account for any additional energy considerations which may arise due to other components. Enumerating the terms gives

$$K_f \frac{dt}{dz_1} - K_u \frac{dt}{dz_2} - LKi \geqslant 0 \qquad 2.11$$

The hydraulic gradient, i, may be more rigorously defined as the gradient of the total potential, i.e. ϕ, thus 2.11 may be re-written as

$$K_f \frac{dt}{dz_1} - K_u \frac{dt}{dz_2} - LK \frac{d\phi}{dz} \geqslant 0 \qquad 2.13$$

2.2.3 Potential Gradient

The rate of moisture migration is governed by the laws of soil water flow. Water flows due to a gradient in total potential. Total potential is defined as

$$\phi = \gamma z + (\psi + \epsilon - \xi) \qquad 2.12$$

Where ϕ = total potential

γz = position head or gravitational head

ψ = pressure head or pressure potential

ϵ = osmotic pressure potential

ξ = adsorption potential.

In this problem the osmotic potential and adsorption potential components may be neglected reducing expression 2.12 to

$$\phi = \gamma z + \psi \qquad 2.13$$

However, the presence of tensions in the pore water tends to complicate the problem, hence some formalism in definition and terminology is necessary to avoid confusion. The status of water in a soil can be expressed in terms of free energy relative to free, pure water (Aitchison, Russam and Richards, 1965). In cases where the free energy is less than that of pure water under atmospheric pressure the terms suction and negative pore water pressure are often used. The total potential of soil water is the potential in pure water that will cause the same free energy at the same temperature as in the soil water.

An alternative definition of total potential is the work done per unit quantity to transport reversibly and isothermally an infinitesimal amount of pure water from a pool at a specified elevation at atmospheric pressure to the point in the soil water under consideration. At this point the balance of work done by the pore water must be investigated. In the definition given above, the potential is expressed as the work done transporting water into the sample from a pool at a specified elevation, however, in the frost heave problem there are two components of work: 1) that work done due to the flow of water under the influence of a potential gradient and 2) the work done in lifting the frozen soil and the applied load.

It would appear that the greater the work required to lift the applied load the less will be the energy available to transport water at a given temperature gradient. This in general terms appears to be the action of externally applied loads. Consequently an experimental study of water flux during freezing with varying applied loads and rates of freezing was undertaken to investigate the inter-relationship between these factors.

CHAPTER 3

TEST PROCEDURE AND DESCRIPTION OF EQUIPMENT

3.1 Materials

Testing was carried out using Devon Silt, the properties of which are summarized in Table 3.1 and Fig 3.1. This material was chosen for its high frost susceptibility, availability and its similarity to silty materials found in northern regions.

The samples were prepared as a slurry at a moisture content of about 50%(1 1/2 times its liquid limit) for ease of handling. To ensure saturation the slurry was subjected to vigorous vibration, and a vacuum of approximately 680 mm of mercury was applied to the sample. This proved to be a very succesful method of de-airing the slurry as B values of unity were obtained both before and after several consolidation increments had been applied.

3.2 Testing Program and Procedure

The objective of the program was to investigate the moisture migration characteristics of Devon Silt with respect to stress level and rate of advance of the frost front. Loads were applied using a weights and hanger system and the different heat flux conditions were obtained by applying a constant step temperature to the sample.

Once the slurry had been placed in the apparatus, and

DEVON SILT	
LIQUID LIMIT	— 35.9 %
PLASTIC LIMIT	— 18.5 %
SPECIFIC GRAVITY	— 2.68
% PASSING 200 SIEVE	— 87 %
D_{10}	— 0.0002m.m

Table 3.1 Properties of Devon Silt

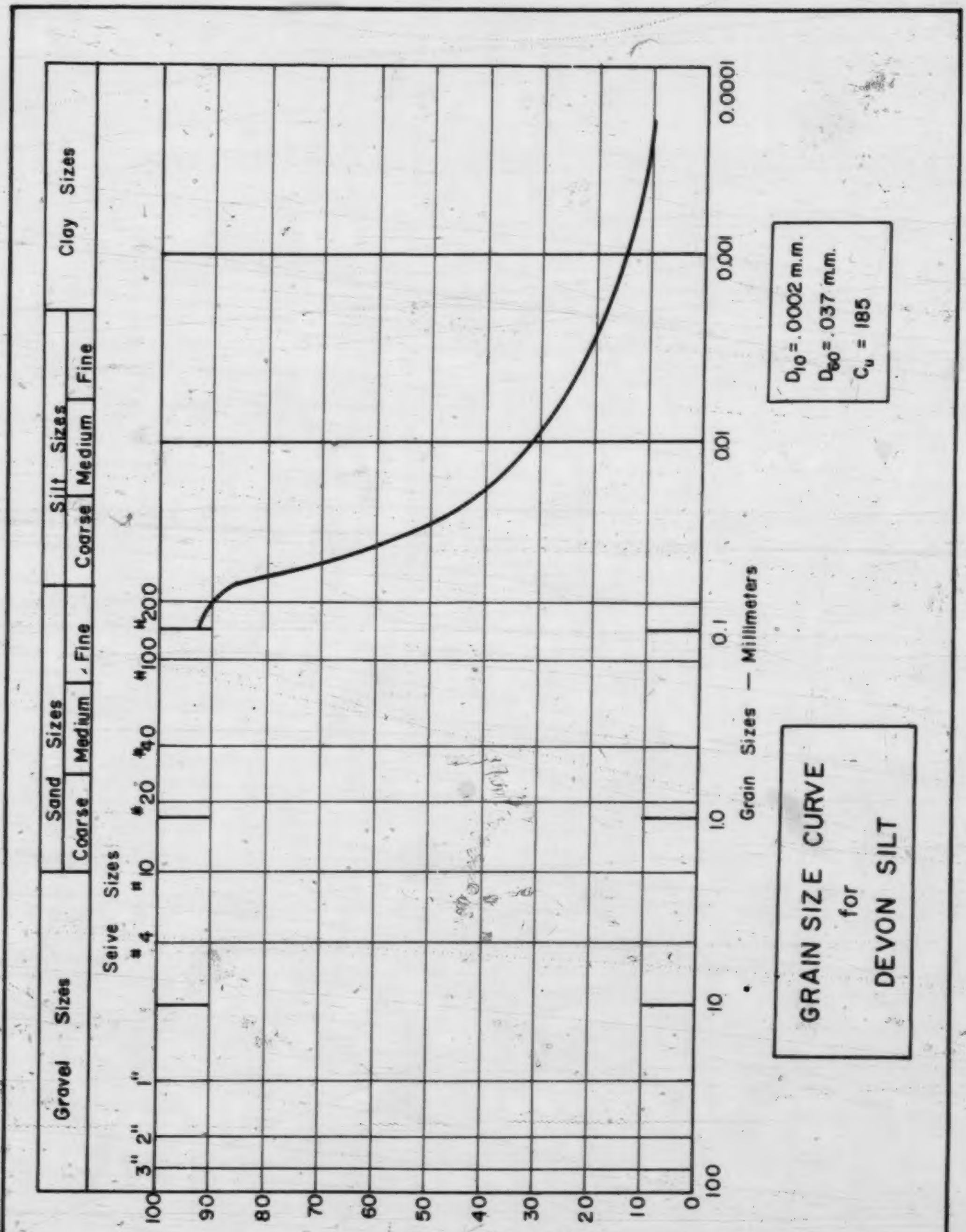
Gravel Sizes
Sand Sizes
Coarse
Medium
Fine
Silt Sizes
Coarse
Medium
Fine
Clay Sizes
Seive Sizes
3"
2"
1"
#4
#10
#20
#40
#100
#200
Percent Finer Than
100
90
80
70
60
50
40
30
20
10
0
100
10
1.0
0.1
.01
0.001
0.0001
Grain Sizes — Millimeters
GRAIN SIZE CURVE
for
DEVON SILT
D10 = .0002 m.m.
D60 = .037 m.m.
Cu = 185

Fig. 3.1

assembly completed, the test equipment was set up in a cold room with a mean air temperature of 1.7°C. The sample was then consolidated to the desired applied load. Temperature equilibration was ensured by leaving the sample for a period of time (usually 18 hours) in a styrofoam cabinet inside the cold room while each consolidation increment was applied. The B test to check the degree of satuation, if desired, was carried out at this stage.

Prior to freezing the soil sample, the desired freeze test boundary conditions were imposed. Bottom drainage was closed and an unrestrained displacement boundary condition applied. The sample had free access to an external water source through the top plate of the apparatus. The volume of water leaving or entering the soil was measured by a volume change indicator system, described below.

To eliminate problems of friction and adfreeze the samples were frozen from the bottom upwards by imposing a negative step temperature on the base of the sample. This temperature was held constant throughout the test and the resultant freeze rate was a function of sample moisture content and magnitude of the step temperature.

The temperature distribution and movement of the 0°C isotherm was monitered continuously. The magnitude of heave was also measured.

3.3 Description of Equipment

The experimental apparatus was a Permode (Permafrost Oedometer) as described by Roggensack (1976) with slight modification to permit the measurement of temperature in the soil sample.

The permode was intended primarily for work with thawing soils, however it lends itself well to work on the freezing of soils.

A schematic diagram of the equipment set-up is shown in Fig 3.2.

The permode (Figs 3.3 to Fig 3.7) is a 100 mm diameter, teflon lined cylinder. The outer jacket of the cell was machined from thick walled P.V.C. pipe thereby preventing lateral strain during the application of load. The load was applied by weights on a counterbalanced hanger, and was transfered to the soil by the top piston. The seal on this piston was a double o-ring seal with grooves for the rings machined in the piston to increase the efficiency of the seal and to reduce side friction. The seal proved effective up to pressures of 1.4 Kg/cm^2 though during the testing program the loading increments were held well below this level.

A coating of high vacuum grease on the teflon reduced friction between the membrance and the walls of the cylinder to almost zero. This was deduced from the results of the B test carried out at various stages of loading. The results

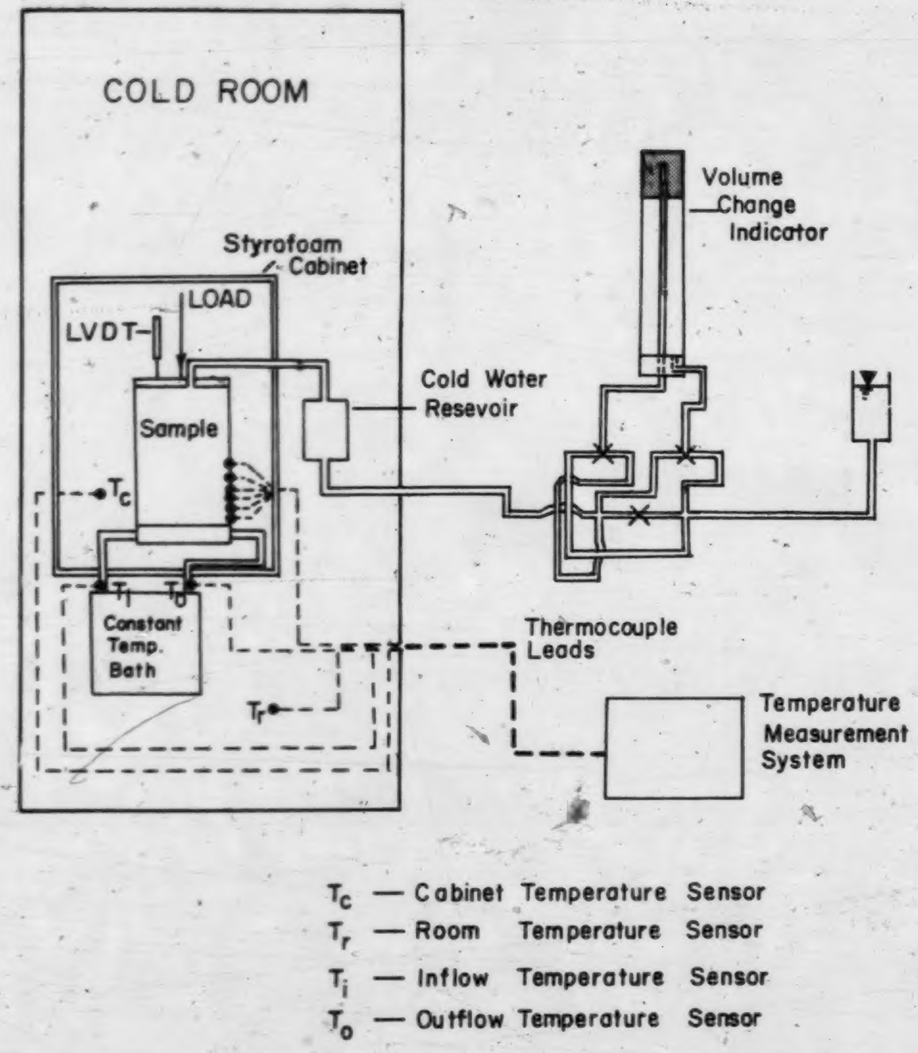
COLD ROOM
Styrofoam Cabinet
LOAD
LVDT
Sample
T_c
T_i
T_o
Constant Temp. Bath
T_r
Cold Water Resevoir
Volume Change Indicator
Thermocouple Leads
Temperature Measurement System
T_c — Cabinet Temperature Sensor
T_r — Room Temperature Sensor
T_i — Inflow Temperature Sensor
T_o — Outflow Temperature Sensor

Fig. 3.2 Schematic Diagram of Experimental Apparatus

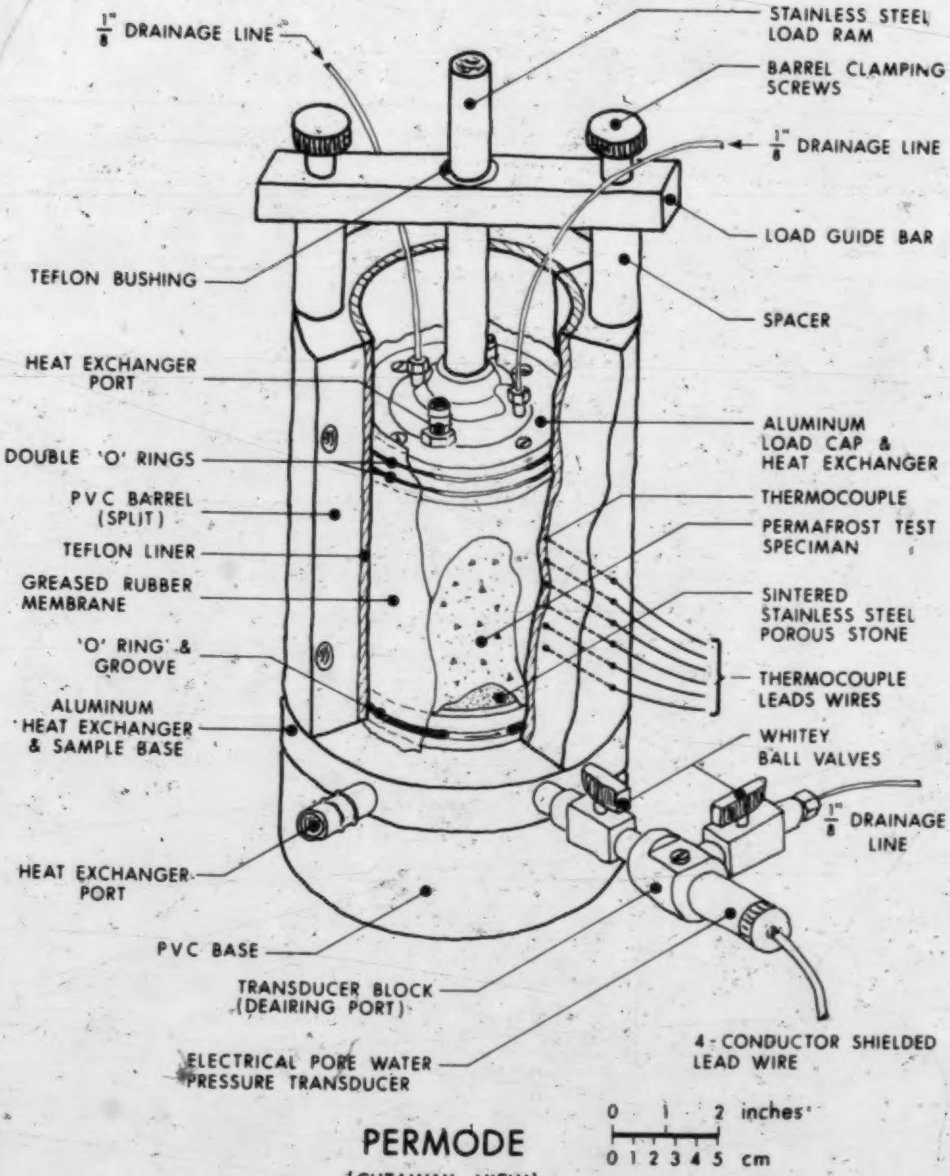
1/8" DRAINAGE LINE
STAINLESS STEEL LOAD RAM
BARREL CLAMPING SCREWS
1/8" DRAINAGE LINE
LOAD GUIDE BAR
TEFLON BUSHING
SPACER
HEAT EXCHANGER PORT
ALUMINUM LOAD CAP & HEAT EXCHANGER
DOUBLE 'O' RINGS
PVC BARREL (SPLIT)
THERMOCOUPLE
TEFLON LINER
PERMAFROST TEST SPECIMAN
GREASED RUBBER MEMBRANE
SINTERED STAINLESS STEEL POROUS STONE
'O' RING & GROOVE
THERMOCOUPLE LEADS WIRES
ALUMINUM HEAT EXCHANGER & SAMPLE BASE
WHITEY BALL VALVES
1/8" DRAINAGE LINE
HEAT EXCHANGER PORT
PVC BASE
TRANSDUCER BLOCK (DEAIRING PORT)
ELECTRICAL PORE WATER PRESSURE TRANSDUCER
4-CONDUCTOR SHIELDED LEAD WIRE
0 1 2 inches
0 1 2 3 4 5 cm

PERMODE
(CUTAWAY VIEW)

Fig. 3.3

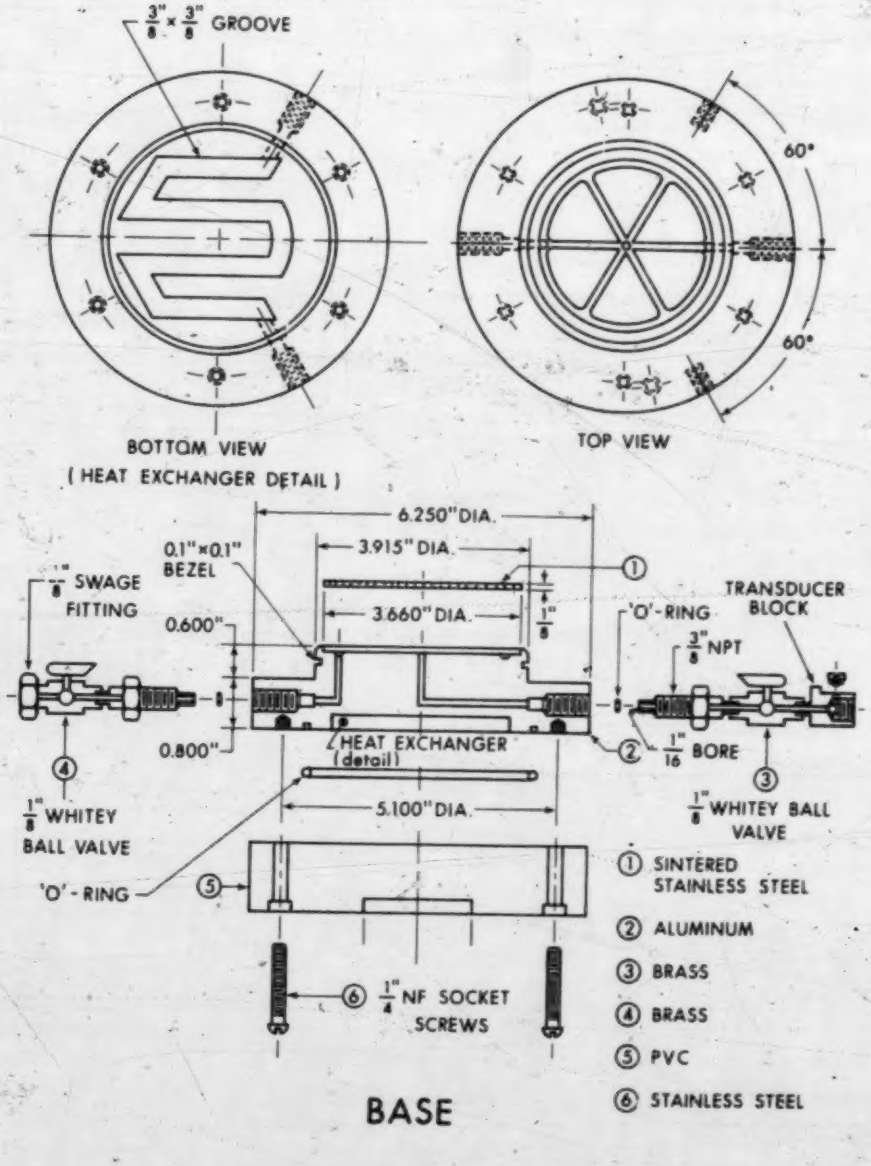
3/8" × 3/8" GROOVE
60°
60°
BOTTOM VIEW
(HEAT EXCHANGER DETAIL)
TOP VIEW
6.250" DIA.
3.915" DIA.
3.660" DIA.
0.1" × 0.1" BEZEL
1/8" SWAGE FITTING
0.600"
0.800"
1/8"
①
'O'-RING
TRANSDUCER BLOCK
3/8" NPT
HEAT EXCHANGER (detail)
②
1/16" BORE
③
1/8" WHITEY BALL VALVE
④
1/8" WHITEY BALL VALVE
5.100" DIA.
'O'-RING
⑤
⑥
1/4" NF SOCKET SCREWS
① SINTERED STAINLESS STEEL
② ALUMINUM
③ BRASS
④ BRASS
⑤ PVC
⑥ STAINLESS STEEL
BASE

Fig. 3.4

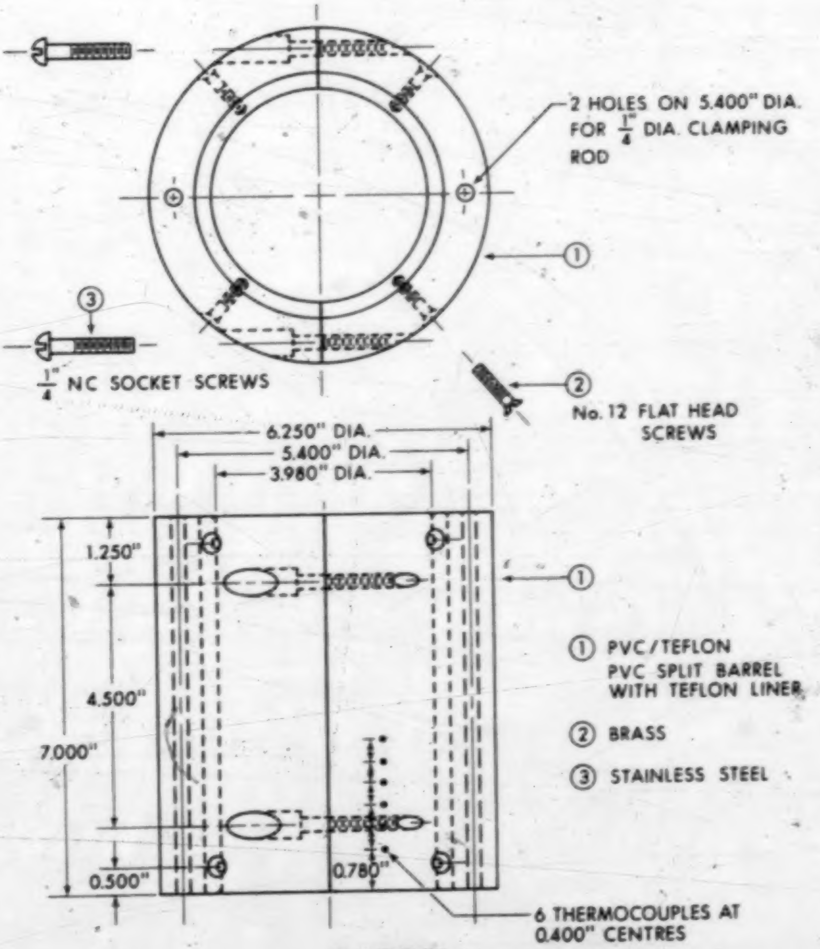
2 HOLES ON 5.400" DIA. FOR $\frac{1}{4}$" DIA. CLAMPING ROD
①
③
$\frac{1}{4}$" NC SOCKET SCREWS
②
No. 12 FLAT HEAD SCREWS
6.250" DIA.
5.400" DIA.
3.980" DIA.
1.250"
①
4.500"
7.000"
0.500"
0.780"
① PVC/TEFLON
PVC SPLIT BARREL WITH TEFLON LINER
② BRASS
③ STAINLESS STEEL
6 THERMOCOUPLES AT 0.400" CENTRES

BARREL

Fig. 3.5

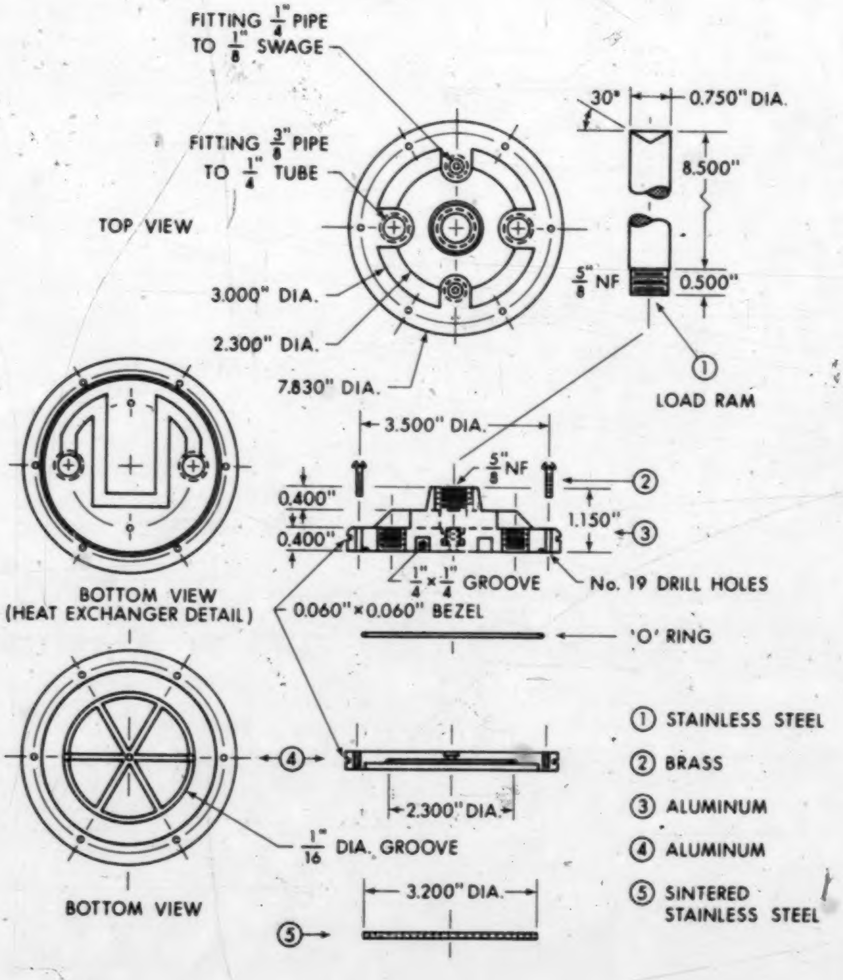
FITTING $\frac{1}{4}$" PIPE TO $\frac{1}{8}$" SWAGE
FITTING $\frac{3}{8}$" PIPE TO $\frac{1}{4}$" TUBE
TOP VIEW
3.000" DIA.
2.300" DIA.
7.830" DIA.
30°
0.750" DIA.
8.500"
$\frac{5}{8}$" NF
0.500"
①
LOAD RAM
BOTTOM VIEW (HEAT EXCHANGER DETAIL)
3.500" DIA.
$\frac{5}{8}$" NF
②
0.400"
0.400"
1.150"
③
$\frac{1}{4}$" × $\frac{1}{4}$" GROOVE
No. 19 DRILL HOLES
0.060" × 0.060" BEZEL
'O' RING
④
2.300" DIA.
$\frac{1}{16}$" DIA. GROOVE
BOTTOM VIEW
3.200" DIA.
⑤
① STAINLESS STEEL
② BRASS
③ ALUMINUM
④ ALUMINUM
⑤ SINTERED STAINLESS STEEL

LOAD CAP

Fig. 3.6

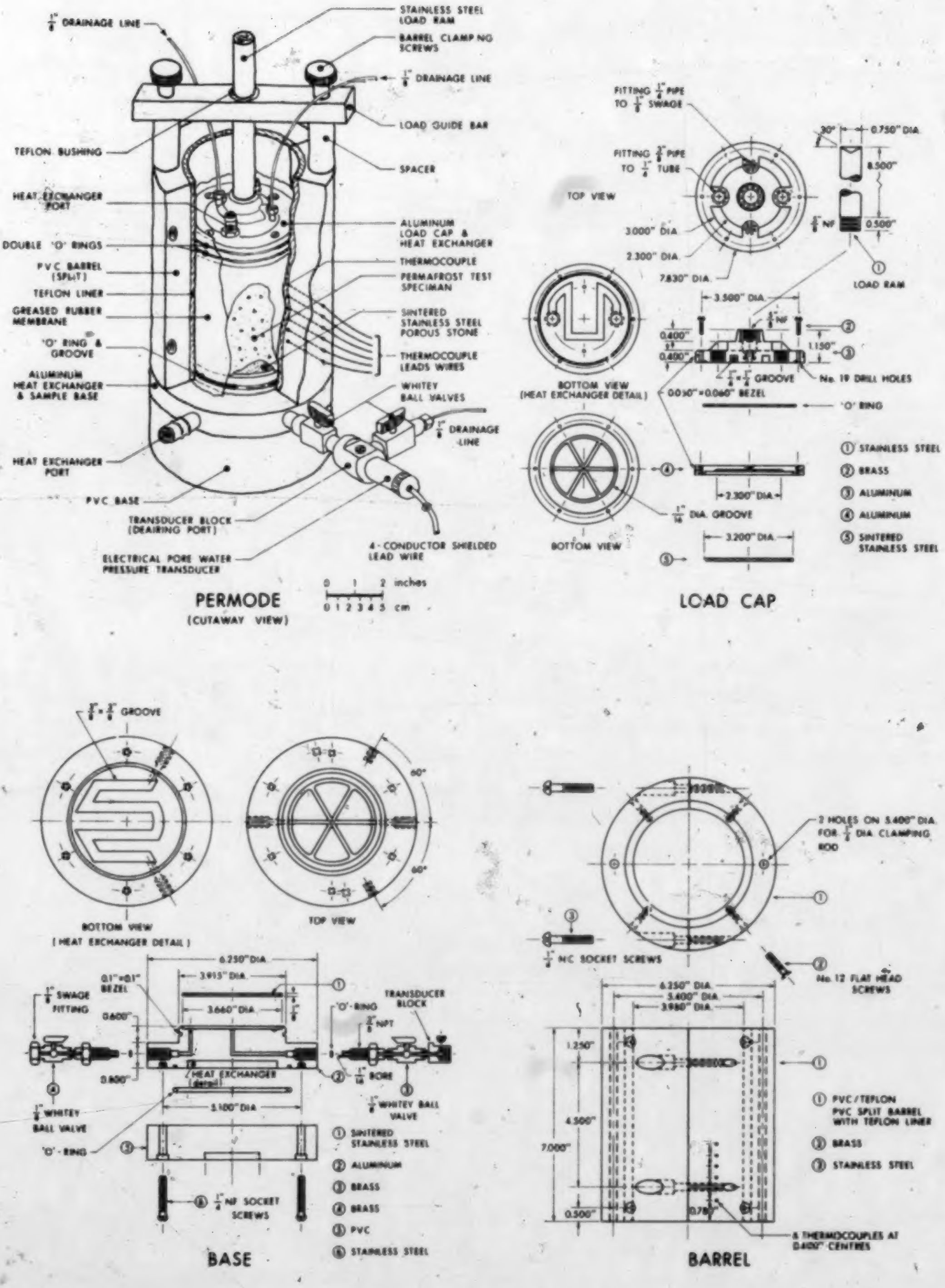
1/8" DRAINAGE LINE
STAINLESS STEEL LOAD RAM
BARREL CLAMPING SCREWS
1/8" DRAINAGE LINE
LOAD GUIDE BAR
TEFLON BUSHING
SPACER
HEAT EXCHANGER PORT
ALUMINUM LOAD CAP & HEAT EXCHANGER
DOUBLE 'O' RINGS
THERMOCOUPLE
PVC BARREL (SPLIT)
PERMAFROST TEST SPECIMAN
TEFLON LINER
GREASED RUBBER MEMBRANE
SINTERED STAINLESS STEEL POROUS STONE
'O' RING & GROOVE
THERMOCOUPLE LEADS WIRES
ALUMINUM HEAT EXCHANGER & SAMPLE BASE
WHITEY BALL VALVES
1/8" DRAINAGE LINE
HEAT EXCHANGER PORT
PVC BASE
TRANSDUCER BLOCK (DEAIRING PORT)
ELECTRICAL PORE WATER PRESSURE TRANSDUCER
4-CONDUCTOR SHIELDED LEAD WIRE
0 1 2 inches
0 1 2 3 4 5 cm
PERMODE
(CUTAWAY VIEW)
FITTING 1/8" PIPE TO 1/8" SWAGE
FITTING 3/8" PIPE TO 1/4" TUBE
TOP VIEW
30°
0.750" DIA.
8.500"
3/8" NF
0.500"
3.000" DIA.
2.300" DIA.
7.830" DIA.
① LOAD RAM
BOTTOM VIEW (HEAT EXCHANGER DETAIL)
3.500" DIA.
3/8" NF
②
0.400"
1.150"
③
0.400"
1/4" × 1/4" GROOVE
No. 19 DRILL HOLES
0.030" × 0.060" BEZEL
'O' RING
④
2.300" DIA.
1/16" DIA. GROOVE
BOTTOM VIEW
3.200" DIA.
⑤
① STAINLESS STEEL
② BRASS
③ ALUMINUM
④ ALUMINUM
⑤ SINTERED STAINLESS STEEL
LOAD CAP
3/8" × 3/8" GROOVE
60°
60°
BOTTOM VIEW
(HEAT EXCHANGER DETAIL)
TOP VIEW
6.250" DIA.
3.915" DIA.
0.1" × 0.1" BEZEL
①
1/8" SWAGE FITTING
3.660" DIA.
1/8"
'O'-RING
TRANSDUCER BLOCK
0.600"
3/8" NPT
0.800"
HEAT EXCHANGER (detail)
② 1/16" BORE
④ 1/8" WHITEY BALL VALVE
③ 1/8" WHITEY BALL VALVE
5.100" DIA.
'O'-RING
⑤
① SINTERED STAINLESS STEEL
② ALUMINUM
③ BRASS
④ BRASS
⑤ PVC
⑥ STAINLESS STEEL
⑥ 1/4" NF SOCKET SCREWS
BASE
2 HOLES ON 5.400" DIA. FOR 1/4" DIA CLAMPING ROD
①
③
1/4" NC SOCKET SCREWS
②
No. 12 FLAT HEAD SCREWS
6.250" DIA.
5.400" DIA.
3.980" DIA.
1.250"
①
4.500"
7.000"
0.500"
0.750"
① PVC/TEFLON PVC SPLIT BARREL WITH TEFLON LINER
② BRASS
③ STAINLESS STEEL
8 THERMOCOUPLES AT 0.400" CENTRES
BARREL

Fig. 3.7

of the $\bar{B}$ tests carried out on sample NDS-6 are included in Chapter 4.

The bottom seal ~~was~~ an O-ring and groove construction, effective to pressures above 1.8 Kg/cm^2 due to the thickness of the O-ring. However, as mentioned before the efficiency of ths seal was never tested to its limit during the program because of the low load increments that were applied.

Drainage was provided at both top and bottom through sintered steel porous stones. This is an improvement over previous apparatus as time for complete pore pressure dissipation after load application is greatly reduced.

The base plate acted as a heat sink to induce freezing. It contained the coolant circulation maze which was designed to provide as high a flow rate as possible without denying adequate distribution of the fluid throughout the base.

Thermocouples were placed in the side walls of the cylinder to measure the temperature distribution in the soil sample. This system will be described in detail below.

Freezing from the bottom was adopted for several reasons. The problems of adfreeze and side friction and the resulting restraining forces induced by trying to heave a plug of frozen soil upwards, (as in freezing from the top) was considered to be a major problem. If freezing was induced from the bottom upwards the soil being heaved would be unfrozen and hence side friction would be minimal and adfreeze non-existent.

Freezing from the base also eliminates the problem of having to know, very accurately, the sample height since the distance from the plane of application of the step temperature to each thermocouple is the same in each experiment, and hence temperature/time data may be easily correlated to observe and compare rates of penetration of the freezing front.

The negative step temperature imposed on the base of the sample was attained by the circulation of a coolant through a maze in the base plate . The fluid temperature was maintained by a constant temperature bath to 0.1°C. The fluid used was an anti-freeze/water mix (50% by volume) which was pumped through the maze at a rate of 80ml/sec.

Thermocouples set into the walls of the cylinder were used to monitor temperature. A Honeywell 24 channel strip chart recorder recorded temperature distribution through the sample with time. Accuracy of 0.3°C was possible with this arrangement. However a slight time lag between the soil temperature and that measured will occur due to the low thermal conductivity of the membrance and the grease. This time lag will be constant for each set of tests and is thus a negligible source of error.

Six thermocouples were installed at 10mm intervals and were numbered 7 to 12 from the base upwards. Four other thermocouples were employed to monitor coolant bath temperature, coolant return temperature, room temperature and the temperature inside the styofoam cabinet.

Heat flux removed from the sample may be calculated from the above data. The temperature difference between the exit and entry lines of the heat exchanger is directly proportional to the heat flux or alternatively knowing the temperature gradient in the frozen zone, and the thermal conductivity of frozen soil, the heat flux may be calculated from

$$Q=K_f\frac{dt}{dz}A \qquad 3.1$$

K_f - thermal conductivity of frozen soil

A - sample cross-sectional area

$\frac{dt}{dz}$ - temperature gradient

Pore water pressure measurements were recorded using a pressure transducer calibrated to 0.01 Kg/cm². These measurements were taken during $\bar{B}$ tests to ensure 100% saturation and complete load transfer to the sample.

The volume change of the sample in terms of pore fluid entering or leaving the sample was measured in a 10cc volume change indicator as in Fig 3.8.

Vertical displacements both during consolidation and freezing were monitored using a 6 volt excitation LVDT

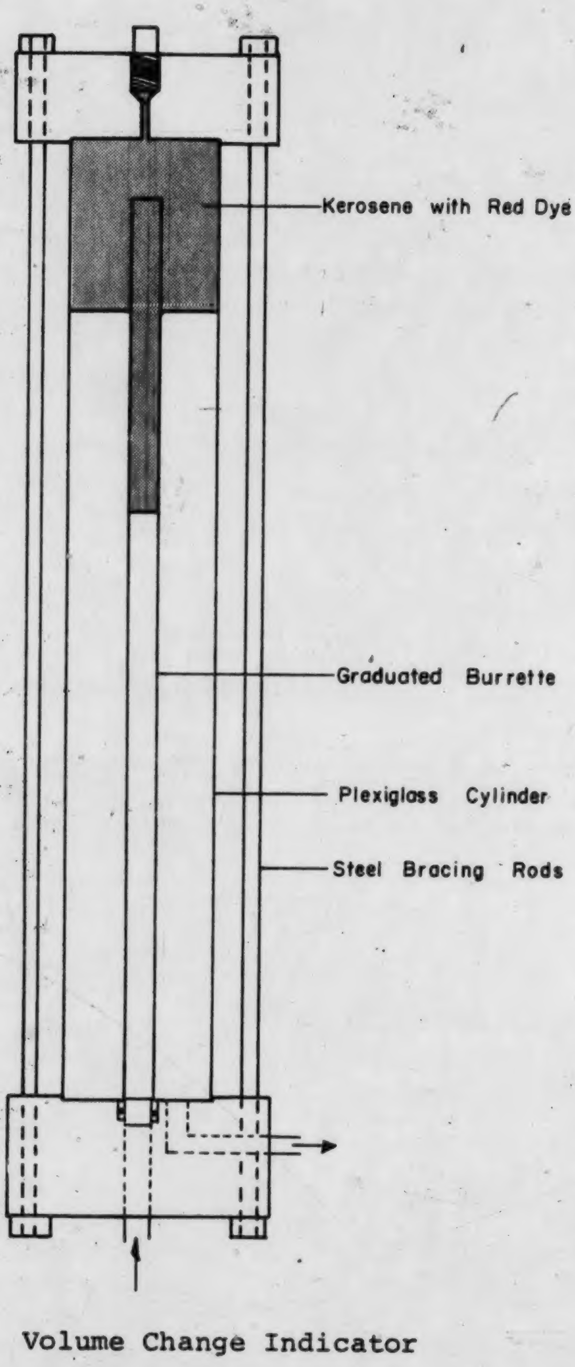
Kerosene with Red Dye
Graduated Burrette
Plexiglass Cylinder
Steel Bracing Rods

Fig. 3.8 Volume Change Indicator

(Linear Voltage Displacement Transdocer) accurate to 0.025mm. The output was recorded on a Hewlett Packard data aquisition system employing a digital voltmeter.

The apparatus, although not originally intended for this application, performed extremely well. Side friction was found to be negligible and no other major problems were encountered during testing. However, slight difficulty was found during set up. Since the slurry when first placed in the cylinder has zero strength the sample was unable to stand unsupported when the permode cylinder jackets were removed to install the top piston and O-ring seals. This was overcome with the aid of an assistant who would support the slurry and membrane while the outer jacket was removed. The O-rings were then placed and sealed and the cylinder was replaced and tightened to complete the operation. Distilled, de-aired water was then circulated through the drainage system to remove any air bubbles which may have gathered during set-up.

Overall performance was good. The only delays were caused by the failure of ancillary equipment such as the temperature bath, data aquisition system or failure of the room refrigeration system.

CHAPTER 4

TEST RESULTS

4.1 Test Program

The aim of the test program was to obtain the moisture migration characteristics of Devon Silt under varying conditions of applied load and freezing rate. In each experiment water flow into or out of the sample, vertical displacement and temperature were observed and plotted against time. The program consisted of 4 series of experiments. The step temperature applied to all the samples in a particular series was the same, only the stress level was varied, giving a complete description of the moisture migration characteristics with respect to applied load for a given freezing rate. The step temperatures used were -5°C, -2.5°C, -1.0°C and -13°C for the NDS series, NDSB series, NDSC series and NDSD series respectively. In series NDSB and NDSC an initial step temperature of -10°C was necessary to initiate nucleation, however once the sudden heave due to nucleation occurred, the temperature of the boundary was returned to the desired test temperature and the system allowed to equilibrate.

To give a complete picture of the experimental procedure and interpretation of results, the description of a typical test is given in detail (NDS-7).

The sample was prepared as described in Chapter 3 and the experiment was commenced by loading the sample. Since the sample was prepared as a slurry, and the top seal on the piston was efficient to only 1.5 Kg/cm². The initial load increments were small, about 0.5 Kg/cm² to 1.0 Kg/cm² to prevent extrusion. The excess pore pressures generated during each loading phase were allowed to dissipate completely before the next increment was applied. In test NDS-7, three load increments of approximately 0.73 Kg/cm² were applied to give a total load of 2.2 Kg/cm². When the sample was fully consolidated to the desired load, the initial sample temperature distribution was examined by monitoring the readout from the six thermocouples placed in the side of the jacket of the apparatus. The requirements for temperature stabiity were that all the thermocouples had the same temperature, and that this value remained almost constant, any fluctuations reflecting only the small variation of room temperature with time. If the fluctuations of sample temperature were less than 0.5°C the sample was considered thermally stable. The temperature of the coolant was noted to ensure that the constant temperature bath had attained the required fluid temperature.

Initial readings of the burette measuring pore water volume change and the LVDT measuring vertical displacement were taken and at a convenient time, eg., on the hour, the experiment was started. The temperature of the sample was continuously monitored on the strip chart recorder, and the readings of vertical displacement and volume change were recorded manually at ten minute intervals for the first hour and at longer intervals, usually twenty minutes, for the remainder of the experiment.

The results of experiment NDS-7 are presented in graphical form in Fig 4.1. The experiment was allowed to run for such time as was necessary to ensure that equilibrium had been achieved. Equilibrium was defined as the development of a constant slope on the moisture migration versus time plot.

The graphs obtained for NDS-7 were typical of the other tests. Considering the pore water volume change versus time curve, it was noted that at first a small volume of water was expelled. This trend lasted only for the first hour at which time the overall volume change was zero. After this point, equilibrium was quickly developed and maintained for two hours. The value of moisture migration rate was obtained from this graph and was calculated as the gradient of the line once equilibrium had been developed. This value was then used as a point on the moisture migration versus applied load curve, from which a more complete picture of migration characteristics may be obtained.

The primary expulsion can be interpreted as a result of two factors. First the application of the cold temperature boundary condition caused the temperature of the soil close to the boundary to cool very rapidly. In time the pore water temperature dropped below the freezing point, however

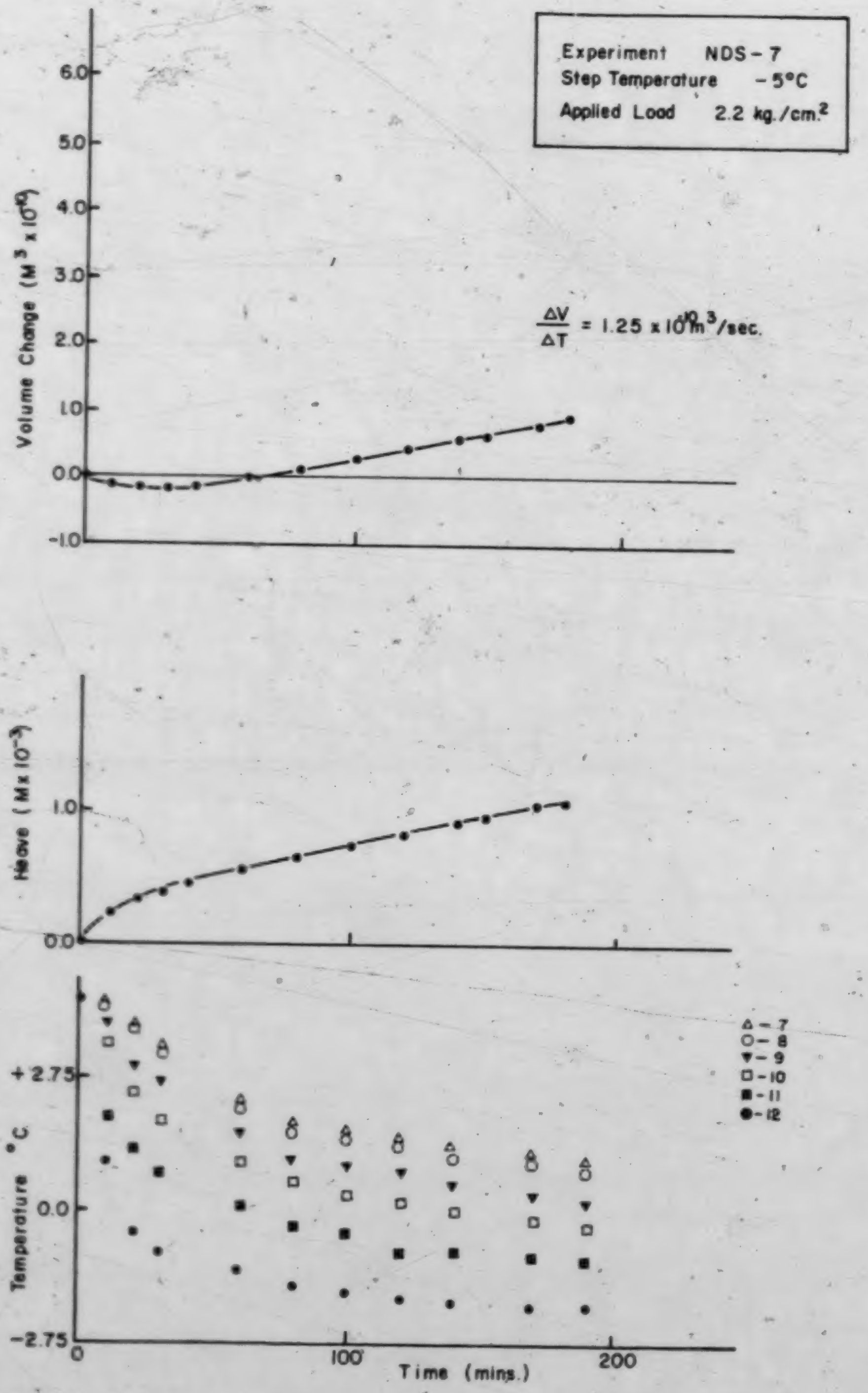

Fig. 4.1 Sample Experimental Results NDS 7

nucleation did not occur immediately, as explained in Chapter 2,and the soil matrix close to the boundary continued to cool. At this point there were no excess pore pressures, since to generate these nucleaction or volume change due to phase change is necessary. As nucleation occurred the frost front propagated rapidly through the soil matrix that had been supercooled, which caused a distinct volumetric increase at the base of the sample. The resulting upward force against the applied load generated a pulse of excess pore pressure which immediately expelled some water and hence the pore pressure dissipated. However due to nucleation, suctions were being generated at the frost front resulting in a change of direction of moisture flow, i.e. the sample started to suck in water.

The heave versus time curve for NDS-7 had a very slight curvature. Heave due only to segregated ice plotted as a straight line due to the constant rate of water inflow,however the non-linear advance of the frost front, and the corresponding non-linear heave due to freezing of in-situ water induced this curvature into the total heave behaviour. The heave rate was taken as the slope of the heave versus time graph once stability had been achieved.

The temperature data from the strip chart recorder was plotted as in Fig 4.1. From this data a graph of depth of penetration of the zero degree isotherm versus the square root of time was plotted and the rate of advance of the frost front calculated. A slight time lag between the true sample temperature and that measured by the thermocouples due to the insulating effects of the membrane and grease was inevitable. It was felt that this was a minor source of error, since the frost front was moving sufficiently slowly that a lag of one minute would have a negligible effect on the calculation of freezing rate.

After termination of the experiment, the apparatus was disassembled and the sample removed for visual inspection. The presence or absence of ice was noted, and then the sample moisture content and void ratio for both before and after the experiment was calculated. The void ratio against effective stress curve for the sample material is given in Fig 4.2.

4.2 Results of Series NDS

The moisture migration, heave, and temperature characteristics of the experiments in Series A are presented in Figs A.1 to A.13 (Appendix A) and are summarized in Table 4.1.

The dependence of moisture migration rate on applied load is shown in Fig A.1. The load at which zero flow rate in or out of the sample occurred was 3.1 Kg/cm². All the data points lie within acceptable limits ,however, experiments NDS-8 and NDS-9 experienced problems with temperature control of the room and the coolant bath. In

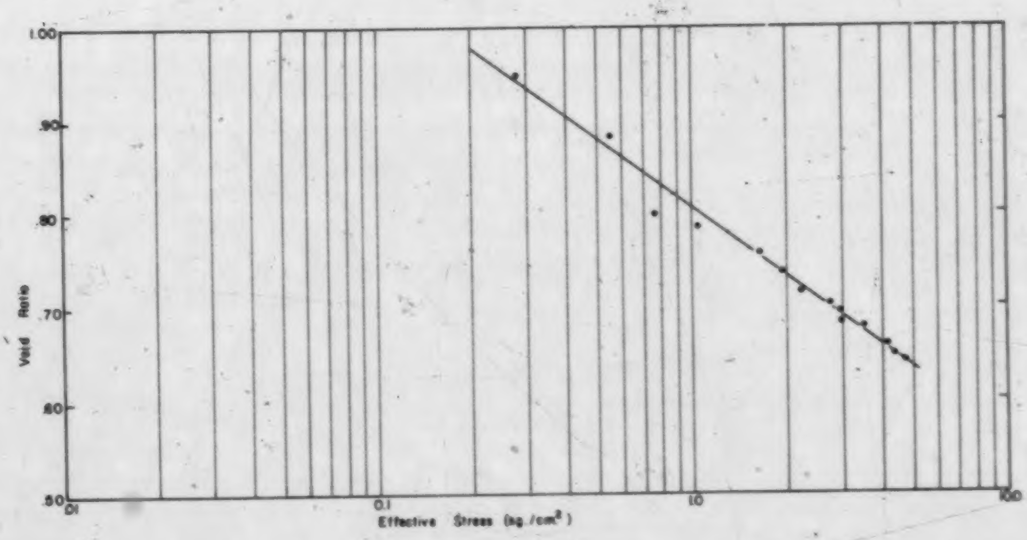

Fig. 4.2 Void Ratio v's Applied Load

Results of Series NDS

STEP TEMPERATURE = -5°C					
EXPERIMENT	APPLIED LOAD	α THERMO-COUPLE	α THEORY	HEAVE RATE	PORE WATER VOL. CHANGE
—	kg./cm^2	M/$\sqrt{\text{sec.}}$	M/$\sqrt{\text{sec.}}$	m./sec.	m^3/sec.
NDS-1	0.28	2.74×10^{-5}	3.78×10^{-5}	9.50×10^{-8}	6.00×10^{-10}
NDS-2	0.55	3.90 "	3.90 "	1.42×10^{-7}	5.42 "
NDS-3	0.78	2.80 "	4.00 "	1.22 "	5.42 "
NDS-4	1.05	2.80 "	3.90 "	1.01 "	4.42 "
NDS-5	1.66	2.85 "	3.90 "	9.00×10^{-8}	2.37 "
NDS-6	1.93	3.36 "	4.00 "	7.69 "	1.91 "
NDS-7	2.20	3.80 "	4.07 "	7.56 "	1.25 "
NDS-8	2.72	3.60 "	4.10 "	5.84 "	0.81 "
NDS-9	2.95	———	4.14 "	5.55 "	0.70 "
NDS-10	3.50	4.30 "	4.10 "	4.76 "	- 0.22 "
NDS-11	4.20	3.36 "	4.20 "	3.32 "	- 0.33 "
NDS-12	4.815	———	4.25 "	2.50 "	- 0.42 "

Table 4.1

spite of the premature termination of these experiments a value of was obtained but used with caution.

In the low stress range (0-2.5Kg/cm²) the rate of moisture migration is particularly sensitive to applied load yet above the shut-off pressure it is found to become asymptotic to a value approximately $0.75\text{x}10^{10}$ m^3/sec. Since overall volume expansion was almost completely restrained at these high loads, this value reflected the amount of moisture expelled from the soil voids by the expansion of in-situ water on freezing as the frost front advanced through the soil.

The temperature data was plotted as depth of penetration against the square root of time (Fig 4.3 and Fig 4.4). Freezing rates were described in terms of X where

$$X=\alpha\sqrt{t}$$

Where X = depth of frost penetration

α = a constant

t = time

values of $2.74\text{x}10^{-6}$ m/ $sec^{1/2}$ to $4.3\text{x}10^{-5}$ m/ $sec^{1/2}$ when found. Predictions using the simplified Stefan solution (Nixon 1973) of $3.78\text{x}10^{-6}$ m/ $sec^{1/2}$ to $4.25\text{x}10^{-6}$ m/ $sec^{1/2}$ were obtained. The correlation between observed and predicted was best at high applied loads because of the lower rates of moistue migration in this range, a factor not considered in the development of the Stefan solution.

B tests to ensure full load transfer to the sample were

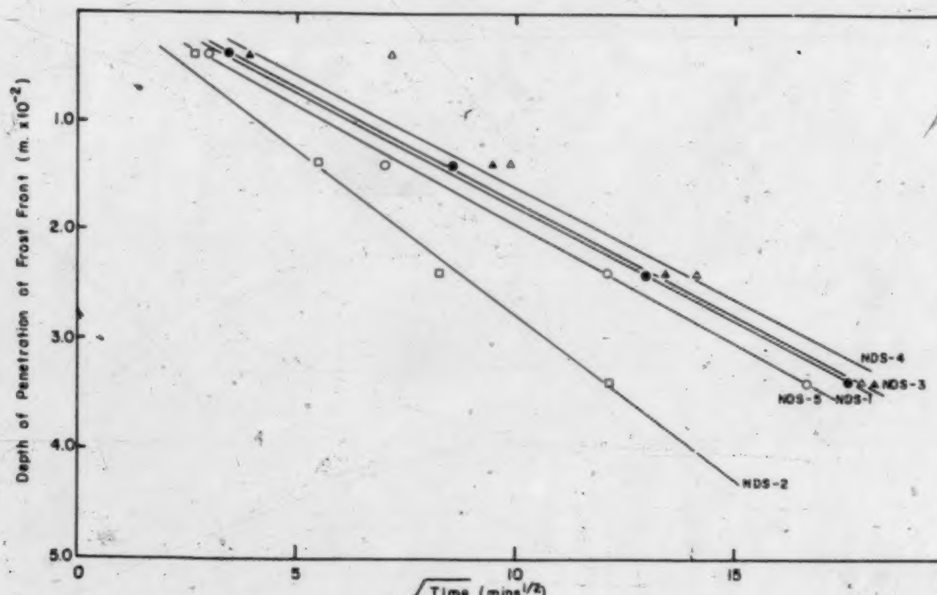

Fig. 4.3 Thermal Data NDS 1 - NDS 6

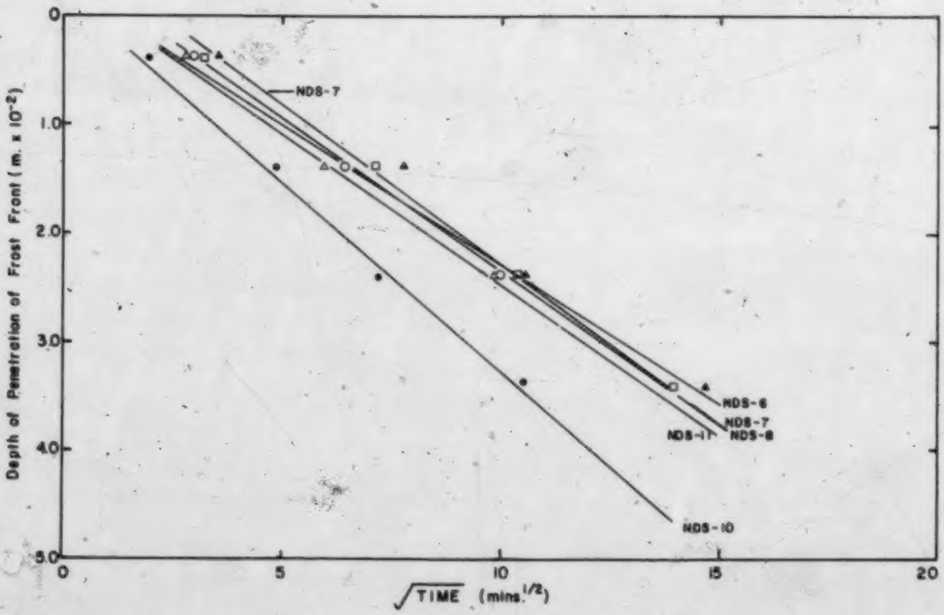

Fig. 4.4 Thermal Data NDS 7 - NDS 12

carried out in test NOS 6 before and after application of some of the load increments. $\bar{B}$ values of unity were obtained (Figs 4.5 and 4.6) showing that full load transfer was being achieved and that the samples were completely saturated.

The total heave rate in each experiment decreased with increased applied load due to the reduced rate of water migration. Heave due to freezing of in situ moisture was approximately constant in each experiment since the rate of advance of the frost front was similar in all the tests.

Visual inspection of the samples after disassembly of the apparatus was carried out, and it was noted that the occurrence of segregation ice lenses, both horizontal and vertical, were more evident in the low applied load samples (Plate 1). The thickness and spacing of the horizontal lenses varied along the length of the sample. Close to the base plate where the velocity of the frost front was relatively high, the lenses were thin and barely visible. The lenses became progressively thicker and farther apart with increasing distance from the cold side boundary. The increased thickness and spacing is caused by the difference between the rate of advance of the frost front and the rate of ice lens growth, which is limited by moisture availability, i.e. if the frost front passed rapidly through a soil element as in the case of the soil close to the cold boundary, that element would be unable to suck in an appreciable amount of moisture during the interval required

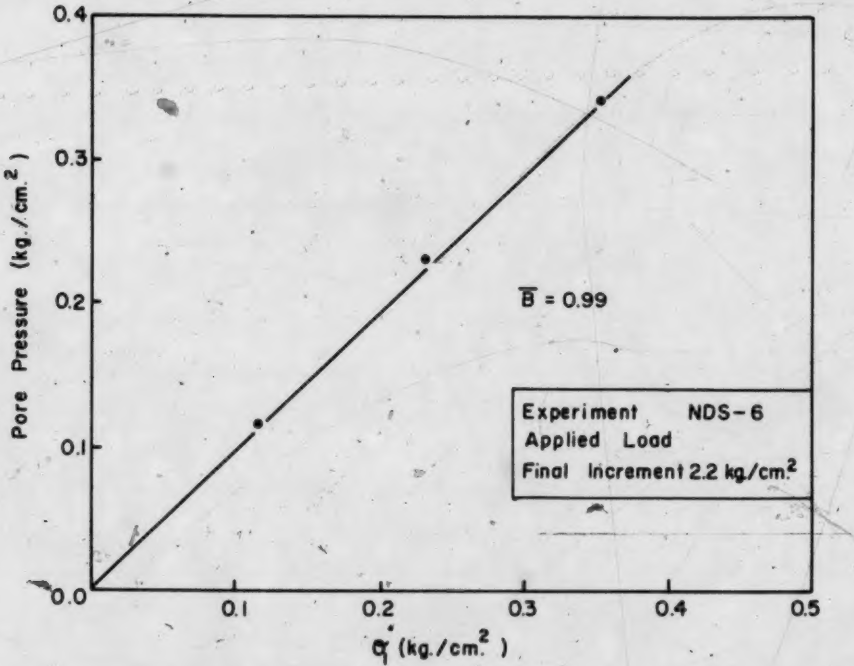
Pore Pressure (kg./cm.^{2})
0.0
0.1
0.2
0.3
0.4
0.1
0.2
0.3
0.4
0.5
σ_1 (kg./cm.^{2})
$\overline{B}$ = 0.99
Experiment NDS-6
Applied Load
Final Increment 2.2 kg./cm.^{2}

Fig. 4.5

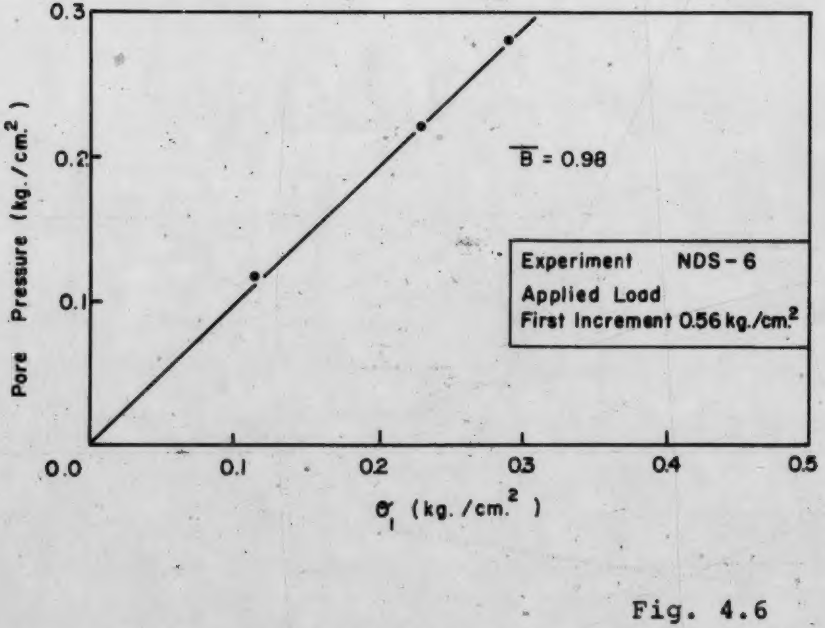
Pore Pressure (kg./cm.^{2})
0.0
0.1
0.2
0.3
0.1
0.2
0.3
0.4
0.5
σ_1 (kg./cm.^{2})
$\overline{B}$ = 0.98
Experiment NDS-6
Applied Load
First Increment 0.56 kg./cm.^{2}

Fig. 4.6

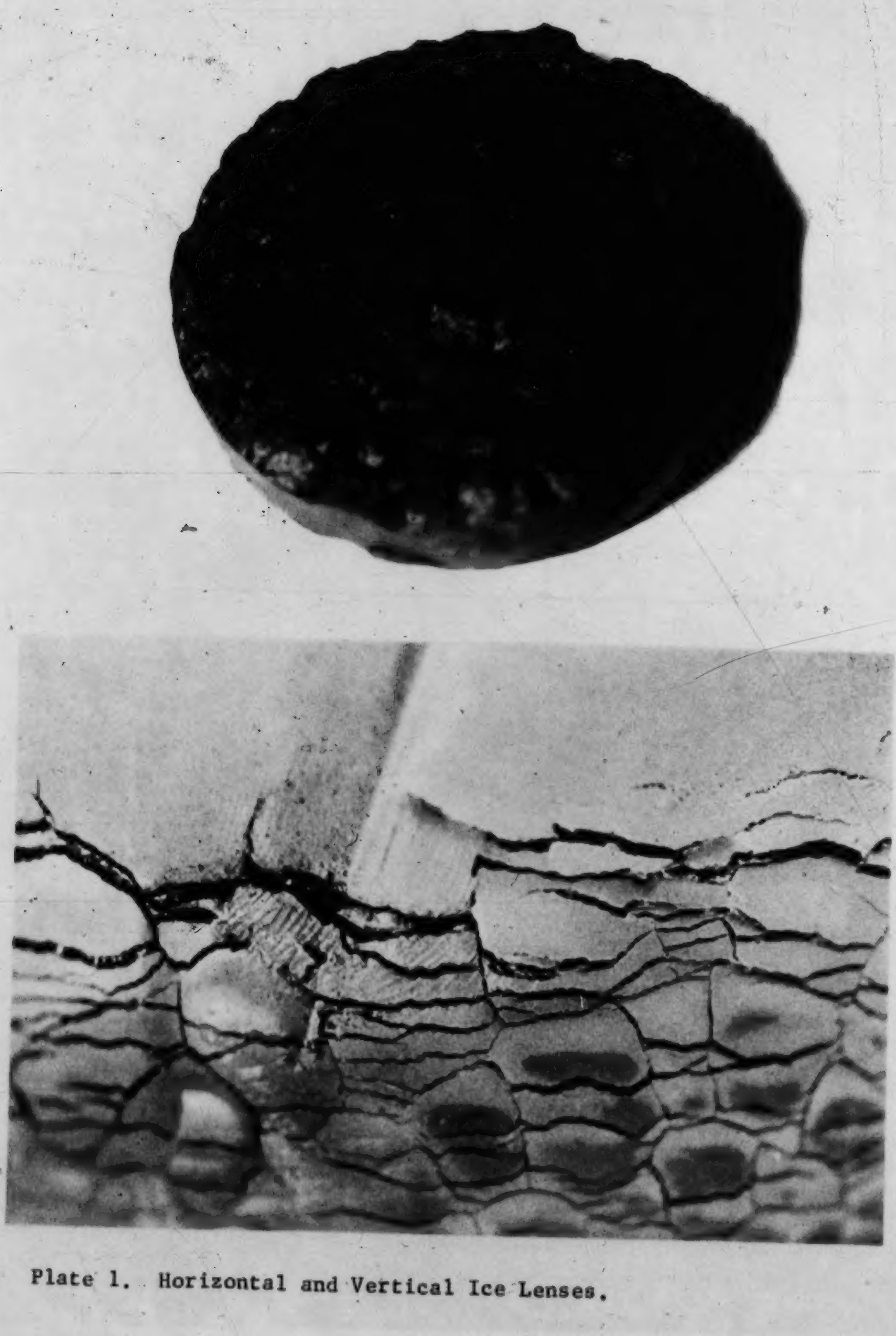

Plate 1. Horizontal and Vertical Ice Lenses.

for freezing of the element. Consequently segregated ice lens growth at this position was subdued. However as the frost front progressed through the sample and its velocity reduced, a larger volume of migrated water may enter the same volume of element in the time necessary for freezing, resulting in thicker ice lenses at depth.

Vertical lensing occurred at very low stress levels. The negative pore pressures induced by freezing had the effect of increasing the effective stress on the unfrozen soil. The soil experienced a volumetric contraction which manifested itself in the form of hexagonal tension cracks which then filled with water and subsequently froze, giving the vertical lenses, refered to by MacKay(1972) as reticulate ice forms.

With increasing load, lensing was progressively more subdued and at applied loads of 1.5 Kg/cm² or greater was barely visible at any point in the sample.

4.3 Results of Series NDS-B

Experimental results are presented in graphical form in Fig A.14 to A.20 (Appendix A) and summarized in Table 4.2. Fig A.14 summarizes the moisture migration characteristics due to a change in applied load. In test NDSL-T-1 the sample was consolidated to 5.0 Kg/cm² and freezing was permitted to continue for a much longer time period than the other tests, and an important characteristic was noticed (Fig A.19 and

Results of Series NDS-B

STEP TEMPERATURE = -2.5°C					
EXPERIMENT	APPLIED LOAD	α THERMO-COUPLE	α THEORY	HEAVE RATE	PORE WATER VOL. CHANGE
—	kg./cm.^{2}	m./$\sqrt{\text{sec.}}$	m./$\sqrt{\text{sec.}}$	m./sec.	m.^{3}/sec.
NDS B-1	0.556	1.70×10^{-5}	2.70×10^{-5}	8.33×10^{-8}	6.067×10^{-10}
NDS B-2	1.505	———	2.80 "	3.50 "	2.35 "
NDS B-3	2.76	1.80 "	2.90 "	2.05 "	1.06 "
NDS B-4	4.70	2.13 "	2.96 "	1.85 "	-0.033 "
NDS L-T-1	5.00	———	3.00 "	0.218 "	0.164 "

Table 4.2

Fig A.20). Expulsion of pore water was the primary mode of behaviour, however after 550 minutes expulsion stopped and water was attracted into the sample. This trend continued for approximately 1400 minutes (1 day) and the test was terminated after this time. This change in moisture transfer characteristics shows very clearly the limitations of the assumption that short term behaviour accurately represents the long term behaviour of a freezing soil. The long term behaviour shows that the shut-off pressure is greater than 5.0 kg/cm² however using short-term data a shut off pressure of 4.0 Kg/cm² is obtained. It is felt that the long term data exhibits the true mode of behaviour and that the moisture migration characteristics obtained in the short term tests must be interpreted with care.

On visual examination of the samples, ice lensing as described in Chapter 4.1 was noted, however the frost front had not penetrated as far into the samples as in the NDS series and consequently only the fine closely spaced lenses typical of those formed close to the cold side boundary were found.

The magnitude of total heave rate decreased with an increase in applied load reflecting the decreasing rate of moisture migration at higher stresses.

The difference between values predicted by the Stefan solution and observed values became greater at this step temperature due to the errors involved in neglecting the effects of migrated moisture and the error in assuming the initial sample temperature to be 0°C.

4.4 Results of Series NDS-C

The results of the experiments in Series NDS-C are presented in graphical form in Figs A.21 to A.28 (Appendix A) and summarized in Table 4.3. The shut-off pressure was found to be 4.2 Kg/cm². The same limitations due to the effects of short term testing apply here as in Series NDS-B.

To check the validity of the use of short duration tests for the low applied load samples, tests NDS C-1 NDS C-2 and NDS C-3 were permitted to run for 640 minutes, 640 minutes and 1420 minutes respectively, to ensure that the behaviour in the long term was consistent with that assumed from the short term tests. The long term data points fell on the projected lines (Figs A.28 A.29 and A.30) confirming this assumption.

The magnitude of the rates of migration of water are lower for a given applied load than in the previous series, the implications of which will be discussed in detail later.

In this series of experiments the frost front became stationary thus making the calculation of values meaningless and since the frost front did not pass any of the thermocouples derivation of rate of advance by this

Results of Series NDS-C

STEP TEMPERATURE = −13 °C

EXPERIMENT	APPLIED LOAD	α THERMO-COUPLE	α THEORY	HEAVE RATE	PORE WATER VOL. CHANGE
—	kg./cm^2	m./$\sqrt{\text{sec.}}$	m./$\sqrt{\text{sec.}}$	m./sec.	m^3/sec.
NDS D-1	0.555	4.26×10^{-5}	6.28×10^{-5}	2.08×10^{-7}	5.55×10^{-10}
NDS D-2	3.20	5.03 "	6.66 "	3.42×10^{-8}	0.58 "
NDS D-3	4.75	5.16 "	6.70 "	5.83 "	−0.50 "

Table 4.3

Results of Series NDS-D

STEP TEMPERATURE = −1.0°C

EXPERIMENT	APPLIED LOAD	α THERMO-COUPLE	α THEORY	HEAVE RATE	PORE WATER VOL. CHANGE
—	kg./cm^2	m./$\sqrt{\text{sec.}}$	m./$\sqrt{\text{sec.}}$	m./sec	m^3/sec.
NDS C-1	0.62	—	—	2.50×10^{-8}	2.10×10^{-10}
NDS C-2	0.95	—	—	2.47 "	1.75 "
NDS C-3	2.63	—	—	1.11 "	0.763 "
NDS C-4	4.75	—	—	0.21 "	−0.22 "

Table 4.4

method was impossible.

The total heave rates were also reduced in comparison with the previous series due to the decreased rates of moisture migration.

Lensing was noted in the samples at low applied load especially NDS C-1 which sucked in 6.0×10^{-4} m^3 to a stationary frost front, building up a comparatively thick layer of ice.

4.5 Results of Series NDS-D

The results of the experiments in Series NDS-D are presented in graphical form in Figs A.29 to A.32 (Appendix A) and summarized in Table 4.4.

The shut-off pressure was found to be 4.0 Kg/cm^2 (Fig A.29) The graph of rate of pore water volume change against applied load has the same shape as the curves obtained in the NDSA series and the NDS-B series.

The volume change against time curve in experiment NDS D-1 exhibited continuous curvature due to the very rapid advance of the frost front. Thus to obtain a value of $^{\Delta Q}/_{\Delta t}$, the gradient of the curve was taken at a time when the frost front was well inside the middle third of the sample.

Lensing was not visible in any of these samples.

The total heave rates were similar to those in the NDS

Series, in response to the similar rates of moisture migration.

Correlation between predicted and observed values is not good, ranging from 24% error to 30%. It is thought that the extreme value of step temperature applied may have caused problems such as heat conduction into the sample through the walls due to the high temperature gradient and induced these errors into the system.

4.6 Conclusions From Observations

In all of the four series of experiments, an increase in applied load was accompanied by a decrease in rate of moisture migration due to a combination of two factors.

1) A decrease in the total potential gradient of the pore water with increase in applied load,

2) A decrease in the soil permeability due to increase in applied load.

At high applied loads the moisture migration characteristics obtained from short duration tests did not not reflect the long term behaviour, as found in test NDS L-T-1. Consequently the values of shut-off pressure obtained in each series must be considered inaccurate. Hence the evidence obtained in this test program which showed that the shut-off pressure was independent of temperature distribution is inconclusive since it is felt that the true value of shut-off pressure was greater than 5 Kg/cm², and not about 4.0 Kg/cm² as indicated by the short term tests.

Comparison of the moisture migration characteristics obtained at low applied loads in short duration tests is valid, since long term testing in series C showed that the behaviour of freezing soil at low applied load remained unchanged with time. Comparison of the moisture migration rate against applied load curves for series NDS, NDS B, and NDS D show the initial portion (0 Kg/cm² to 3.0 Kg/cm²) to be identical, however the series NDS C curve falls well below these. Considering an experiment from each series at a given stress level, the permeability is the same in each case, hence the reduction in water flow in to the sample must be a result of a reduction in the suction generated at the frost front. The cause of this reduciton will be discussed in Chapter 5. These results imply that the suction generated at very low heat energy flow is small, increasing as the heat flux is increased, until a plateau value of suction, independent of heat flux, is maintained. This value of suction is probably a function of soil particle size distribution and stress history.

The magnitude of the total heave ratio obtained by measurements in each experiment and the segregational heave rate obtained from the moisture migration characteristics were plotted against applied load. (Figs 4.7 to 4.15). It is clear that both the total heave rate and the segregational heave rate were reduced by an increase in applied load. The

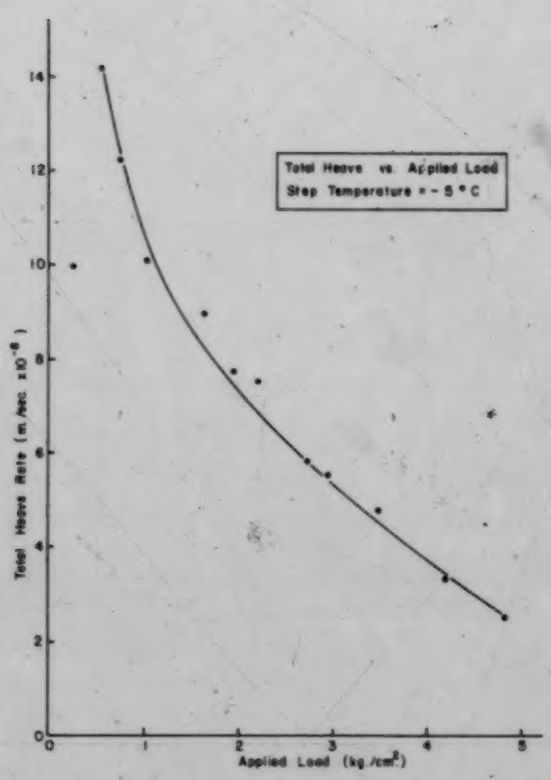
Total Heave vs. Applied Load
Step Temperature = - 5 °C
Total Heave Rate (m./sec. x10^{-8})
Applied Load (kg./cm.^{2})
0
2
4
6
8
10
12
14
0
1
2
3
4
5

Fig. 4.7

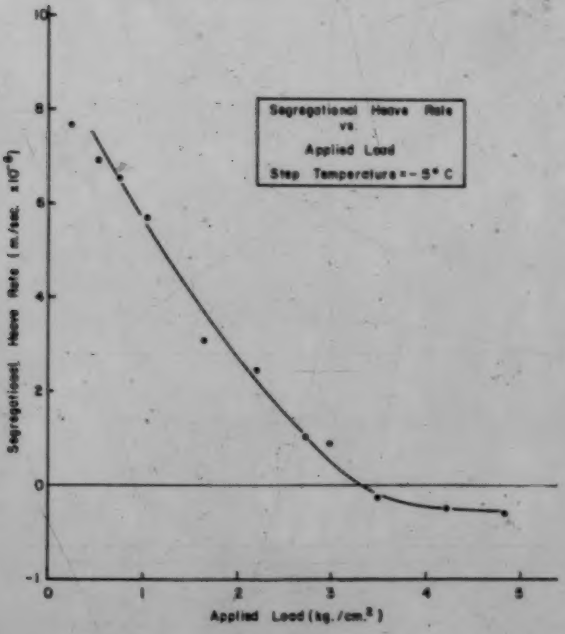
Segregational Heave Rate
vs.
Applied Load
Step Temperature = - 5° C
Segregational Heave Rate (m./sec. x10^{-8})
Applied Load (kg./cm.^{2})
-1
0
2
4
6
8
10
0
1
2
3
4
5

Fig. 4.8

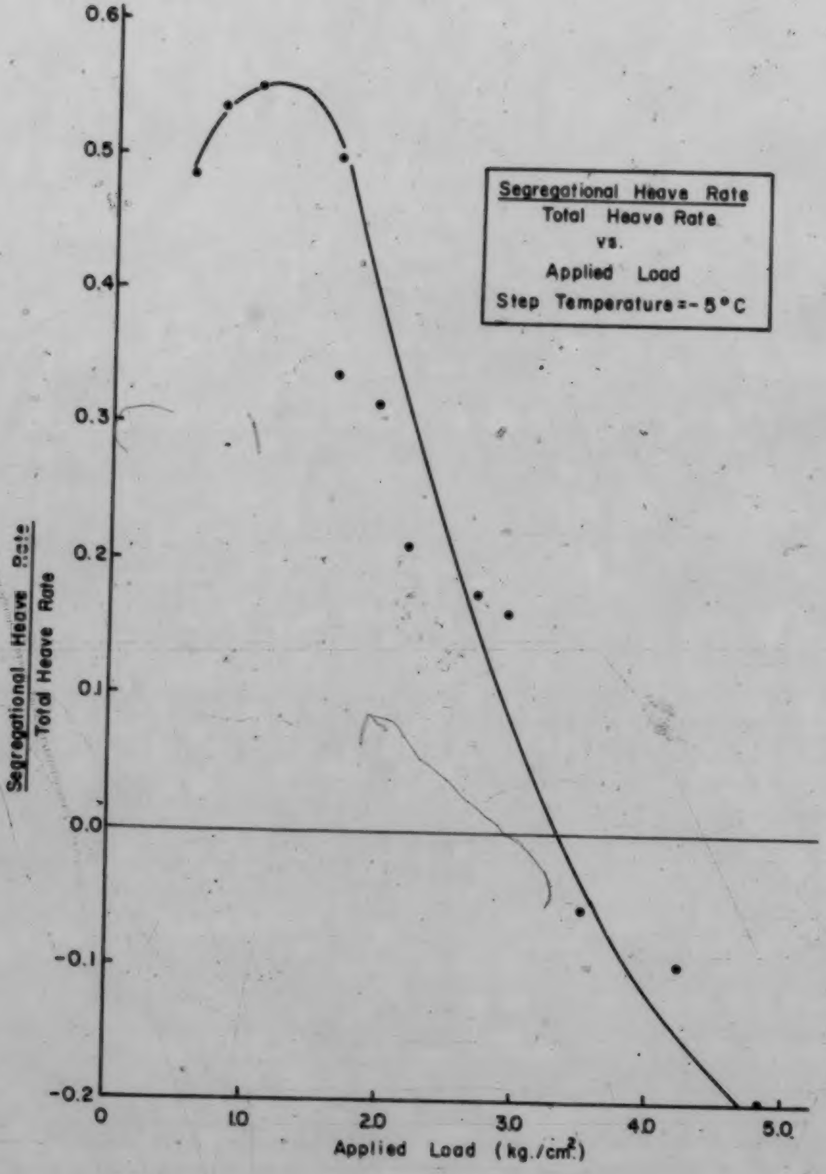

Segregational Heave Rate / Total Heave Rate vs. Applied Load
Step Temperature = -5°C
Segregational Heave Rate / Total Heave Rate
Applied Load (kg./cm.^{2})
0.6
0.5
0.4
0.3
0.2
0.1
0.0
-0.1
-0.2
0
1.0
2.0
3.0
4.0
5.0

Fig. 4.9

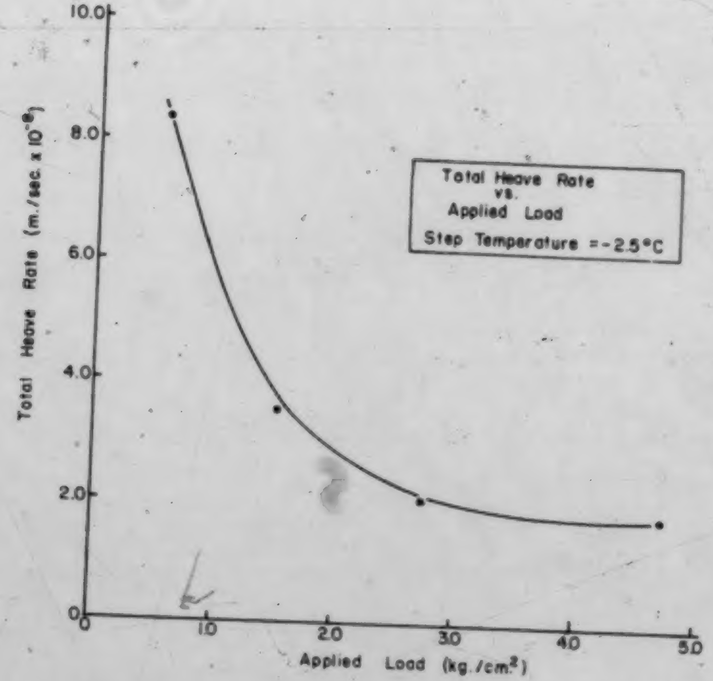

Fig. 4.10

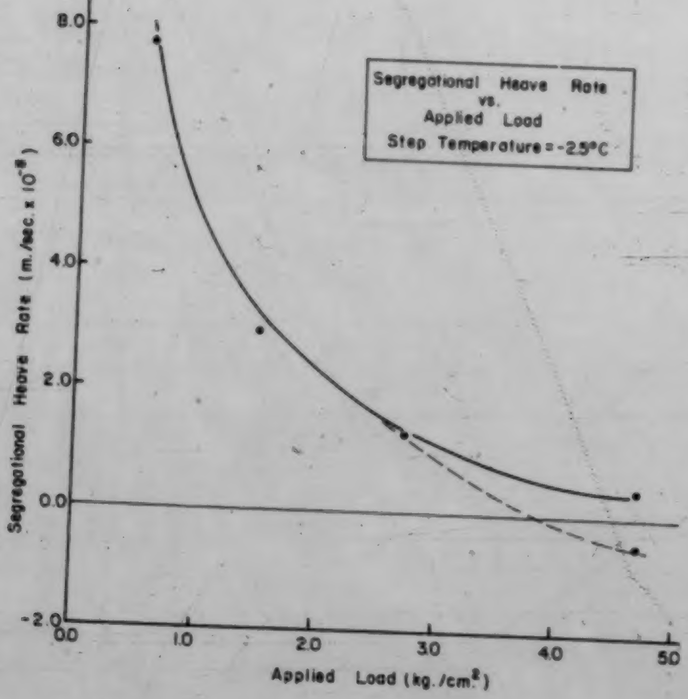

Fig. 4.11

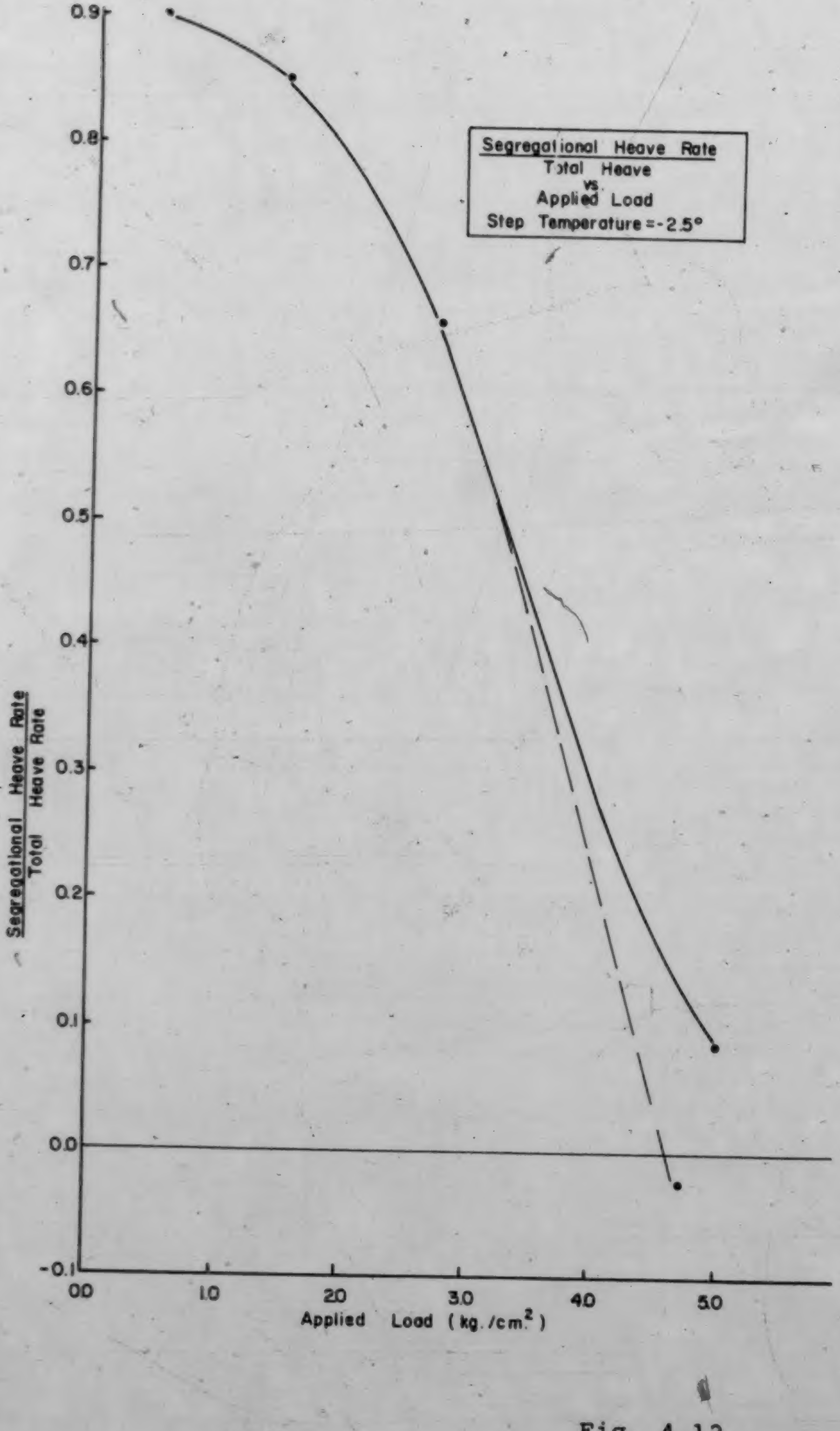
Segregational Heave Rate / Total Heave vs. Applied Load
Step Temperature = -2.5°
Segregational Heave Rate / Total Heave Rate
0.9
0.8
0.7
0.6
0.5
0.4
0.3
0.2
0.1
0.0
-0.1
0.0
1.0
2.0
3.0
4.0
5.0
Applied Load (kg./cm.^{2})

Fig. 4.12

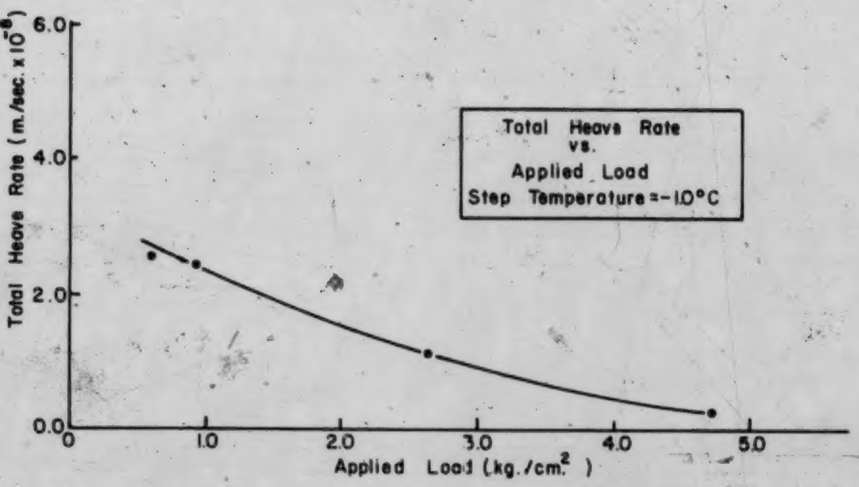

Fig. 4.13

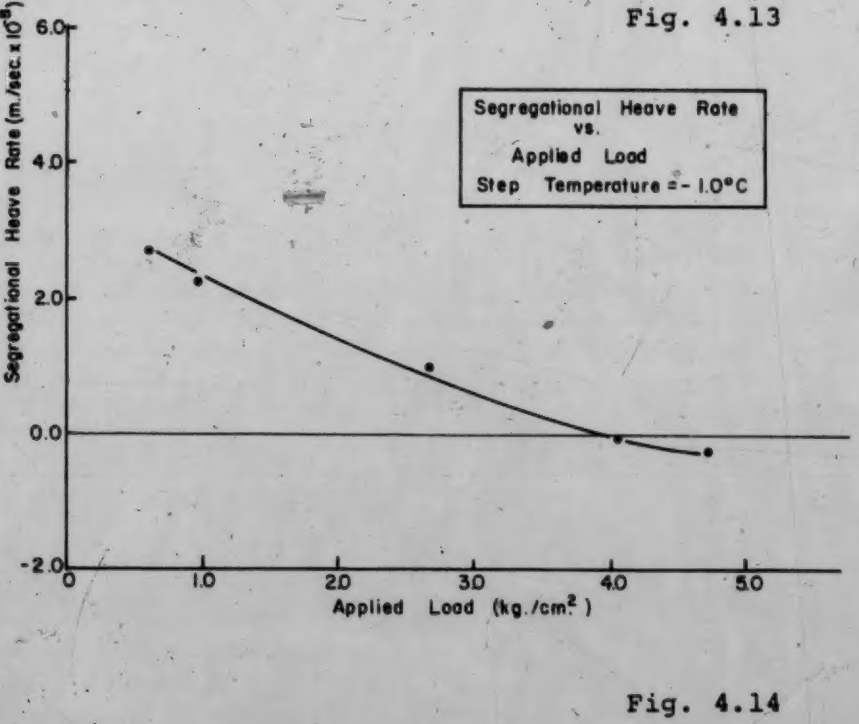

Fig. 4.14

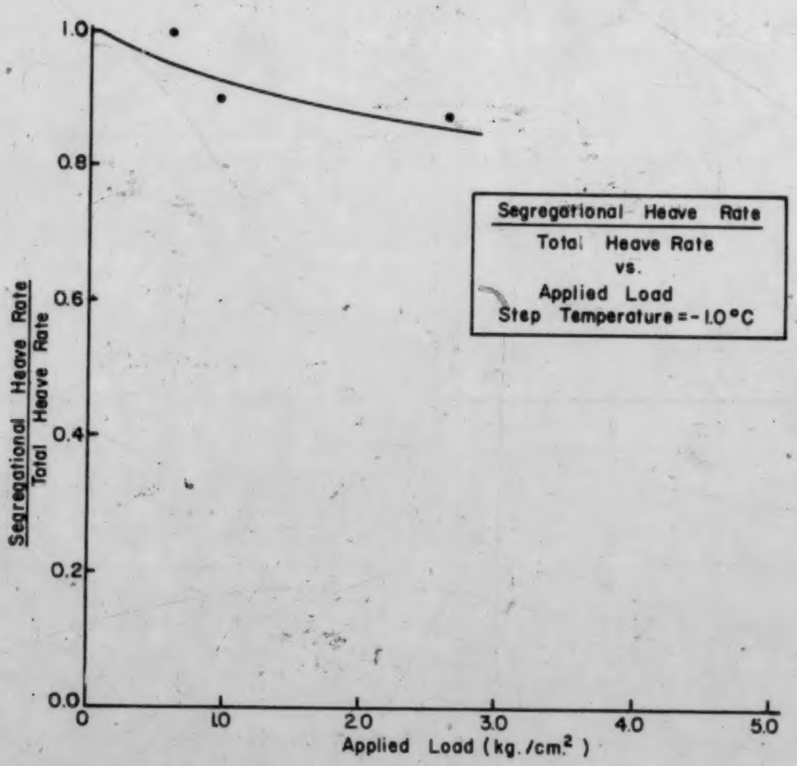
1.0
0.8
0.6
0.4
0.2
0.0
0
1.0
2.0
3.0
4.0
5.0
Applied Load (kg./cm.^{2})
Segregational Heave Rate / Total Heave Rate
Segregational Heave Rate / Total Heave Rate
vs.
Applied Load
Step Temperature = -1.0°C

Fig. 4.15

ratio of these two components of heave was also plotted against applied load. The effects of assuming the expulsion behaviour at high applied load also renders the upper portion of the curve in doubt, however it is clear that at low applied loads the ratio of segregational heave to total heave decreases with an increase in applied load. At the higher step temperatures, the ratio of the heave components is appfoaching unity which implies that fully efficient ice lensing is occurring. If this ratio is defined as the efficiency of the lensing system, the graph of efficiency against the square root of applied step temperature (Fig 4.16) shows that the efficiency of the system decreases as the advance of the frost front through the sample becomes more rapid.

4.7 Limitations of Experimental Data

The major limitation of the experimental data is the validity of the high applied load results. Experiment NDS L-T-1 demonstrated the change in behaviour between short duration and long duration testing at high stress. Consequently in any further research work the importance of the duration of the test must not be underestimated.

In the anaylsis of the test results values of suction developed at the frost front were derived indirectly from the value of moisture migration rate observed in experiments. The main limitation of this derivation is that

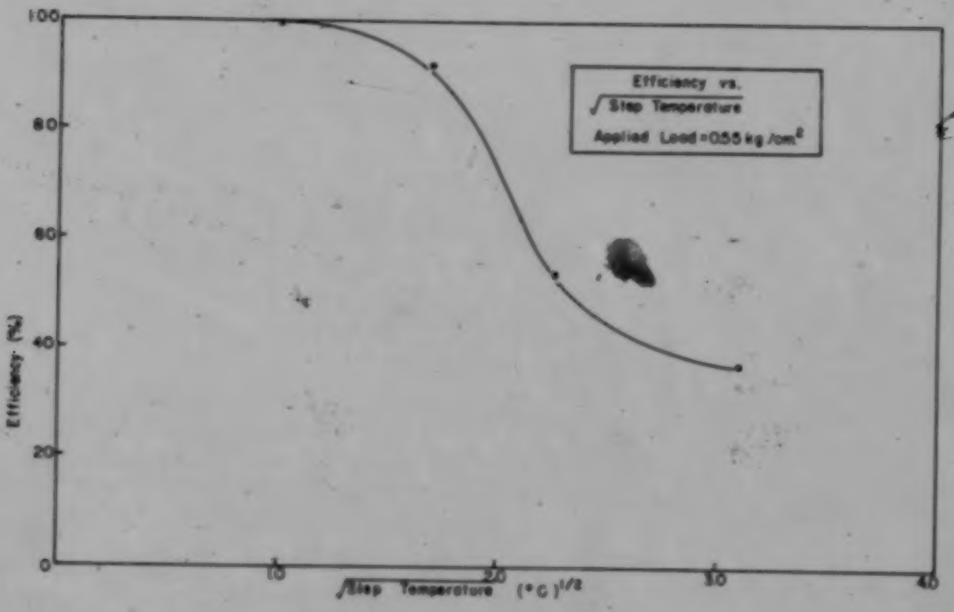

Fig. 4.16 Efficiency versus Square Root of Temperature

the value of suction calculated is very sensitive to the permeability of the soil. The determination of the permeability of the soil is in itself an inexact procedure since permeability is very sensitive to the set-up procedure and handling of the apparatus. The value of permeability used in the calculation of the suctions developed was obtained from a constant head permeability test using the Permode apparatus thus minimizing any inherent errors as much as possible.

Direct measurements of pore water pressure during freezing were not taken since it is necessary to have a closed system drainage condition for the measurement of water pressures at the end of the sample. Since the experimental program was investigating open system behaviour, and it is felt that the application of a closed system boundary condition alters the freezing conditions, these measurements were not attempted.

CHAPTER 5

ANALYSIS OF TEST DATA

5.1 Temperature Data Analysis

When subzero temperatures are applied to the surface of a soil, freezing will be induced. If the surface temperature history is known then a solution for the freezing rate and temperature distribution in the soil with time may be calculated.

If the surface temperature is held constant at some value below 0°C, then the Neumann solution (Carslaw and Jaegar, 1947) is capable of describing the rate of freezing by the equation

$$X = \alpha\sqrt{t} \qquad 5.1$$

Where X = depth of frost penetration

α = constant, depending on the thermal properties of the soil, and the ground and surface temperatures

t = time.

If the ground surface temperature varies with time, the preceding method may no longer be capable of modelling accurately the soil behaviour. For this reason a numerical solution must be adopted to determine the rate of freezing.

The governing differential equation of one dimensional conductive heat transfer from Ho, Harr and Leonards (1970) is

$$\frac{\partial \theta}{\partial t} = \frac{1}{C_o(\theta)} \cdot \frac{\partial}{\partial x}\left\{ K(\theta)\frac{\partial \theta}{\partial x}\right\} - \frac{LW\gamma_d}{C_o(\theta)} \cdot \frac{dW_u(\theta)}{dt} \qquad 5.2$$

Where θ = temperature

$C(\theta)$ = volumetric heat capacity of the soil/ice/water mixture

$K(\theta)$ = thermal conductivity of the soil

L = latent heat of the soil

W = water content

γ_d = dry density

$W_u(\theta)$ = unfrozen water content.

Writing the above in finite difference form assuming a constant discrete interval in the x-direction gives

$$\theta_{i,j+1} = A\theta_{i+1,j} - (A+B-1)\theta_{i,j} + B\theta_{i-1,j} - \frac{LW\gamma_d \quad \Delta W_u}{C_o(\theta_{i,j})} \qquad 5.3$$

Where i and j are the finite difference subscripts in the x and t directions respectively.

$$A = \frac{2\Delta t}{C_o(\theta_{i,j})(\Delta x^2)\left\{\frac{1}{K(\theta_{i+1,j})} + \frac{1}{K(\theta_{i,j})}\right\}} \qquad 5.4$$

$$B = \frac{2\Delta t}{C_o(\theta_{i,j})(\Delta x^2)\left\{\frac{1}{K(\theta_{i,j})} + \frac{1}{K(\theta_{i-1,j})}\right\}} \qquad 5.5$$

Where Co($\theta_{i,j}$) and K($\theta_{i,j}$) represent the value of those functions at the temperature $\theta = \theta_{i,j}$.

For a stable solution the inequality

$$A+B \leqslant 1$$

must be satisfied, and this limitation on the time step t is the chief drawback to this numerical method.

The input data necessary is $K_u, K_f, P, Q, H, T_s, T_g, W$

Where K_u, K_f = thermal conductivities of the fully thawed and fully frozen soil respectively.

P,Q define the unfrozen water content/temperature relationship by the equation

$$W_u = (P+\exp(Q\theta+R))/100 \qquad 5.7$$

Where R = ln(100-P)

P = represents the terminal unfrozen water content at a very low temperature as a percentage of the total water content.

Q = defines the curvature of the Wu(θ) relationship.

H = height of the soil considered

T_s and T_g are the surface and ground temperatures respectively

W is water content expressed as a percentage.

The units used are centimeters, grams, seconds, and degrees

Centigrade.

A listing of the program and a sample output is given in Appendix B.

The results of depth of frost penetration against the square root of time from the computer program are presented in Fig 5.1 and Fig 5.2. These figures represent the propagation of the 0°C isotherm for various configurations of step temperature and applied load. values were calculated for each of these and compared to the α values obtained in the corresponding experiment. Figs 5.3 and 5.4 show the comparison of the values predicted with the values observed for applied loads of 0.55 Kg/cm^2 and 3.0 Kg/cm^2 respectively. Comparison of the predicted and observed is good however limitations to this development exist. As the frost front propagates through the sample and heat is extracted from the unfrozen soil a finite quantity of heat is conducted through the top piston providing an extra source of heat energy. Hence as the frost front advances through the soil the end effects become increasingly pronounced.

In the development of the governing differential equation the flow of migrated moisture was neglected since there was no composite method of predicting water flow to the frost front and its effects in the heat conduction equation. At low stresses where the volumetric flow rate of water to the frost front may be of considerable magnitude

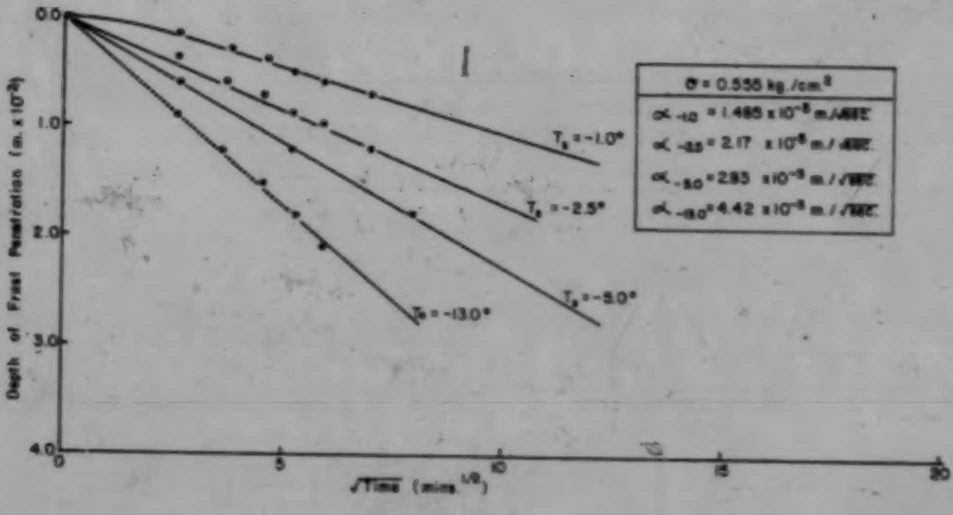
σ = 0.555 kg./cm²
α₋₁.₀ = 1.485 x 10⁻⁵ m./√SEC.
α₋₂.₅ = 2.17 x 10⁻⁵ m./√SEC.
α₋₅.₀ = 2.83 x 10⁻⁵ m./√SEC.
α₋₁₃.₀ = 4.42 x 10⁻⁵ m./√SEC.
Tₛ = -1.0°
Tₛ = -2.5°
Tₛ = -5.0°
Tₛ = -13.0°
Depth of Frost Penetration (m. x 10⁻²)
0.0
1.0
2.0
3.0
4.0
0
5
10
15
20
√Time (mins.^1/2)

Fig. 5.1

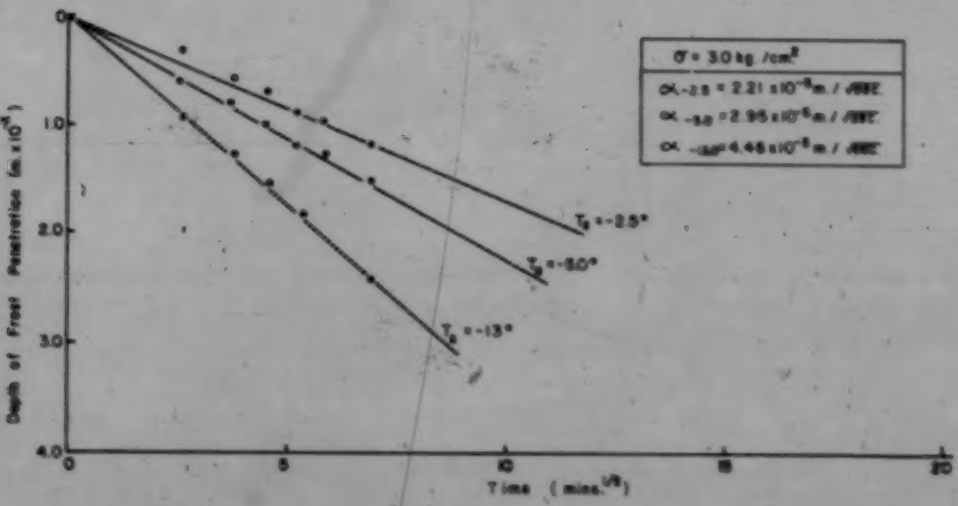
σ = 3.0 kg./cm²
α₋₂.₅ = 2.21 x 10⁻⁵ m./√SEC.
α₋₅.₀ = 2.95 x 10⁻⁵ m./√SEC.
α₋₁₃.₀ = 4.46 x 10⁻⁵ m./√SEC.
Tₛ = -2.5°
Tₛ = -5.0°
Tₛ = -13°
Depth of Frost Penetration (m. x 10⁻²)
0
1.0
2.0
3.0
4.0
0
5
10
15
20
Time (mins.^1/2)

Fig. 5.2

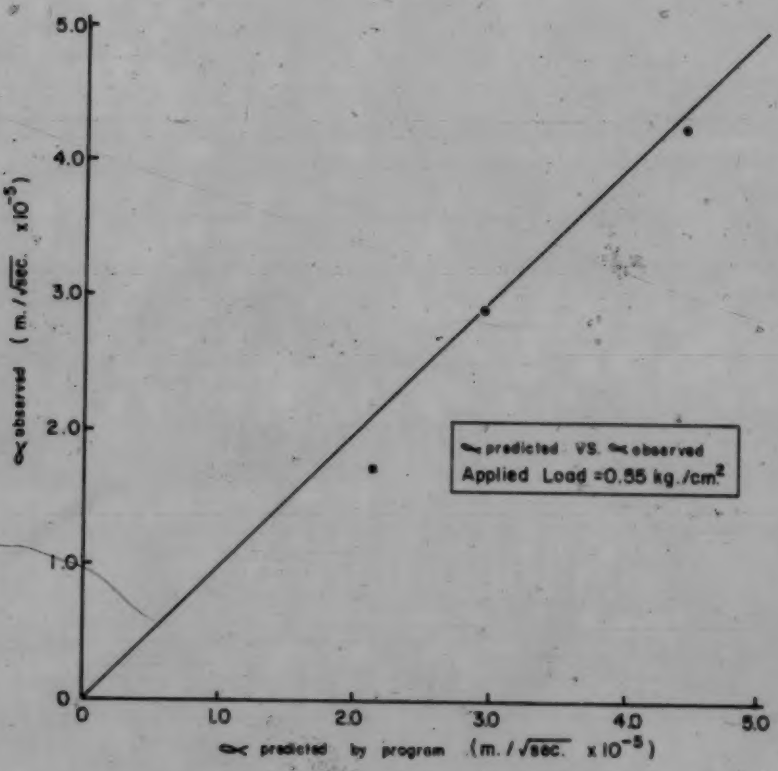
α observed (m./√sec. x10⁻⁵)
5.0
4.0
3.0
2.0
1.0
0
0
1.0
2.0
3.0
4.0
5.0
α predicted by program (m./√sec. x10⁻⁵)
α predicted VS. α observed
Applied Load =0.55 kg./cm²

Fig. 5.3

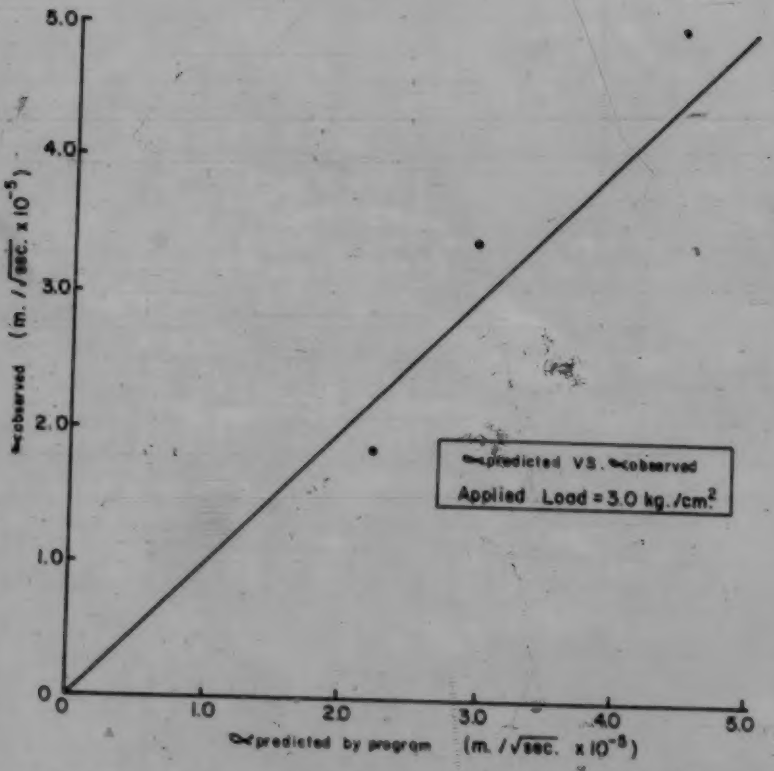
5.0
4.0
3.0
2.0
1.0
0
αobserved (m. / √sec. x 10⁻⁵)
αpredicted VS. αobserved
Applied Load = 3.0 kg./cm²
0
1.0
2.0
3.0
4.0
5.0
αpredicted by program (m. / √sec. x 10⁻⁵)

Fig. 5.4

inaccuracies will be inherent in the calculations. From the moisture migration data observed in the test program it may be noted that at lower heat flux removal rates the heat energy brought to the frost front in the form of latent heat of fusion may be sufficient to be of consideration in the heat balance equation. This is another limitation placed on the use of the program.

A combination of these factors, viz., low applied load and a small negative step temperature, may induce considerable inaccuracies and values of depth of frost penetration should be used with caution.

5.2 Pore Pressures Developed at the Frost Front

The data from the experimental program demonstrated that a potential gradient was induced through the unfrozen zone during freezing causing water to flow into the sample. The moisture migration rate was found to be a function of both applied load and heat flux removal. The affect of increasing the applied load was to decrease the rate of moisture migration. The behaviour may be interpreted in terms of two factors: 1) decreased permeability of the soil and 2) a decrease in potential gradient through the soil. As the applied load is increased the permeability of the soil decreases reflecting the decrease in void ratio. Thus even if the potential gradient through the soil was independent of applied load, the moisture migration rate would still decrease with applied load due to the effects of soil permeability alone. However, the potential gradient also varies due to a change in applied load as predicted by the Kelvin equation and demonstrated by Penner (1959). The interaction of both these factors makes investigation of the actual value of suction developed due to a change in applied load impossible, without recourse to direct measurement of suctions in experiments using special techniques.

The decrease in rate of moisture migration due to a decrease in heat removal at low step temperatures is not affected by changes in permeability since the water flow rates are compared at the same applied load. Consequently the decrease in flow rate must be solely a reflecton of a decrease in potential gradient.

From the moisture migration characteristics, values of the suction generated at the frost front may be calculated if the permeability of the soil is known. The soil structure is assumed to be incompressible, hence no moisture transfer due to consolidation will occur. The development of a constant value of suction at the frost front will induce a linear pore pressure distribution through the soil sample ie. the hydraulic gradient is a constant.

Using D'arcys law,

$$v = Ki \qquad 5.8$$

Where v = velocity of the water

K = permeability

i = hydraulic gradient

The hydraulic gradient may be back calculated and hence the suction generated at the frost front.

$$\frac{\Delta Q}{\Delta t} = KiA \qquad 5.9$$

Where A = area of sample

$\frac{\Delta Q}{\Delta t}$ = rate of moisture migration

Calculation of the magnitudes of suction developed are given in Table 5.1. These results indicate that at low heat flux the suction developed is a function of heat energy flow, however after a certain level this dependency stops and the suction reaches a maximum plateau value which cannot be exceeded. The factors limiting the magnitude of the suction are probably pore size (itself a function of the grain size distribution) and cavitation effects in the pore water. Fig 5.5 shows this behaviour in graphical form.

This is a mode of behaviour which may well embrace the findings of two previous studies. Beskow (1935) demonstrated that the heaving rate was not influenced by the rate of frost penetration however his experimental temperatures were in the range of -3°C to -10°C, confirming the 'plateau' concept deduced from this investigation. Penner (1959) showed that the heave rate was dependent on heat flux. It was demonstrated that increasing the rate of heat flow induced higher moisture migration rates and consequently higher heave rates. It is felt that the marriage of these

Test	Applied Load kg./cm.^{2}	Step Temperature °C	$\frac{\Delta Q}{\Delta T}$ m. x 10^{-10}	u kg./cm.^{2}
NDS-2	0.55	-5.0	5.5	0.27
NDS B-1	0.55	-2.5	6.06	0.30
NDS C-1	0.62	-1.0	2.10	0.15
NDS D-1	0.55	-13.0	5.55	0.279

Table 5.1 Suction Developed at the Frost Front

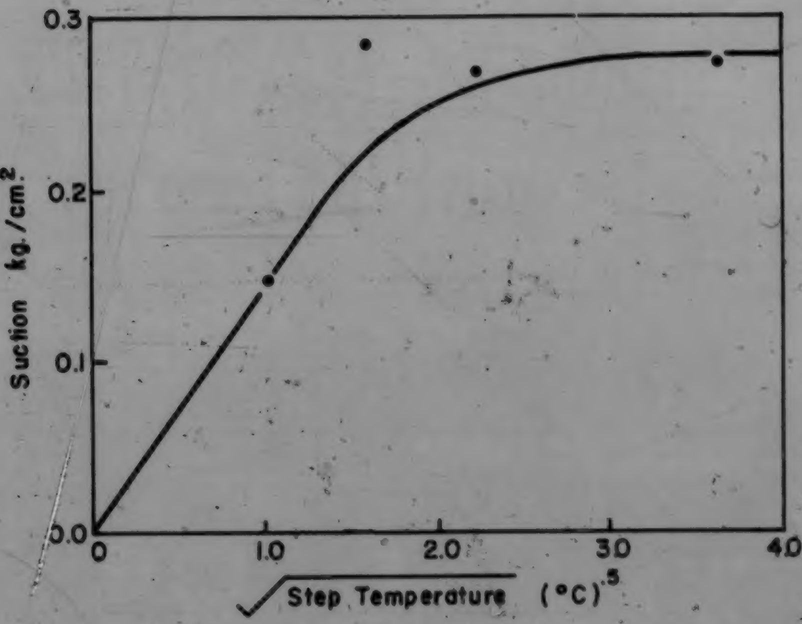

Fig. 5.5 Suction Developed at the Frost Front

two modes of behaviour may give the complete picture of the effects of heat flux.

The physical interpretation of the variance of the suction developed may be made with respect to the concept of an energy budget. At low step temperatures where the rate of heat flow is low there is a limit to the amount of water which can be attracted to the frost front. This is due to the fact that the water flowing towards the front carries a certain amount of heat energy in the form of latent heat of fusion. This heat flux is in addition to that brought to the frost front by conduction and this total cannot exceed that removed from the frost front by conduction through the frozen zone. Thus if the magnitude of heat flux removal was very low a reduction in moisture migration rate would be anticipated, and was in fact observed in the experimental program.

The validity of the linear pore pressure distribution assumption is of interest. Since the soil structure is not an incompressible medium, the pressure gradient through the sample will not be constant until a finite amount of consolidation has occurred. Also the dynamics of the frost front further complicate the problem. The effect of these factors is to introduce curvature into the suction gradient (Fig 5.6).

This curvature is most pronounced immediately after nucleation. The development of equilibrium conditions is

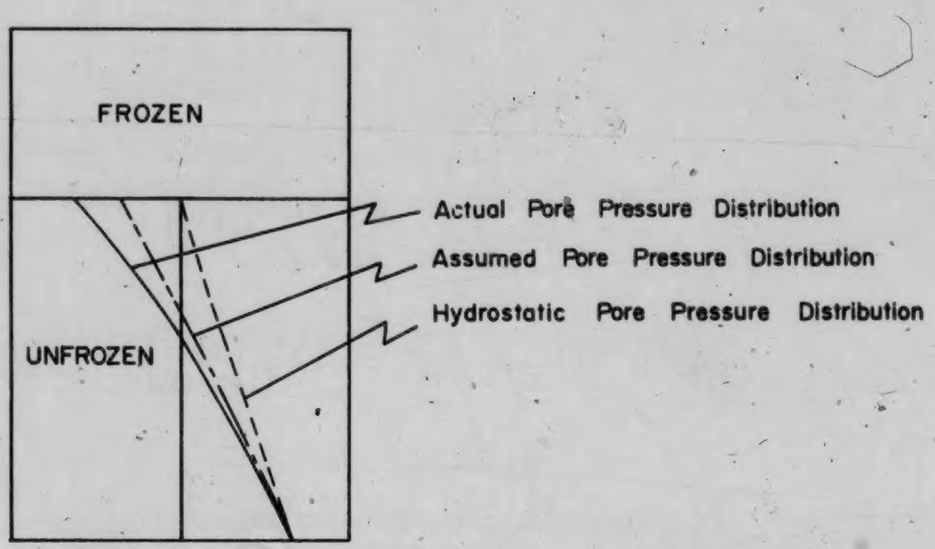
FROZEN
UNFROZEN
Actual Pore Pressure Distribution
Assumed Pore Pressure Distribution
Hydrostatic Pore Pressure Distribution

Fig. 5.6 Schematic Diagram of Pore Pressure Distribution of the Soil Sample

also hindered by the advancing frost front. As the frost front moves through the soil consolidation has to occur through the sample, and equilibrium will only be developed if the frost front remains stationary sufficiently long for dissipation of excess pore pressures to occur.

The application of a very low step temperature would cause a rapid advance of the frost front and hence would not permit the development of equilibrium conditions. Consequently a high suction gradient would exist at or near the frost front lending support to the observation of MacKay (1974) that during rapid freezing of freshly exposed fine-grained sediments in the high Arctic, water is drawn from an area close to the freezing front.

CHAPTER 6

CONCLUSIONS AND RECOMMENDATIONS

6.1 Conclusions

a) There is a relationship between the rate of moisture migration into a soil on freezing and the applied load. The rate of moisture migration falls sharply with an increase in applied load until the situation of no flow into or out of the sample occurs. The values of shut-off pressure obtained from the experimental program cannot be compared with each other since the high applied load data (greater than 3.5 Kg/cm^2) is inconclusive due to the effects of short term testing.

b) To obtain the true moisture migration characteristics at high applied loads, long duration testing must be employed since it was shown that migration behaviour may change after some time at high loads. This is thought to be the due to the effects of secondary consolidation.

c) The rate of moisture migration is a function of the rate of heat energy removal. As the rate of heat energy removal increases the rate of moisture migration also increases until a maximum 'plateau' value is reached. The suction causing this maximum value of rate of water flow is probably a function of grain size distribution and stress history.

d) The temperature distribution during freezing may be calculated using one dimensional heat conduction equations. A finite difference formulation of the equations was found to predict to a high degree of accuracy the advance of the 0°C isotherm through the soil samples.

6.2 Equipment Performance and Procedure

The apparatus, although not designed for work with freezing soils, performed well. The problems encountered with other freezing cells which employ different sealing systems were avoided by the use of the O-ring and groove construction. Leakage did not occur since the load increments applied during the consolidation phase were small. Full saturation of the soil samples was obtained using the vacuum and vibration technique,however care must be taken when placing the sample in the apparatus to avoid trapping pockets of air between the soil and the side walls of the cylinder. Friction was also virtually eliminated and full load transfer to the samples was obtained. $\bar{B}$ tests were carried out on various experiments to check for saturation and load transfer. The data obtained from the experimental program indicates that the overall performance of the apparatus was good.

Two major improvements could be made to the apparatus. The use of the thermistors set into the walls of the cylinder instead of thermocouples would give much better temperature data. At times the data obtained from the existing temperature measurement system appeared erratic and unstable, and interpolation between points where the thermal data appeared stable had to be carried out on occasions. It is felt that the increased stability and accuracy anticipated by the use of thermistors would be a major improvement. Another problem was that of supporting the slurry while the cylinder was removed during the installation of the piston. This problem may be eliminated by cutting the cylinder jackets at the required initial sample height. With this configuration the bottom portion of the cylinder may be used to support the slurry during placement. If the sample height corresponds to the top of the cylinder the piston may be installed without the necessity of removing the cylinder jacket. Having installed the piston, the upper portion of the cylinder may be placed and assembly completed.

The test procedure as set out in Chapter 3 gave good results showing the trends of behaviour due to the varying conditions of applied load and heat flux removal. There may however be some anomaly between the results obtained and the actual moisture migration characteristics at high applied loads. Although the apparatus functioned adequately it is felt that the interpretation of the results may have been incorrect in some cases. In all the experiments the duration of testing depended on the shape of the moisture migration characteristics of the experiment i.e. only after equilibrium had been developed and maintained for some time was the test terminated. In the case of the high applied load tests where the mode of behaviour was considered to be expulsion some difficulty may have arisen. In these cases the moisture migration characteristics which were assumed to have been in equilibrium may have in fact been a quasi-stable situation, i.e. in the short term the results indicated that a constant rate of expulsion had been achieved and the test was terminated, yet perhaps if the experiment had been permitted to run for a considerably longer period the mode of behaviour may have changed and water may have migrated into the sample. Thus the initial expulsion found in these tests may have exhibited such slight curvature that in the short term the moisture migration characteristics plotted as a straight line.

Another factor which may have had some affect on the high load tests was that of secondary consolidation. In each test complete dissipation of excess pore pressures was ensured by plotting the vertical compression of the soil sample against the logarithm of time. If the curve indicated that the primary consolidation was completed, freezing of the sample could then be commenced. Hence when freezing was first started the sample would still have been undergoing secondary consolidation. In most engineering situations the magnitude of secondary consolidation is negligible in comparison with that of primary consolidation. However in this case where the rate of pore water volume change was very small, the effects of secondary consolidation may have been comparatively important for the first 5 hours of the test, during which time the sample was trying to establish equilibrium conditions. Hence the very small volume of water expelled due to secondary consolidation may have also contributed to a misinterpretation of the short term data. Consequently the data points at high applied loads which were plotted as pore water expulsion may not be correct. It is felt that if in the long term the sample did attract water, the magnitude of the rate of pore water volume change would be very small and the trend of decreasing moisture transfer with increased applied load would be continued.

This is a point of interest in further research, however the author is confident that all the other experiments, in which the mode of behaviour was attraction, had developed true equilibrium and that short term behaviour can represent accurately the long term freezing behaviour of soils.

The problem of misinterpretation of the expulsion data does not affect the finding of lower moisture transfer rates for a given applied load due to a decrease in heat flux removal.

6.3 Recommendations

The distribution of pore pressure through the sample is of major importance in developing a comprehensive solution to the frost heave problem. The change in this distribution with time due to an advancing frost front, and the time taken for development of equilibrium conditions for a stationary frost front are of much interest. It is felt that any deformation of the unfrozen soil and the change in pore pressure distribution with time are functions of the conventional soil mechanics parameters m_v, the co-efficient of volume compressibility and C_v, the co-efficient of consolidation. If the magnitude of the suction generated at the frost front is known for a given set of conditions of applied load and heat flux removal, some method of predicting the pore pressure distribution with time may be developed.

A finite difference approach may be of help in predicting the pore pressure distribution in the non- steady state condition of an advancing frost front. Calculation of the pore pressure distribution through the sample with each time step would give a theoretical prediction which could be examined in the light of experimental findings.

LIST OF REFERENCES

Aitcheson, G. D., Russam, D. and Richards, B. G., 1965. "Engineering Concepts in Moisture Equilibrium and Moisture Changes in Soils." Moisture Equilibrium and Moisture Changes in Soils Beneath Covered Areas, Butterworths, Sydney, Australia. pp. 7-14.

Aitken, G. W., 1963. "Reduction of Frost Heaving by Surcharge Loading." Proc. 1st Int. Conf. on Permafrost, Purdue Univ., Lafayette, Indiana. pp. 319-324.

Anderson, D. M., and Morgenstern, N. R., 1973. "Physics, Chemistry and Mechanics of Frozen Ground." Proc. 2nd Int Int. Conf. on Permafrost, Yakuskt. pp. 257-288.

Anderson, D. M., 1968. "Undercooling, Freezing Point Depression and Ice Nucleation in Soil Water." Israel Jnl. Chem., Vol 6, pp. 349-354.

Arvidson, W. D. and Morgenstern, N. R., 1974. "Water Flow Induced by soil Freezing." Proc. 27th Can. Geotch. Conf., Edmonton, Alberta. pp. 137-143.

Arvidson, W. D., 1973, "Water Flow Induced by Soil Freezing." Unpub. M.Sc. Thesis, Dept. of Civil Eng., Univ of Alberta., Edmonton, Alta.

Beskow, G., 1935. "Soil Freezing and Frost Heaving with Special Application to Roads and Railroads."

Bresler, E. and Miller, R. D., 1974. "Estimation of Pore Blockage Induced by Freezing of Unsaturated Soil." Manuscript, Dept of Agronomy, Cornell Univ.

Dirksen, C. and Miller, R. D., 1966. "Closed System Freezing of Unsaturated Soil." Soil Science Soc. of America, Proc. 30 pp. 168-173.

Everett, D. H., 1961. "Thermodynamics of Frost Action in Porous Soils." Trans. Faraday Soc. 57 pp. 1541-1551.

Glasstone, S. and Lewis, D. 1964. "Elements of Physical Chemistry." 2nd Edition, Van Nostrand Co. Inc., Toronto, Ontario. pp.

Harlan, R. L., 1973. "Analysis of Coupled Heat Fluid Transport in Partially Frozen Soil." Water Resources Res., Vol. 9, No. 5. pp. 1314-1323.

Harlan, R. L., 1974. "Dynamics of Water Movement in Permafrost." Proc. of Workshop Seminar, Can. Nat. Committee, Int. Hydrological Decade pp. 69-77.

Hoekstra, P., 1966. "Moisture Movement in Soils under a Temperature gradient with the Cold Side Temperature below Freezing." Water Resource Res. 2 pp. 241-250.

Hoekstra, P., 1969. "The Physics and Chemistry of Frozen Soils." Highway Research Board, Spec. Rep. 103 pp. 78-90.

Kaplar, C. W., 1970. "Phenomenon and Mechanism of Frost Heaving." Highway Res. Rec. 304 pp. 1-13.

Loch, J. P. G. and Miller, R. D. 197. "Tests on the Concept of Secondary Frost Heaving." Manuscript.

Low, P. F., Anderson, D. M. and Hoekstra P., 1968. "Some Thermodynamic Relationships for Soils at or below the Freezing Point." Part 2 "Freezing Point Depression and Heat Capacity." Water Resource Res. 4 379-394 (Also U.S.A. C.R.R.E.L. Res. Rep. 221, Part 1.)

McGraw, R., 1972. "Frost Heaving versus Depth to the Water Table." Highway Res. Rec. 393 pp. 45-54.

McKay, J. R., 1972. "The World of Underground Ice." Annals of the Assoc. of American Geographers, Vol. 62 No. 1 pp. 1-22.

McRoberts, E. C. and Nixon, J. F., 1975. "Reticulate Ice Veins in Permafrost, Northern Canada." Discussion, Can. Geotech. Jn.. Vol. 12 pp. 159-162.

McRoberts, E. C., and Morgenstern, N. R., 1975. "Pore Water Expulsion During Freezing." Canadian Geotech. Jnl. Vol. 12 No. 1. pp. 130-139.

Miller, R. D., 1966. "Phase Equilibra and Soil Freezing." Proc 1st Int. Conf. on Peramfrost, Purdue University, Lafayette, Indiana pp. 193-197.

Miller, R. D., 1972. "Freezing and heaving of Saturated and Unsaturated soils." Highway Res. Rec. 393, pp. 1-11.

Miller, R. D., 1973. "Soil Freezing in Relation to Pore Water pressure and Temperature." Proc. 2nd Int. Conf. on Permafrost. (Yakuskt) pp. 344-352.

Nixon, J. D. 1973. "The Consolidation of Thawing Soils." Unpub, Ph.D. Thesis, Dept. of Civil Eng., Univ. Of Alberta, Edmonton, Alta.

Palmer, A. C., 1967. "Ice Lensing, Thermal Diffusion and Water Migration in Freezing Soil." Jnl. of Glaciology, Vol. 6 No. 47 pp. 681-694.

Penner, E., 1958, "Soil Moisture Tension and Ice Segregation." Highway Res. Board, Bull. 168 pp. 50-64.

Penner, E., 1959. "The Mechanism of Frost Heaving in Soils." Highway Res. Board, Bull. 225 pp. 1-13.

Penner, E., 1967. "Particle Size as a Basis for predicting Frost Action in Soils." Soils and Foundations, Vol. 8, No. 4, pp. 21-29.

Penner, E., 1967. "Pressures Developed During the Unidrectional Freezing" of water Saturated Porous Materials. Can. Geot. Jnl. Vol 4 pp. 398-408.

Penner, E., 1971. "Heave and Heave Pressures in Frozen Soils." Discussion, Can. Geotech. Jnl., Vol. 8, pp. 499-501.

Penner, E., 1972. "Influence of Freezing Rate on Frost Heaving." Highway Research Res. 393. pp. 56-64.

Roggensack, W. D., 1977. "Geotechnical Properties of Fine Grained Permafrost." Unpub. Ph.D. Thesis. Dept. of Civil Eng., Univ. of Alberta, Edmonton, Alberta. (In press)

Taber, S., 1929. "Frost Heaving." Jnl. of Geol. Vol 37 NO. 1, pp. 428-461.

Taber, S., 1930. "The Mechanics of Frost Heaving." Jnl. of Geol. 38 pp. 303-317.

Tagaki, S., 1970. "An Analysis of Ice Lens Formation." Water Resources Res., Vol 6, No. 3 pp. 736-749.

Takashi, T., Masuda, M. and Yamamoto H., 1974. "Experimental Study on the Influence of Freezing Speed upon Frost Heaving under constant Effective Stress." Manuscript, Seiken Reiki Ltd., Karawayamachi, Saubancho, Minami-Ka, Osaka, Japan.

Williams, P. J, 19 "Pore Pressures at a Penetrating Frost Line and their Prediction." Norwegian Geot. Jnl. No 72 pp. 51-72.

Wissa, A. E. and Martin, R. T., 1968. "Behaviour of Soils under Flexible Pavements, Development of Rapid Frost Susceptibility Tests." Can. Mil. Dept. of Civil Engineering, RR 68-77, Soils Publ 224.

Yong, R. N. and Osler, J. C., 1971. "Heave and Heaving Pressures in Frozen Soils." Can. Geotech. Jnl. Vol. 8 pp. 272-282.

APPENDIX A

EXPERIMENTAL RESULTS

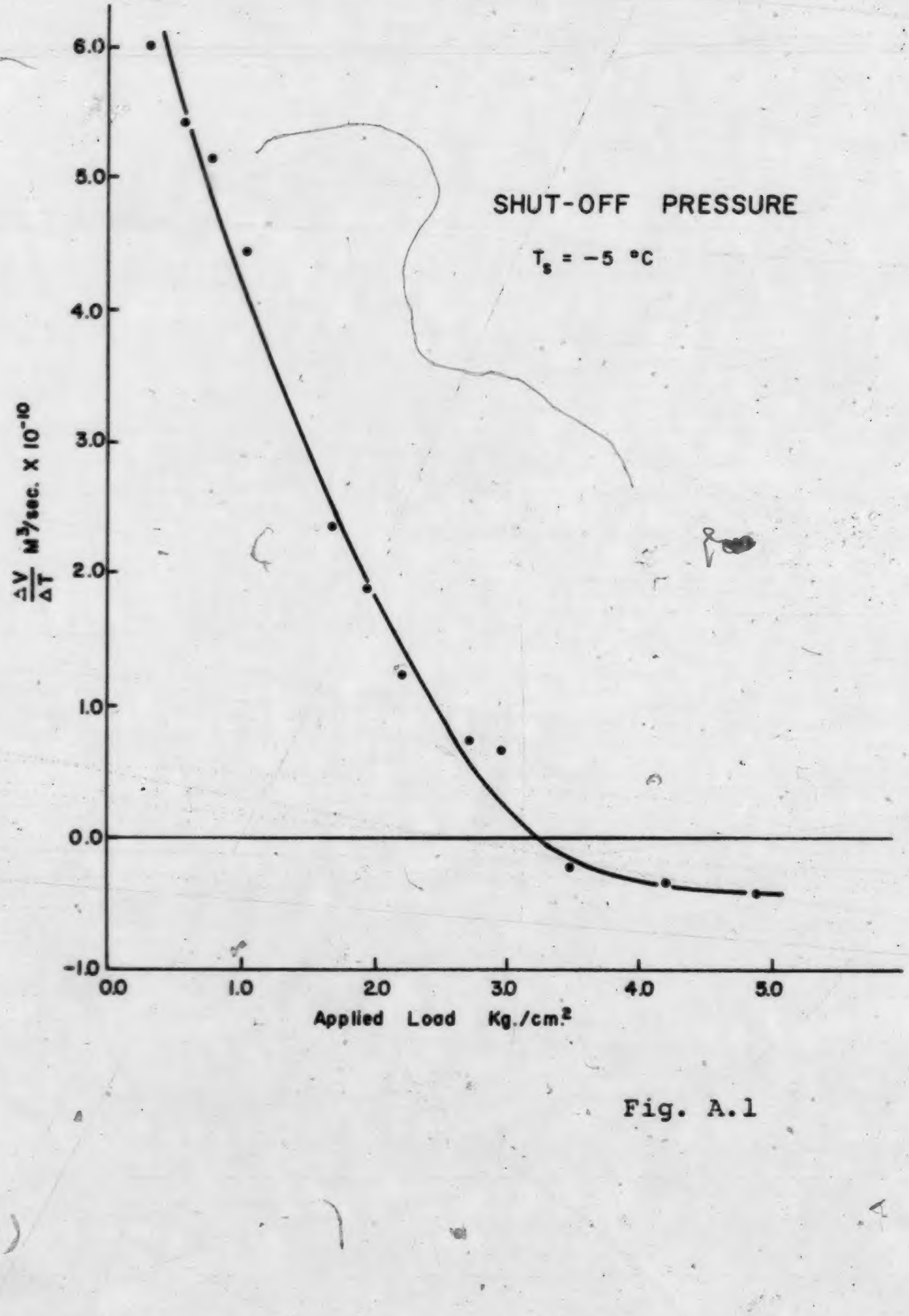
SHUT-OFF PRESSURE
T_s = −5 °C
$\frac{\Delta V}{\Delta T}$ M³/sec. X 10⁻¹⁰
6.0
5.0
4.0
3.0
2.0
1.0
0.0
-1.0
0.0
1.0
2.0
3.0
4.0
5.0
Applied Load Kg./cm.²

Fig. A.1

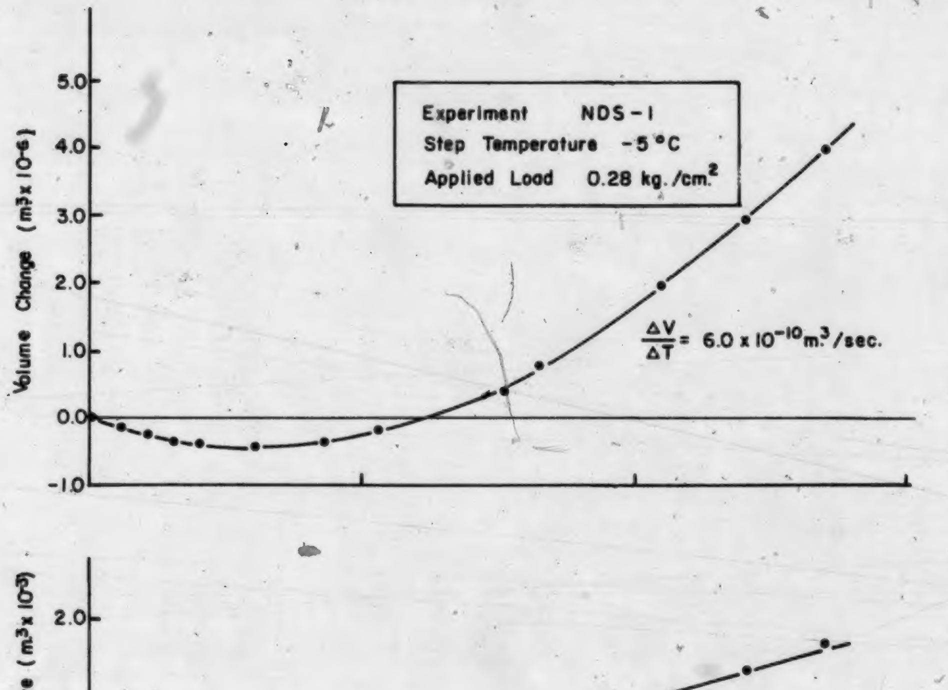
Experiment NDS-1
Step Temperature -5 °C
Applied Load 0.28 kg./cm.^{2}
$\frac{\Delta V}{\Delta T} = 6.0 \times 10^{-10} m^3/sec.$
Volume Change ($m^3 \times 10^{-6}$)
5.0
4.0
3.0
2.0
1.0
0.0
-1.0
Heave ($m^3 \times 10^{-3}$)
2.0
1.0
0.0
Temperature (°C)
△ - 7
○ - 8
▼ - 9
□ - 10
■ - 11
● - 12
2.75
0.0
2.75
0
100
200
300
Time (mins.)

Fig. A.2

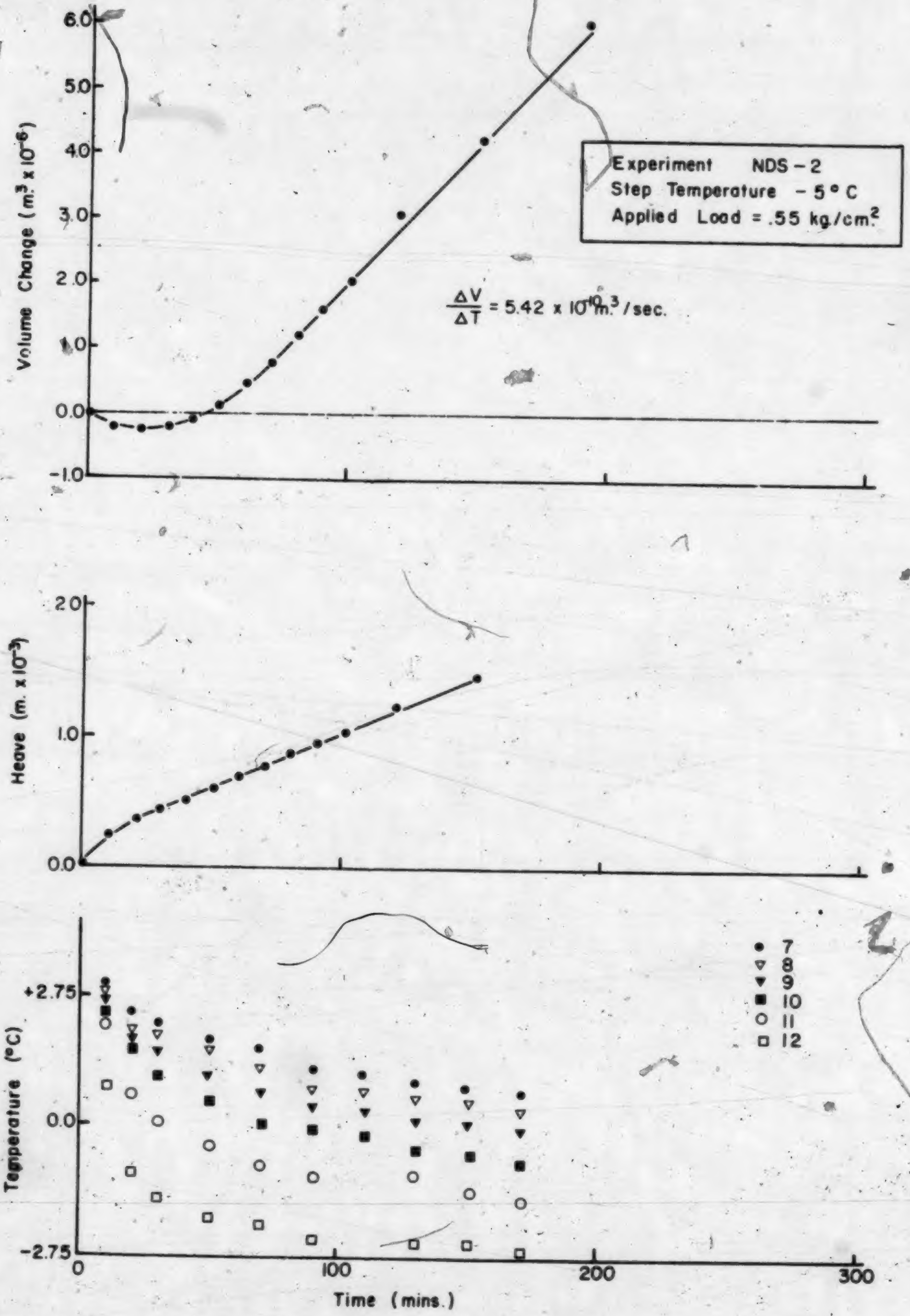
Experiment NDS - 2
Step Temperature - 5 °C
Applied Load = .55 kg/cm²
ΔV/ΔT = 5.42 x 10⁻¹⁰ m.³/sec.
Volume Change (m³ x 10⁻⁶)
6.0
5.0
4.0
3.0
2.0
1.0
0.0
-1.0
Heave (m. x 10⁻³)
2.0
1.0
0.0
Temperature (°C)
+2.75
0.0
-2.75
● 7
▽ 8
▼ 9
■ 10
○ 11
□ 12
0
100
200
300
Time (mins.)

Fig. A.3

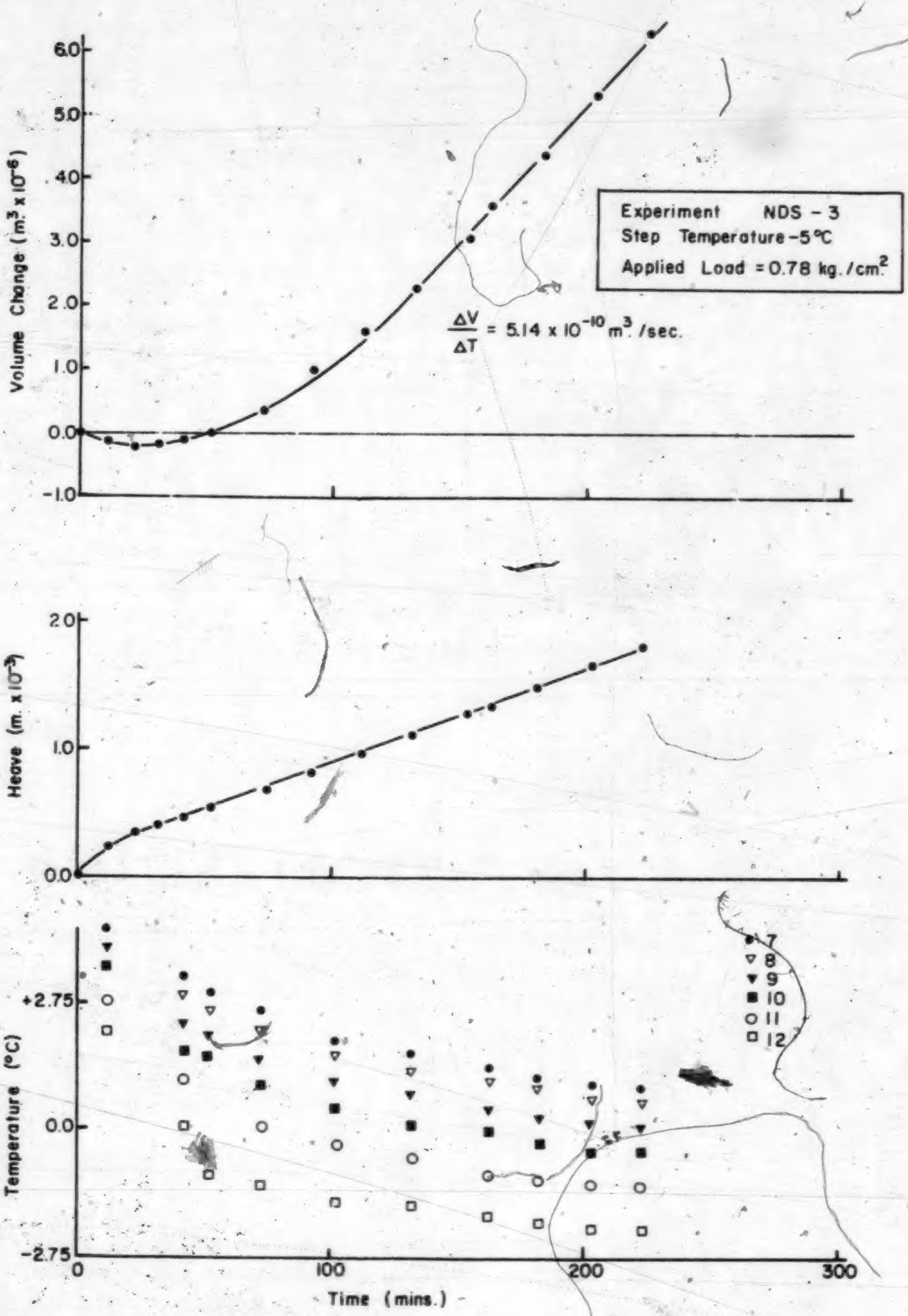
Experiment NDS - 3
Step Temperature -5°C
Applied Load = 0.78 kg./cm²
$\frac{\Delta V}{\Delta T}$ = 5.14 x 10⁻¹⁰ m³/sec.
Volume Change (m³ x 10⁻⁶)
6.0
5.0
4.0
3.0
2.0
1.0
0.0
-1.0
Heave (m. x 10⁻³)
2.0
1.0
0.0
Temperature (°C)
+2.75
0.0
-2.75
0
100
200
300
Time (mins.)
● 7
▽ 8
▼ 9
■ 10
○ 11
□ 12

Fig. A.4

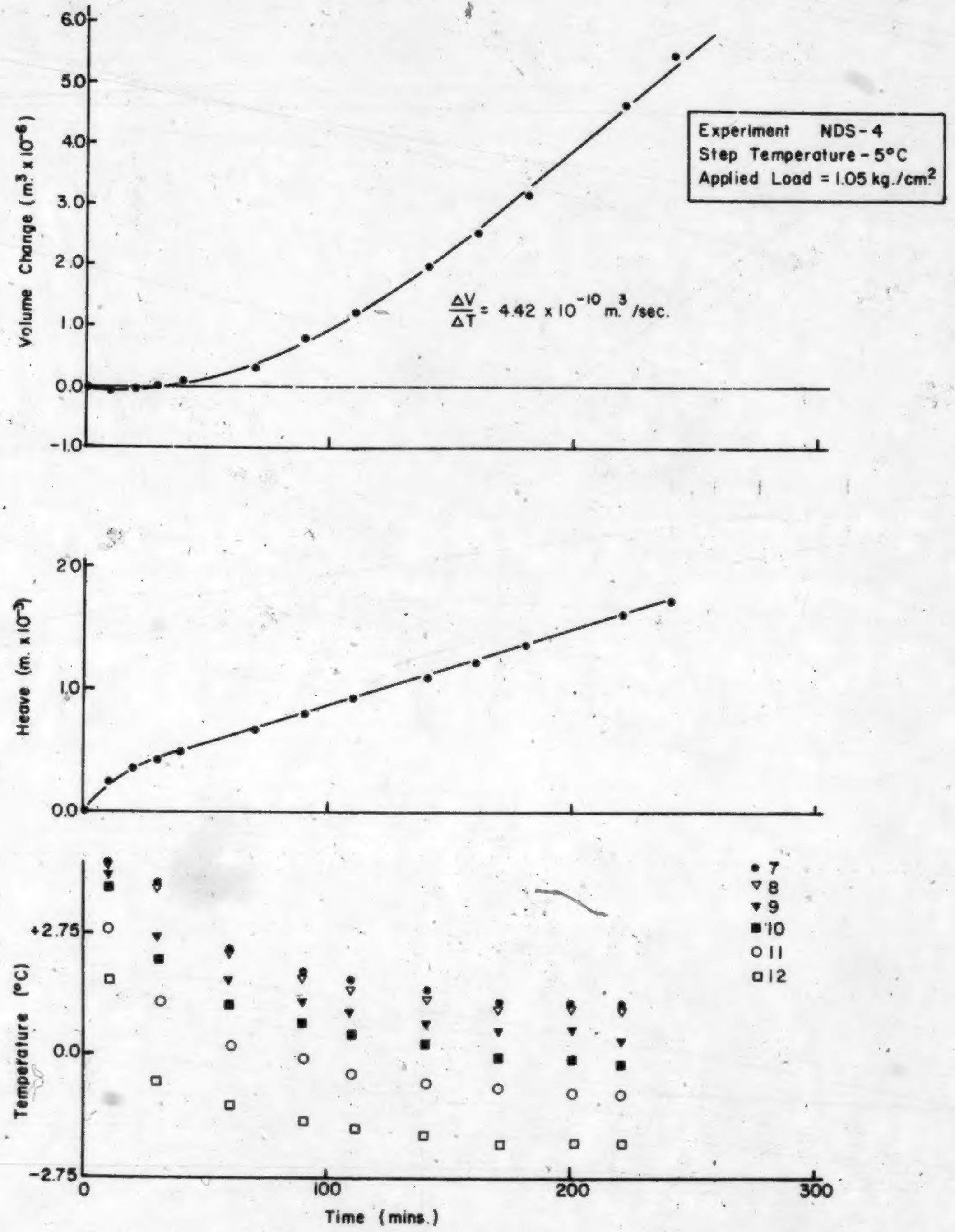
Experiment NDS-4
Step Temperature -5°C
Applied Load = 1.05 kg./cm²
ΔV/ΔT = 4.42 x 10⁻¹⁰ m.³/sec.
Volume Change (m³ x 10⁻⁶)
6.0
5.0
4.0
3.0
2.0
1.0
0.0
-1.0
Heave (m. x 10⁻³)
2.0
1.0
0.0
Temperature (°C)
+2.75
0.0
-2.75
0
100
200
300
Time (mins.)
● 7
▽ 8
▼ 9
■ 10
○ 11
□ 12

Fig. A.5

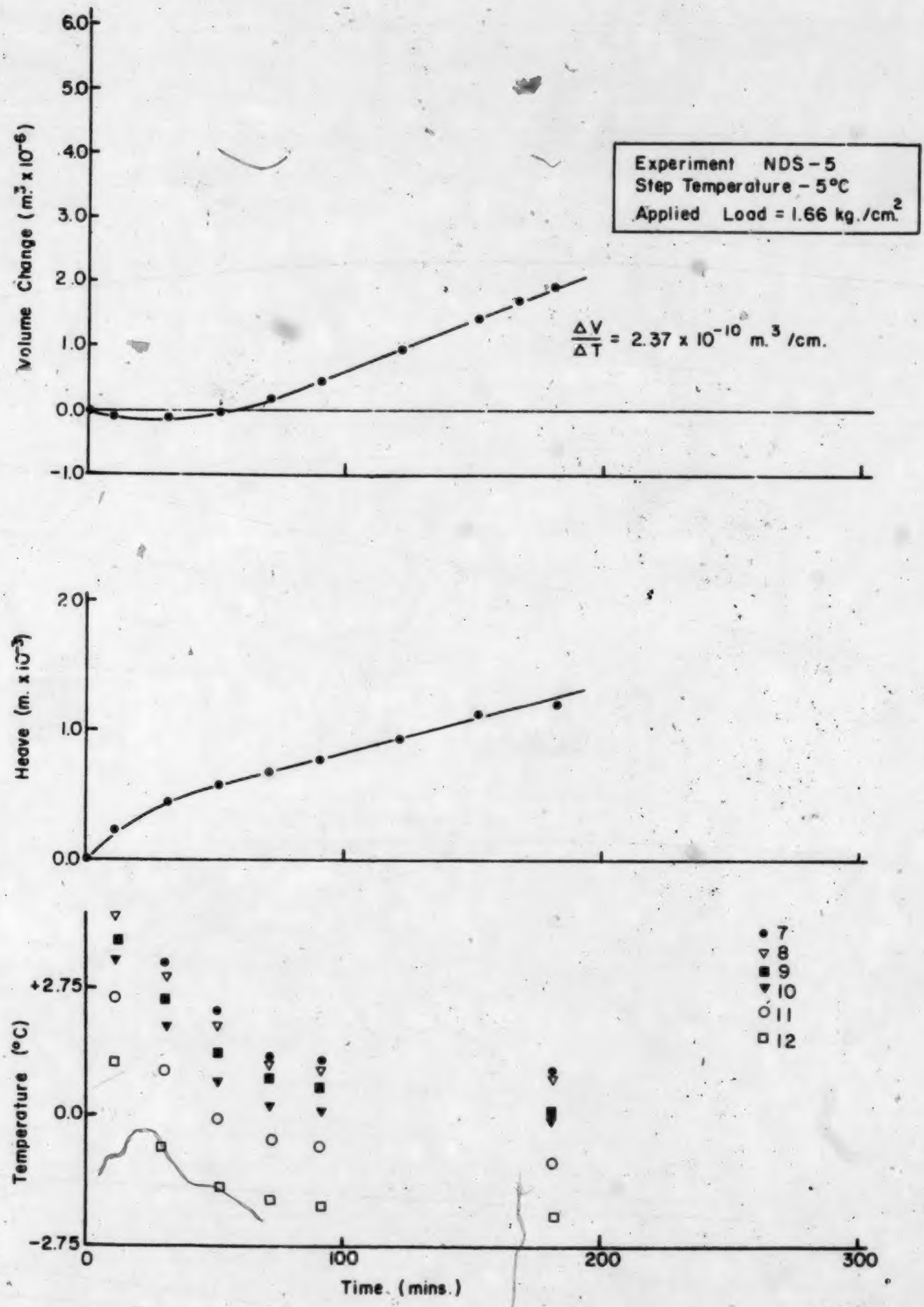
Experiment NDS-5
Step Temperature - 5°C
Applied Load = 1.66 kg./cm.^{2}
Volume Change (m.^{3} x 10^{-6})
6.0
5.0
4.0
3.0
2.0
1.0
0.0
-1.0
$\frac{\Delta V}{\Delta T}$ = 2.37 x 10^{-10} m.^{3}/cm.
Heave (m. x 10^{-3})
2.0
1.0
0.0
Temperature (°C)
+2.75
0.0
-2.75
● 7
▽ 8
■ 9
▼ 10
○ 11
□ 12
0
100
200
300
Time. (mins.)

Fig. A.6

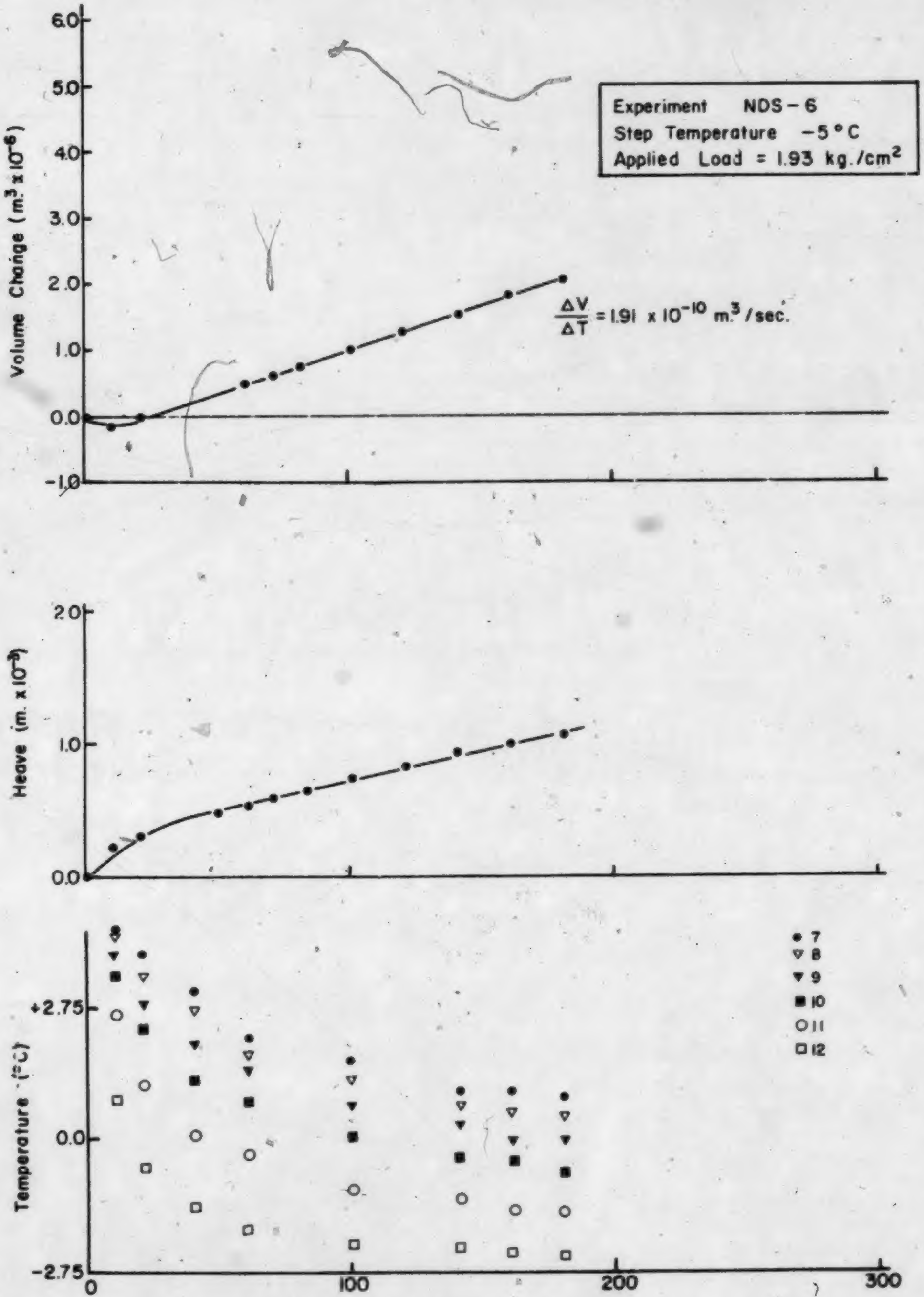
Experiment NDS-6
Step Temperature -5 °C
Applied Load = 1.93 kg./cm²
Volume Change (m³ x 10⁻⁶)
6.0
5.0
4.0
3.0
2.0
1.0
0.0
-1.0
ΔV/ΔT = 1.91 x 10⁻¹⁰ m³/sec.
Heave (m. x 10⁻³)
2.0
1.0
0.0
Temperature (°C)
+2.75
0.0
-2.75
0
100
200
300
Time (mins.)
● 7
▽ 8
▼ 9
■ 10
○ 11
□ 12

Fig. A.7

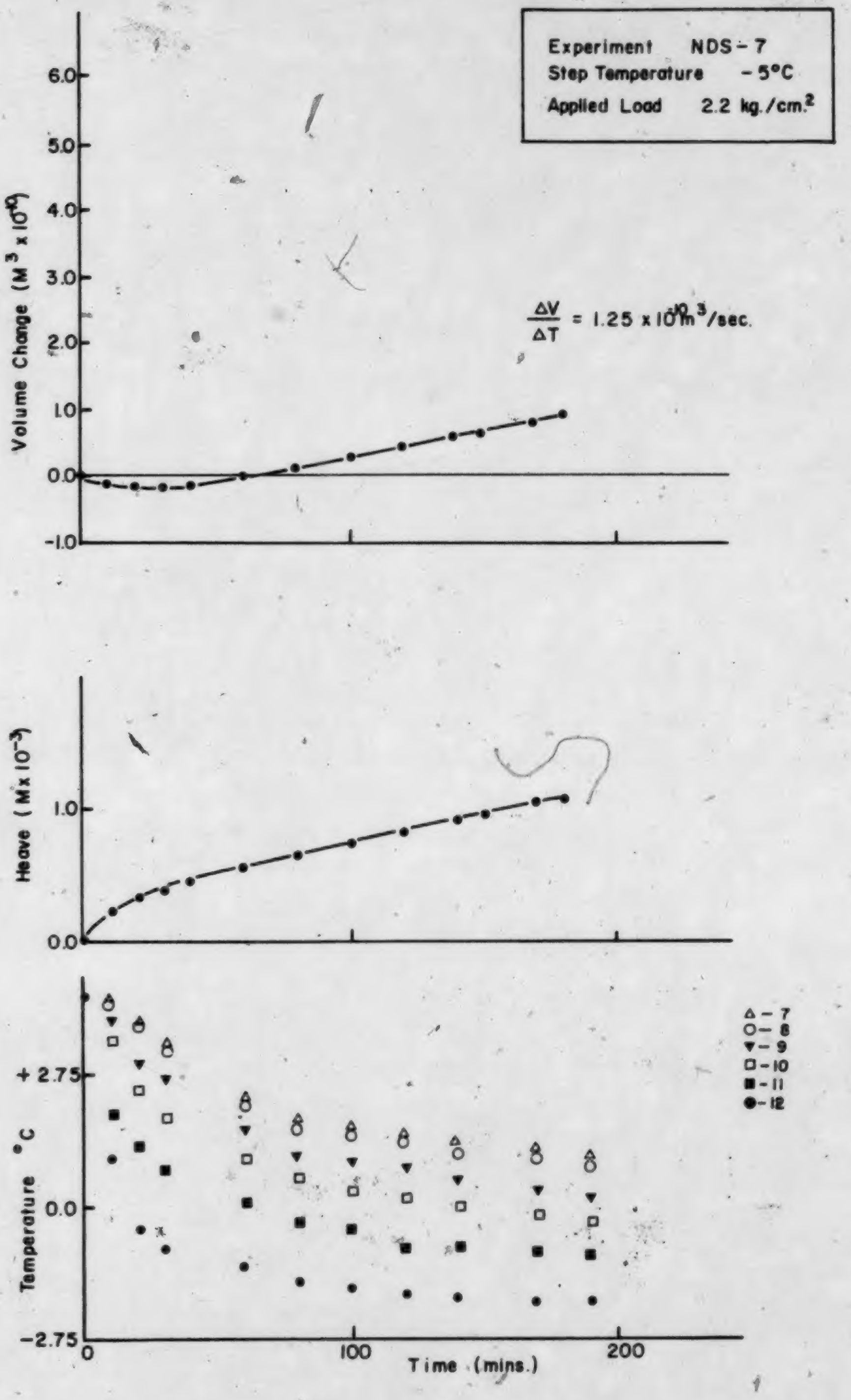
Experiment NDS - 7
Step Temperature - 5°C
Applied Load 2.2 kg./cm.^{2}
Volume Change ($M^3 \times 10^{-6}$)
6.0
5.0
4.0
3.0
2.0
1.0
0.0
-1.0
$\frac{\Delta V}{\Delta T} = 1.25 \times 10^{-10} m^3/sec.$
100
200
Heave ($M \times 10^{-3}$)
1.0
0.0
100
200
Temperature °C
+ 2.75
0.0
-2.75
0
100
200
Time (mins.)
△ - 7
○ - 8
▼ - 9
□ - 10
■ - 11
● - 12

Fig. A.8

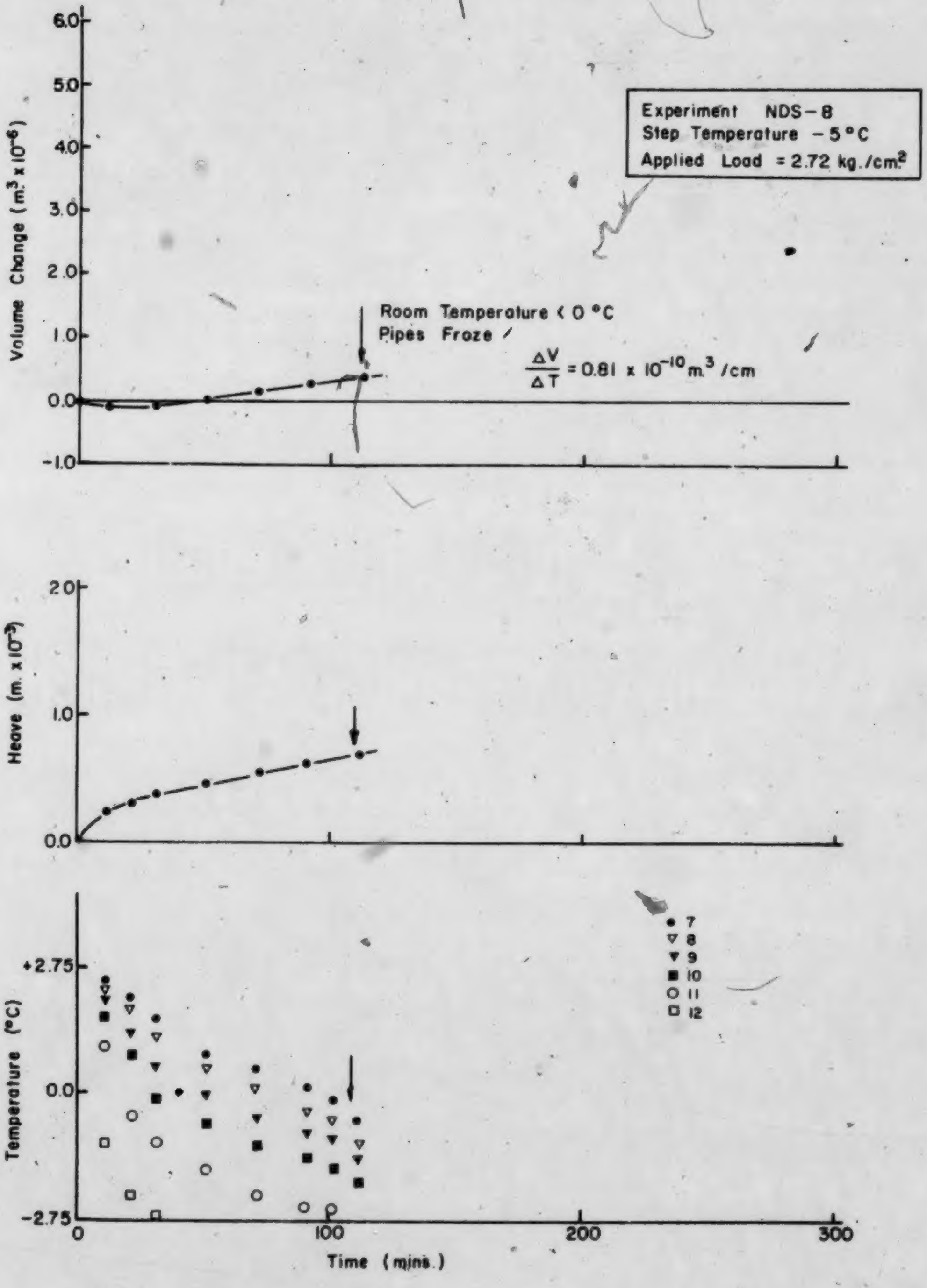
Experiment NDS-8
Step Temperature −5 °C
Applied Load = 2.72 kg./cm²
Volume Change (m³ x 10⁻⁶)
6.0
5.0
4.0
3.0
2.0
1.0
0.0
−1.0
Room Temperature < 0 °C
Pipes Froze /
ΔV/ΔT = 0.81 x 10⁻¹⁰ m³/cm
Heave (m. x 10⁻³)
2.0
1.0
0.0
Temperature (°C)
+2.75
0.0
−2.75
● 7
▽ 8
▼ 9
■ 10
○ 11
□ 12
0
100
200
300
Time (mins.)

Fig. A.9

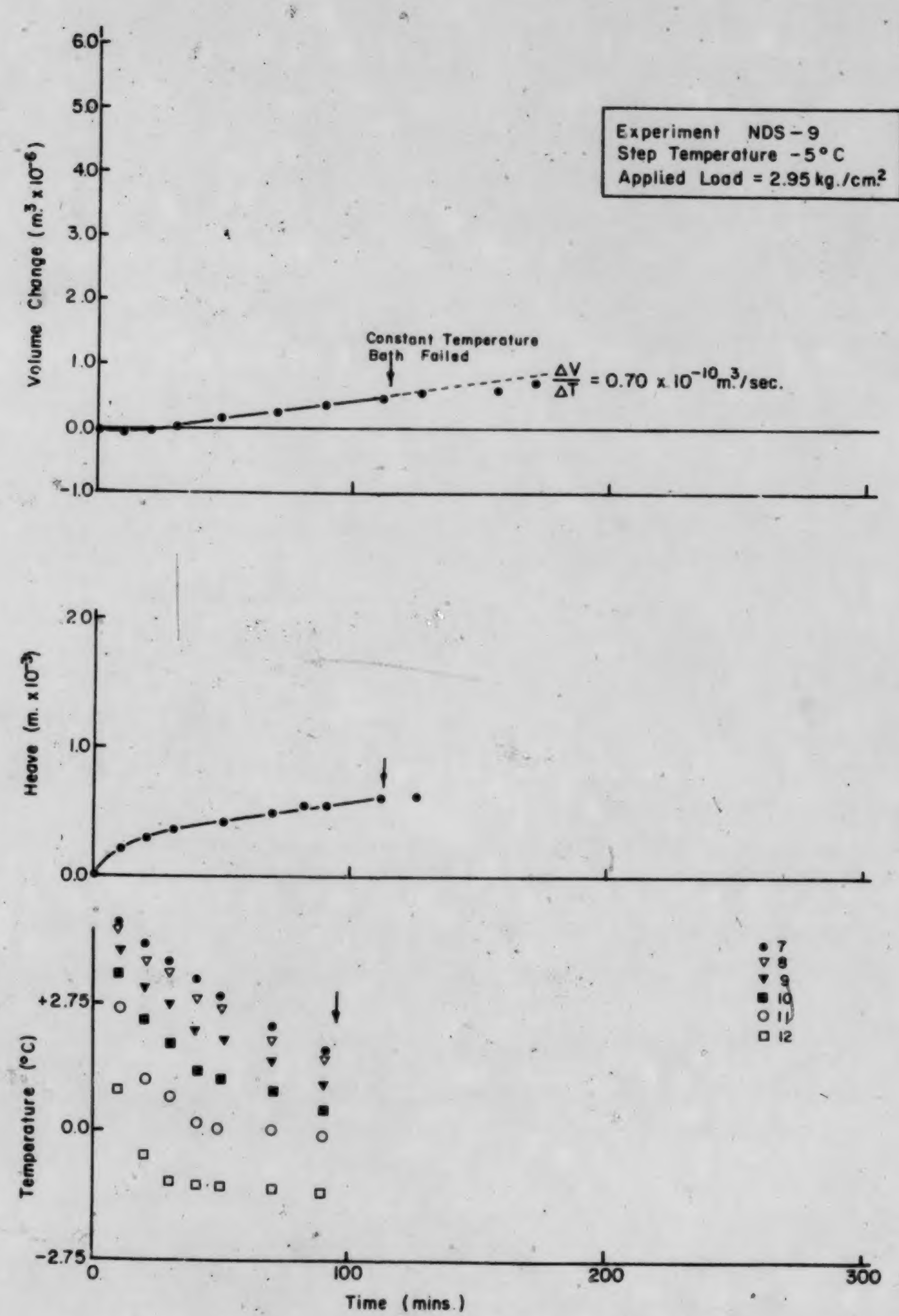
Experiment NDS-9
Step Temperature -5°C
Applied Load = 2.95 kg./cm²
Volume Change (m³ x 10⁻⁶)
6.0
5.0
4.0
3.0
2.0
1.0
0.0
-1.0
Constant Temperature Bath Failed
ΔV/ΔT = 0.70 x 10⁻¹⁰ m³/sec.
Heave (m. x 10⁻³)
2.0
1.0
0.0
Temperature (°C)
+2.75
0.0
-2.75
● 7
▽ 8
▼ 9
■ 10
○ 11
□ 12
0
100
200
300
Time (mins.)

Fig. A.10

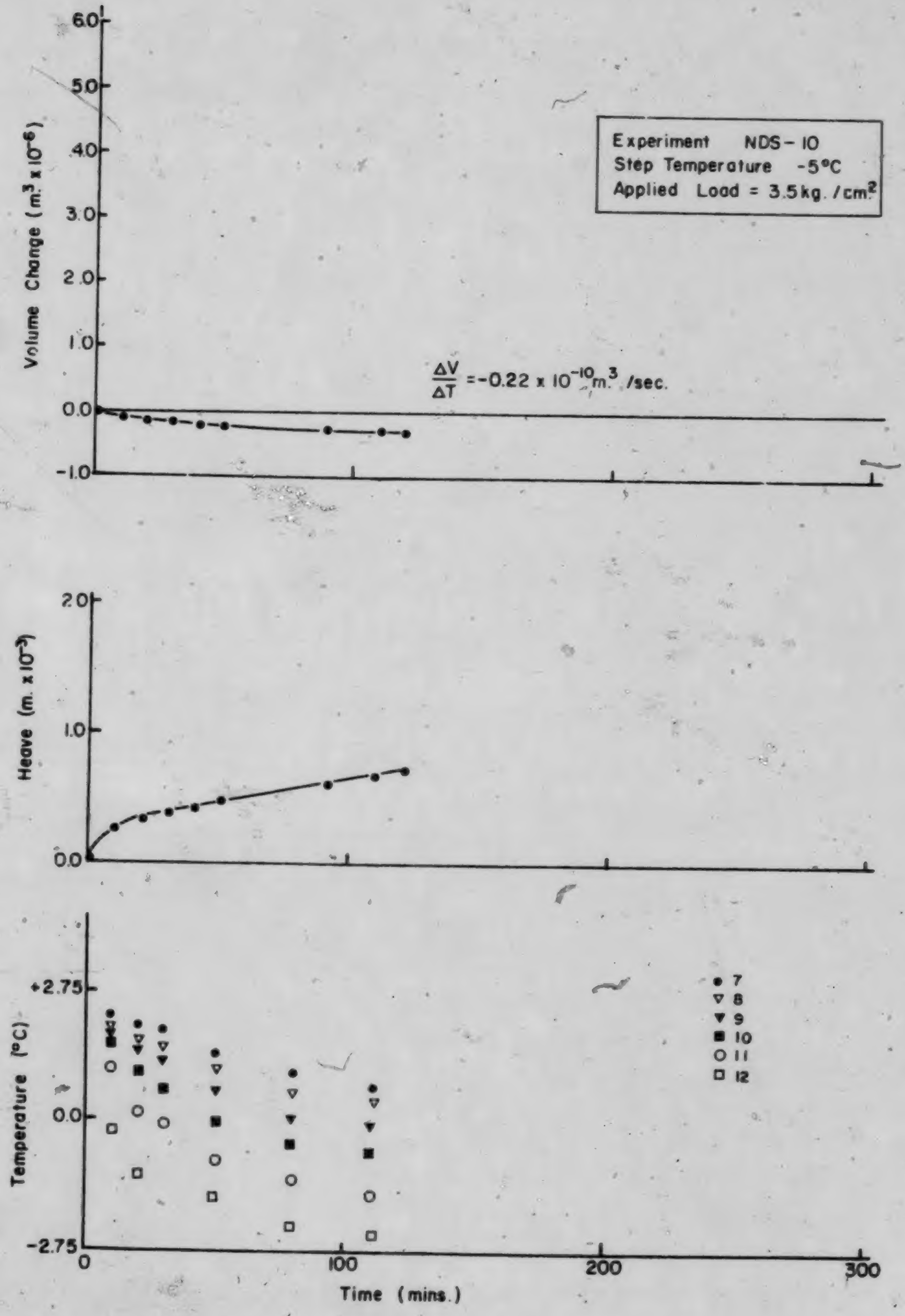
Experiment NDS-10
Step Temperature -5°C
Applied Load = 3.5kg./cm²
Volume Change (m³ x 10⁻⁶)
6.0
5.0
4.0
3.0
2.0
1.0
0.0
-1.0
ΔV/ΔT = -0.22 x 10⁻¹⁰ m³/sec.
Heave (m. x 10⁻³)
2.0
1.0
0.0
Temperature (°C)
+2.75
0.0
-2.75
0
100
200
300
Time (mins.)
● 7
▽ 8
▼ 9
■ 10
○ 11
□ 12

Fig. A.11

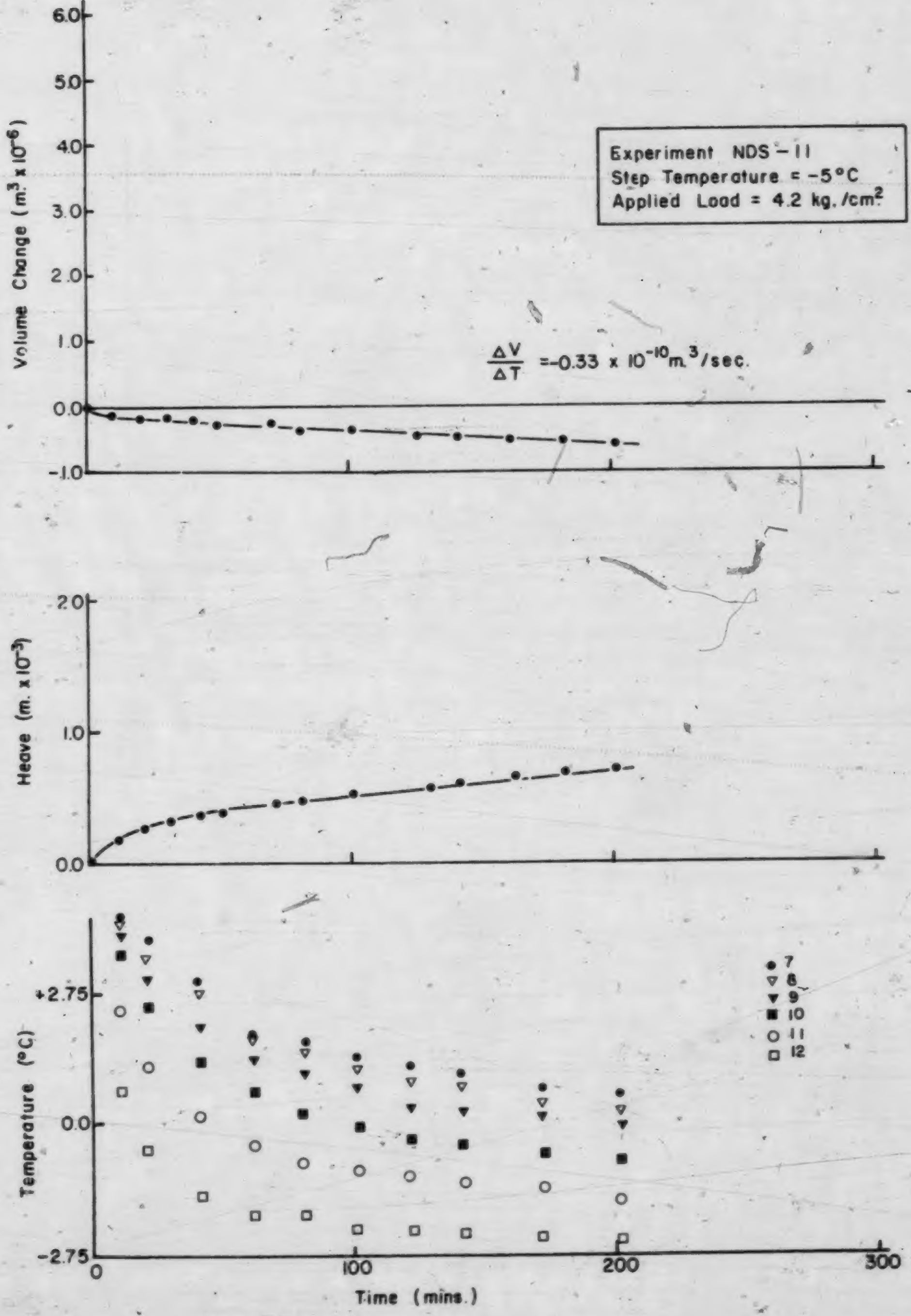
Experiment NDS - 11
Step Temperature = -5°C
Applied Load = 4.2 kg./cm²
Volume Change (m.³ x 10⁻⁶)
6.0
5.0
4.0
3.0
2.0
1.0
0.0
-1.0
ΔV/ΔT = -0.33 x 10⁻¹⁰ m.³/sec.
Heave (m. x 10⁻³)
2.0
1.0
0.0
Temperature (°C)
+2.75
0.0
-2.75
● 7
▽ 8
▼ 9
■ 10
○ 11
□ 12
0
100
200
300
Time (mins.)

Fig. A.12

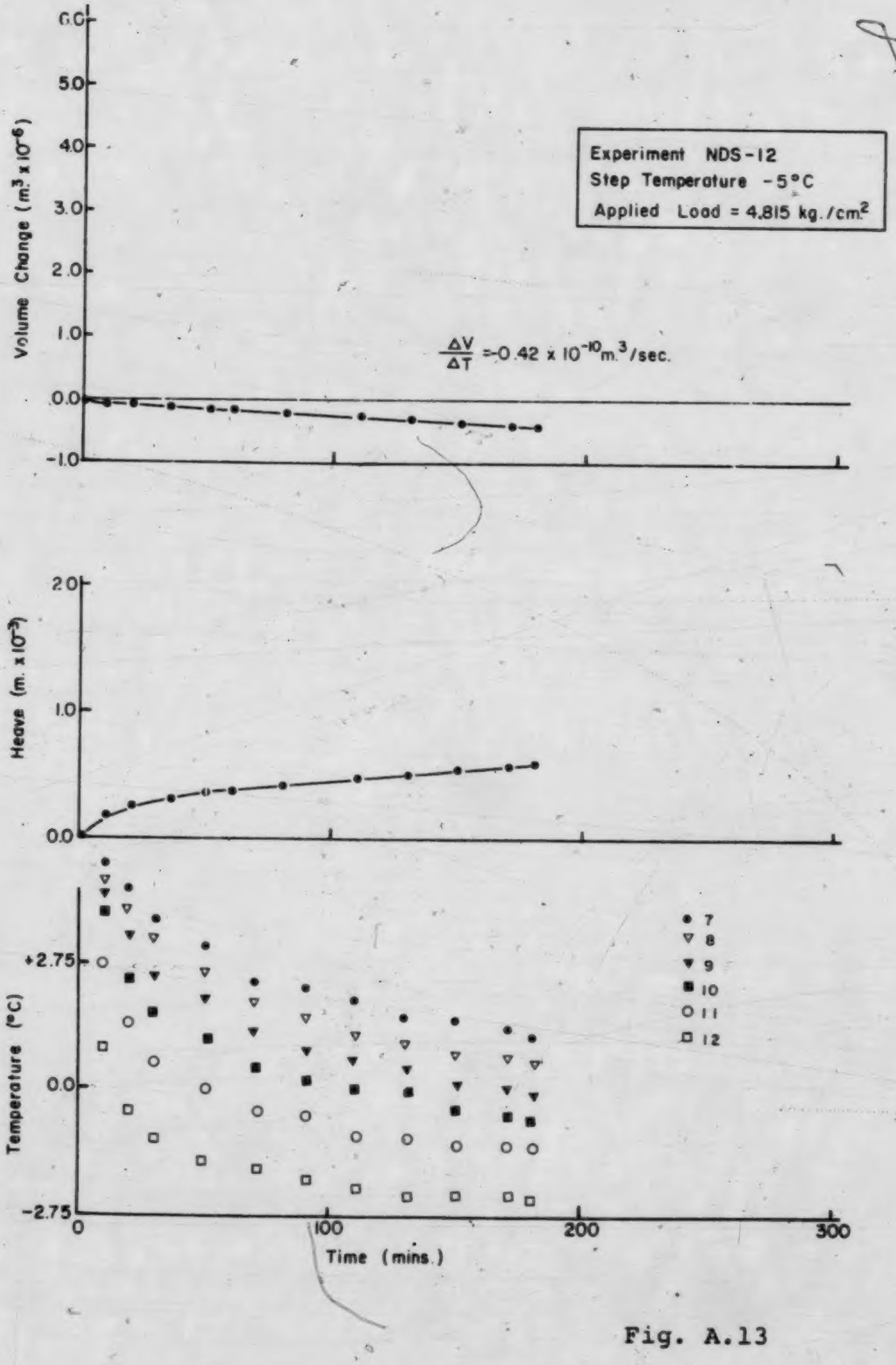

6.0
5.0
4.0
3.0
2.0
1.0
0.0
-1.0
Volume Change (m³ x 10⁻⁶)
Experiment NDS-12
Step Temperature -5°C
Applied Load = 4.815 kg./cm²
ΔV/ΔT = -0.42 x 10⁻¹⁰ m³/sec.
2.0
1.0
0.0
Heave (m. x 10⁻²)
+2.75
0.0
-2.75
Temperature (°C)
0
100
200
300
Time (mins.)
● 7
▽ 8
▼ 9
■ 10
○ 11
□ 12

Fig. A.13

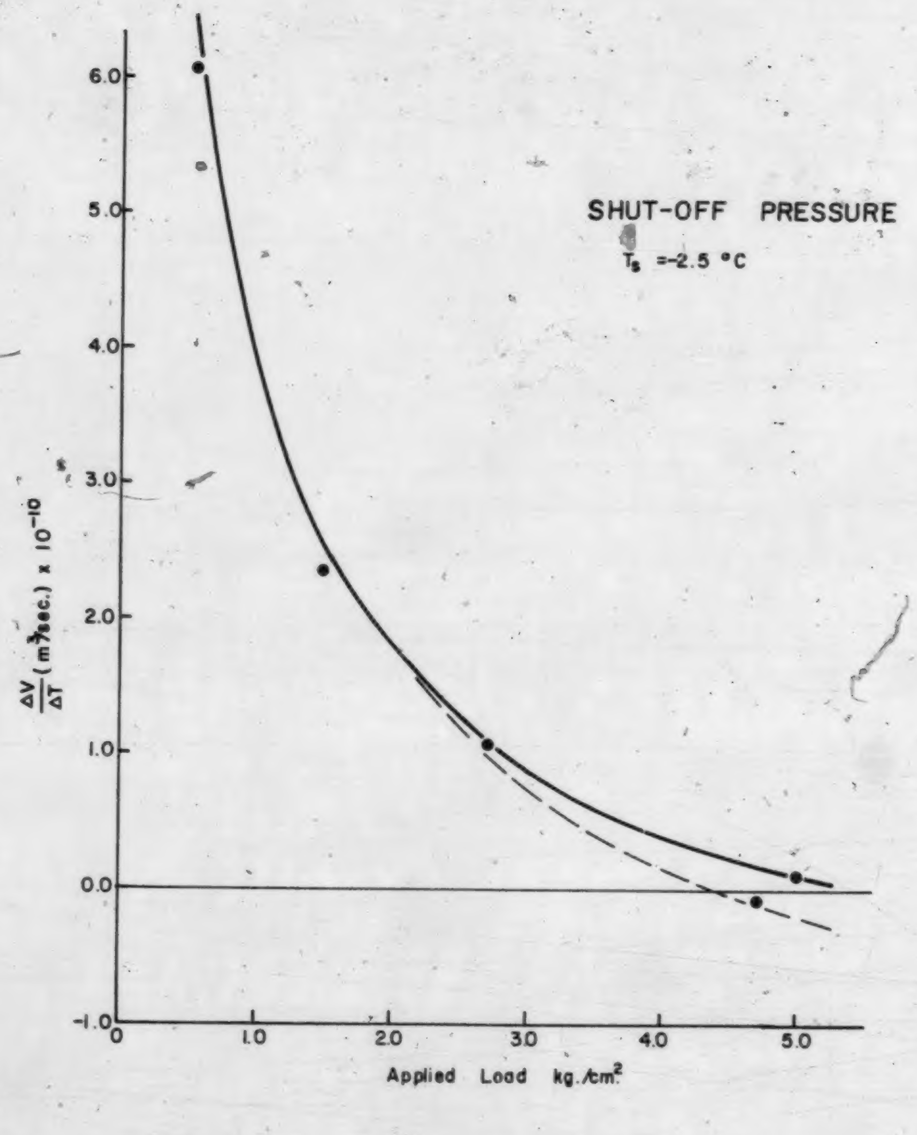
SHUT-OFF PRESSURE
T_s =-2.5 °C
$\frac{\Delta V}{\Delta T}$ (m³/sec.) x 10^{-10}
6.0
5.0
4.0
3.0
2.0
1.0
0.0
-1.0
0
1.0
2.0
3.0
4.0
5.0
Applied Load kg./cm²

Fig. A.14

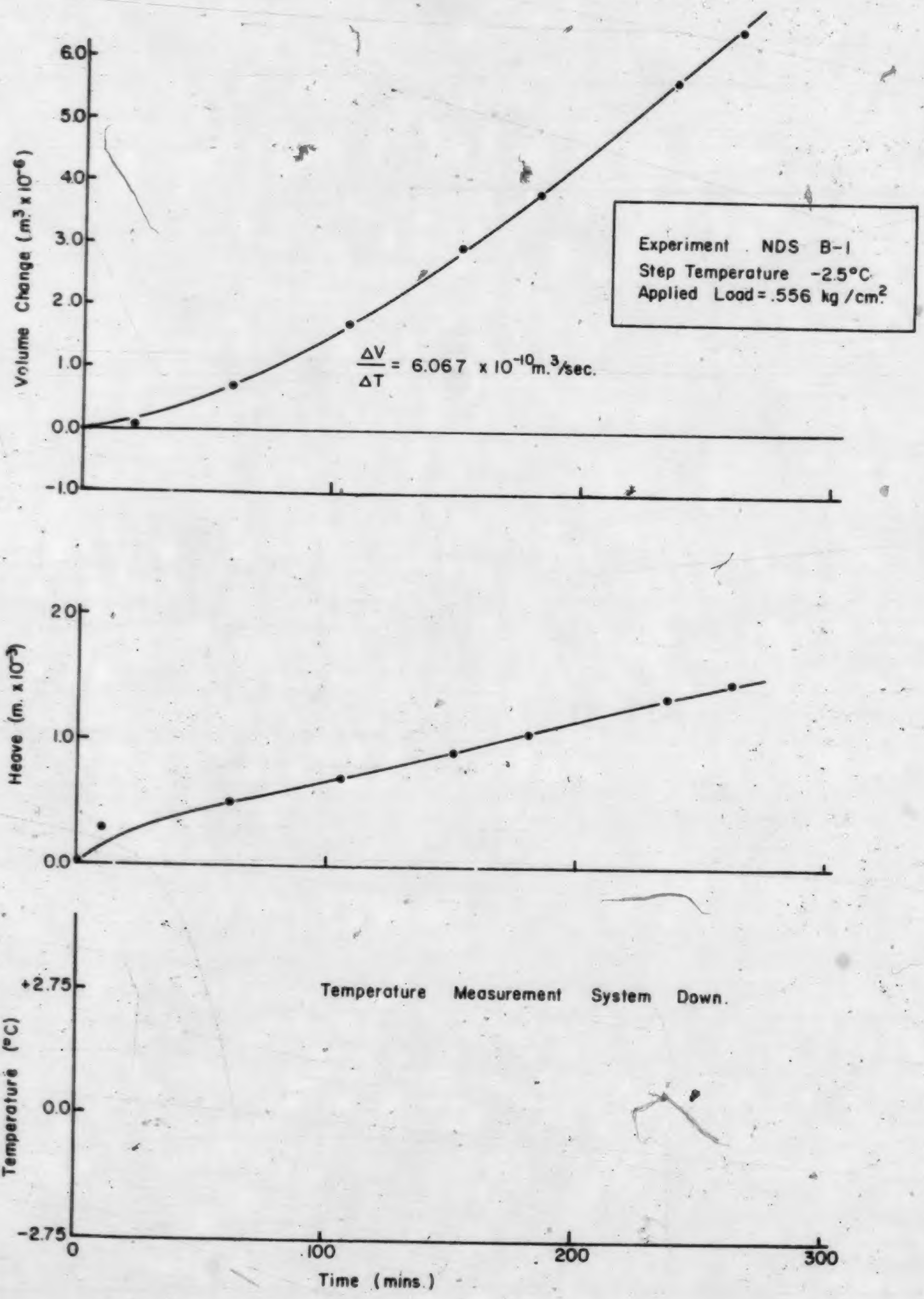
Volume Change ($m^3 \times 10^{-6}$)
6.0
5.0
4.0
3.0
2.0
1.0
0.0
-1.0
Experiment . NDS B-1
Step Temperature -2.5°C
Applied Load = .556 kg/cm^2
$\frac{\Delta V}{\Delta T} = 6.067 \times 10^{-10} m.^3/sec.$
Heave (m. $\times 10^{-3}$)
2.0
1.0
0.0
Temperature (°C)
+2.75
0.0
-2.75
Temperature Measurement System Down.
0
100
200
300
Time (mins.)

Fig. A.15

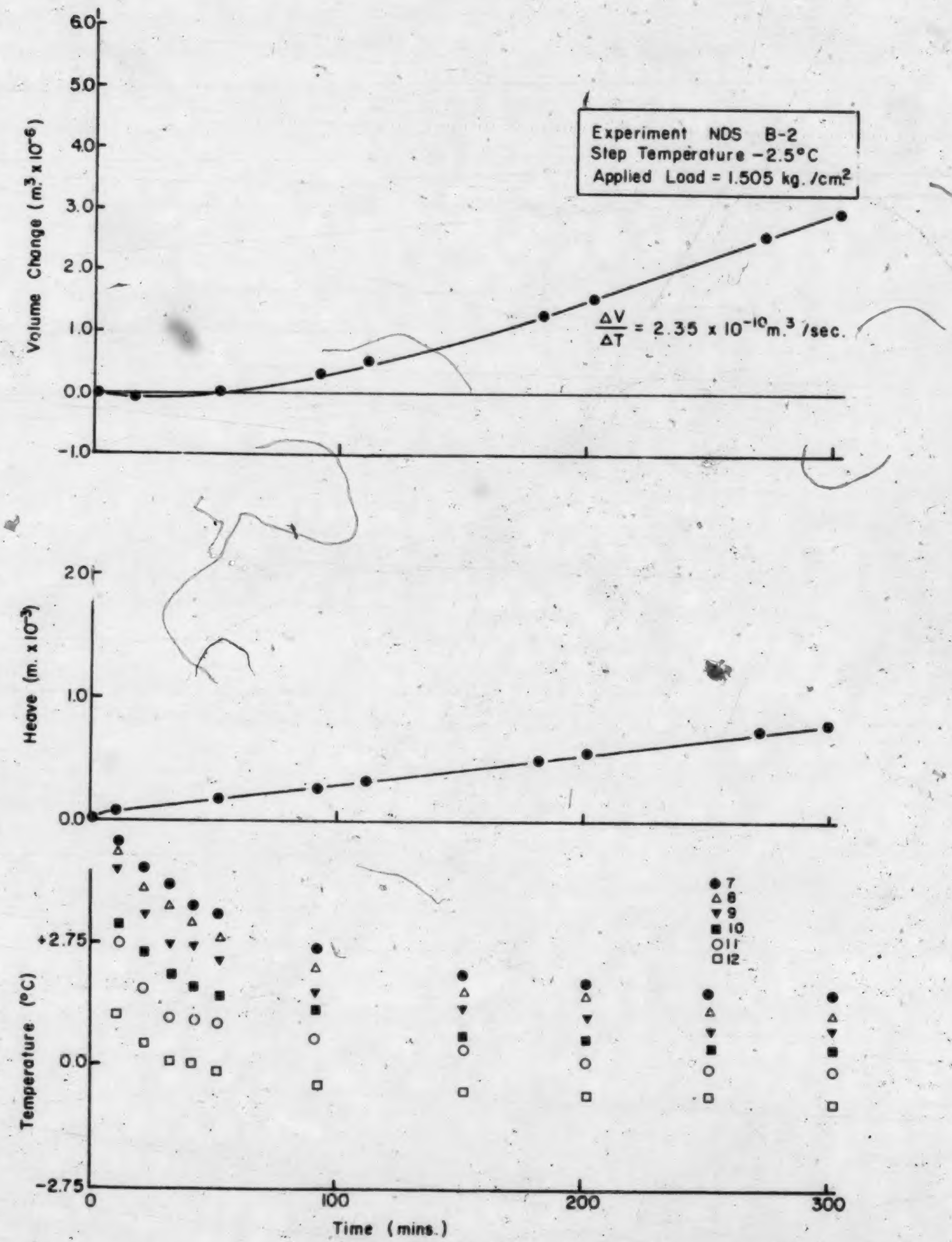
6.0
5.0
4.0
3.0
2.0
1.0
0.0
-1.0
Volume Change (m.³ x 10⁻⁶)
Experiment NDS B-2
Step Temperature -2.5°C
Applied Load = 1.505 kg./cm²
ΔV/ΔT = 2.35 x 10⁻¹⁰ m.³/sec.
2.0
1.0
0.0
Heave (m. x 10⁻³)
+2.75
0.0
-2.75
Temperature (°C)
● 7
△ 8
▼ 9
■ 10
○ 11
□ 12
0
100
200
300
Time (mins.)

Fig. A.16

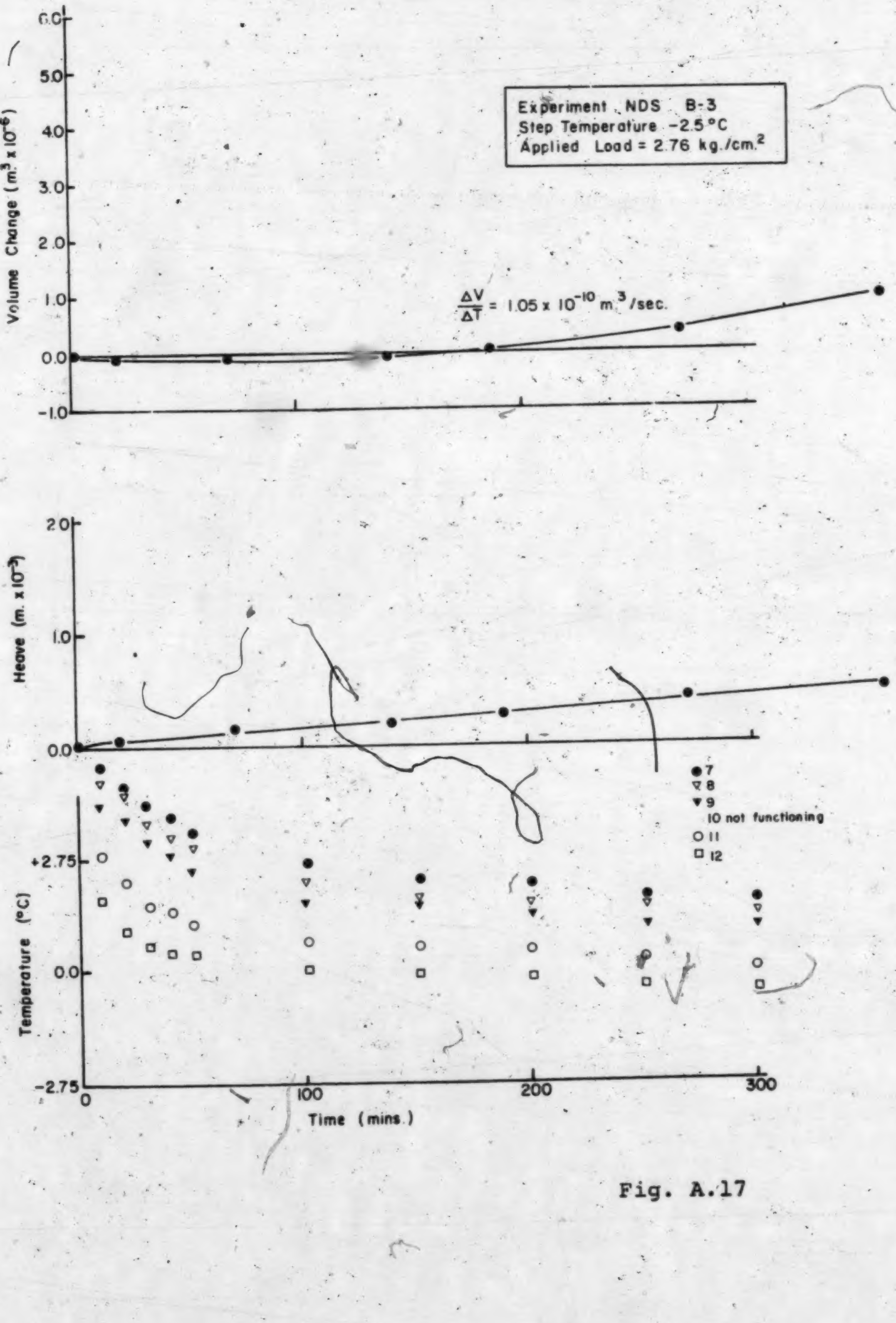
Experiment NDS B-3
Step Temperature -2.5 °C
Applied Load = 2.76 kg./cm.^{2}
Volume Change (m.^{3} x 10^{-6})
6.0
5.0
4.0
3.0
2.0
1.0
0.0
-1.0
ΔV/ΔT = 1.05 x 10^{-10} m.^{3}/sec.
Heave (m. x 10^{-3})
2.0
1.0
0.0
Temperature (°C)
+2.75
0.0
-2.75
0
100
200
300
Time (mins.)
● 7
▽ 8
▼ 9
10 not functioning
○ 11
□ 12

Fig. A.17

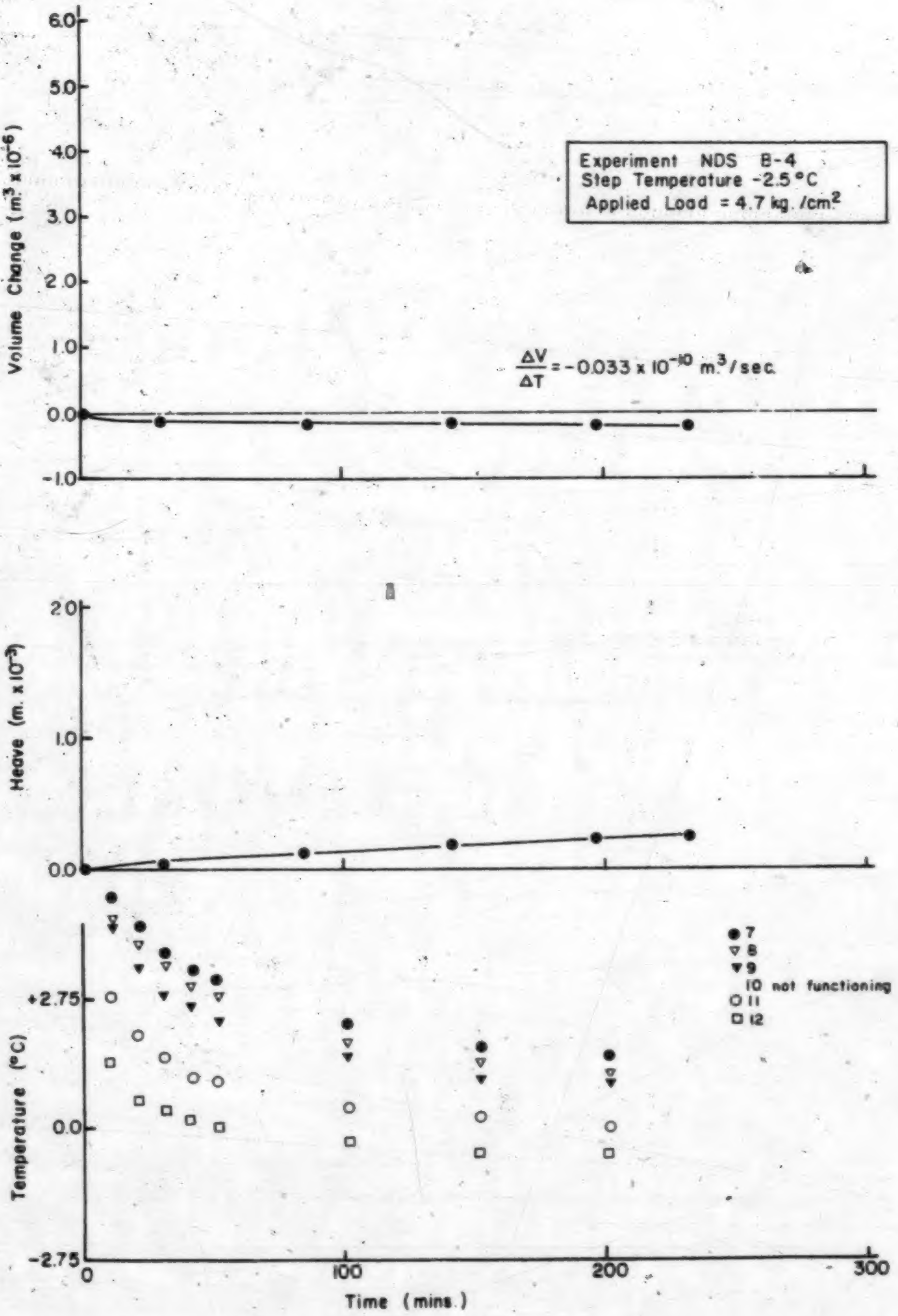
Experiment NDS B-4
Step Temperature -2.5 °C
Applied Load = 4.7 kg./cm²
$\frac{\Delta V}{\Delta T} = -0.033 \times 10^{-10}\ m^3/sec$
Volume Change ($m^3 \times 10^{-6}$)
6.0
5.0
4.0
3.0
2.0
1.0
0.0
-1.0
Heave ($m. \times 10^{-3}$)
2.0
1.0
0.0
Temperature (°C)
+2.75
0.0
-2.75
0
100
200
300
Time (mins.)
● 7
▽ 8
▼ 9
10 not functioning
○ 11
□ 12

Fig. A.18

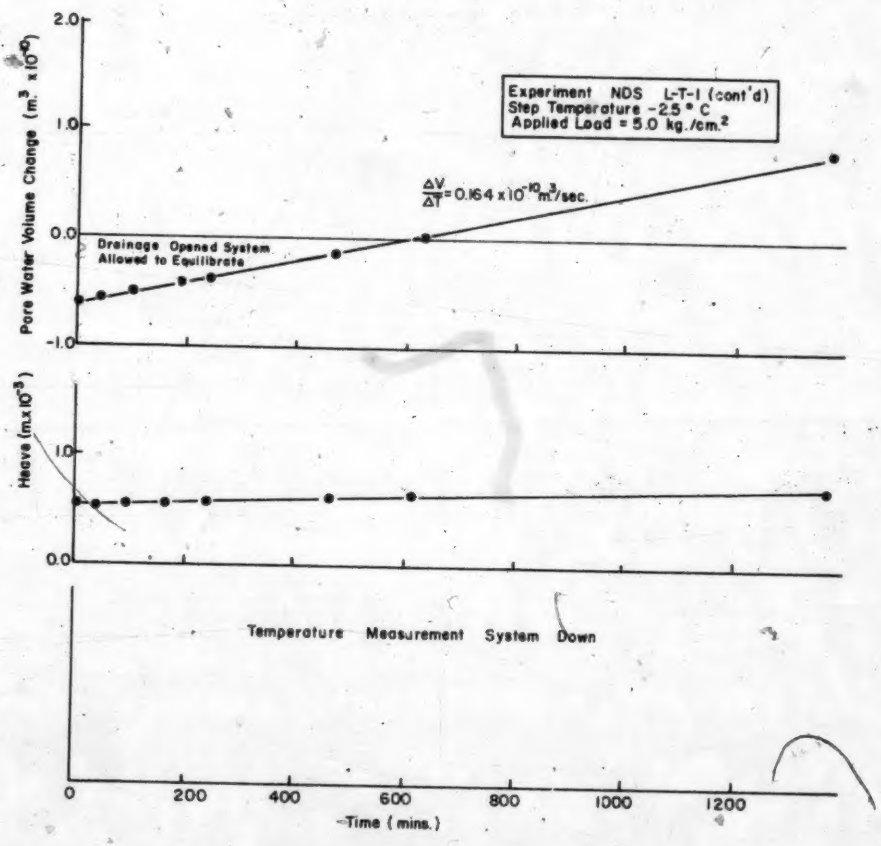
Pore Water Volume Change (m.^{3} x10^{-10})
2.0
1.0
0.0
-1.0
Experiment NDS L-T-I (cont'd)
Step Temperature -2.5 ° C
Applied Load = 5.0 kg./cm.^{2}
$\frac{\Delta V}{\Delta T}$= 0.164 x 10^{-10} m.^{3}/sec.
Drainage Opened System
Allowed to Equilibrate
Heave (m.x10^{-3})
1.0
0.0
Temperature Measurement System Down
0
200
400
600
800
1000
1200
Time (mins.)

Fig. A.19

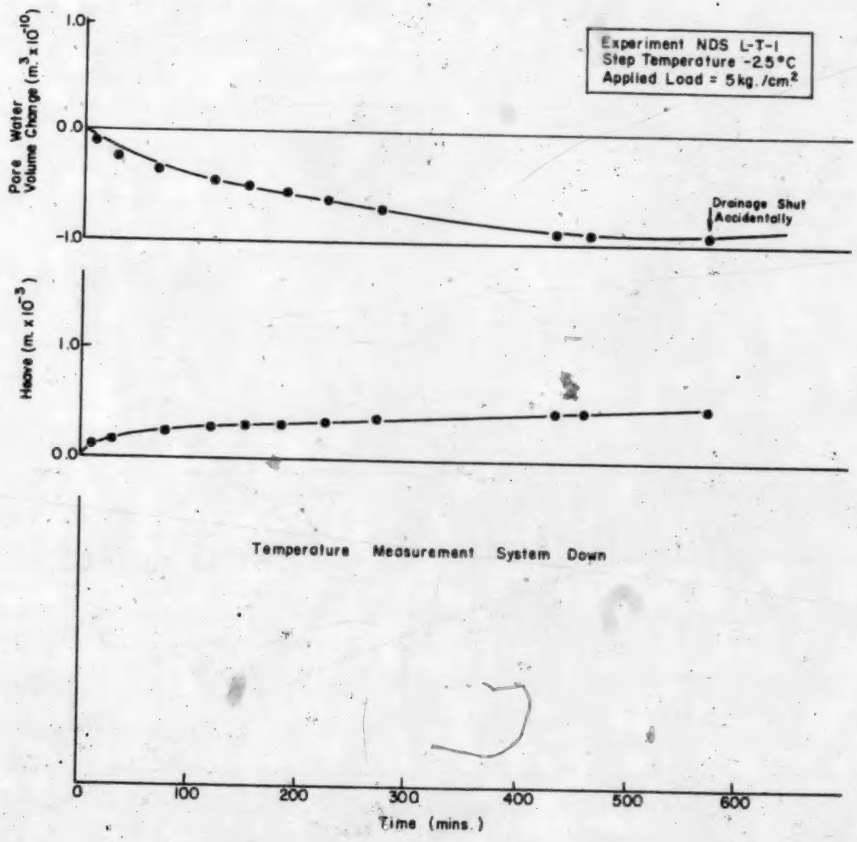
Experiment NDS L-T-1
Step Temperature -2.5°C
Applied Load = 5kg./cm.²
Pore Water Volume Change (m.³ x 10⁻¹⁰)
1.0
0.0
-1.0
Drainage Shut Accidentally
Heave (m. x 10⁻³)
1.0
0.0
Temperature Measurement System Down
0
100
200
300
400
500
600
Time (mins.)

Fig. A.20

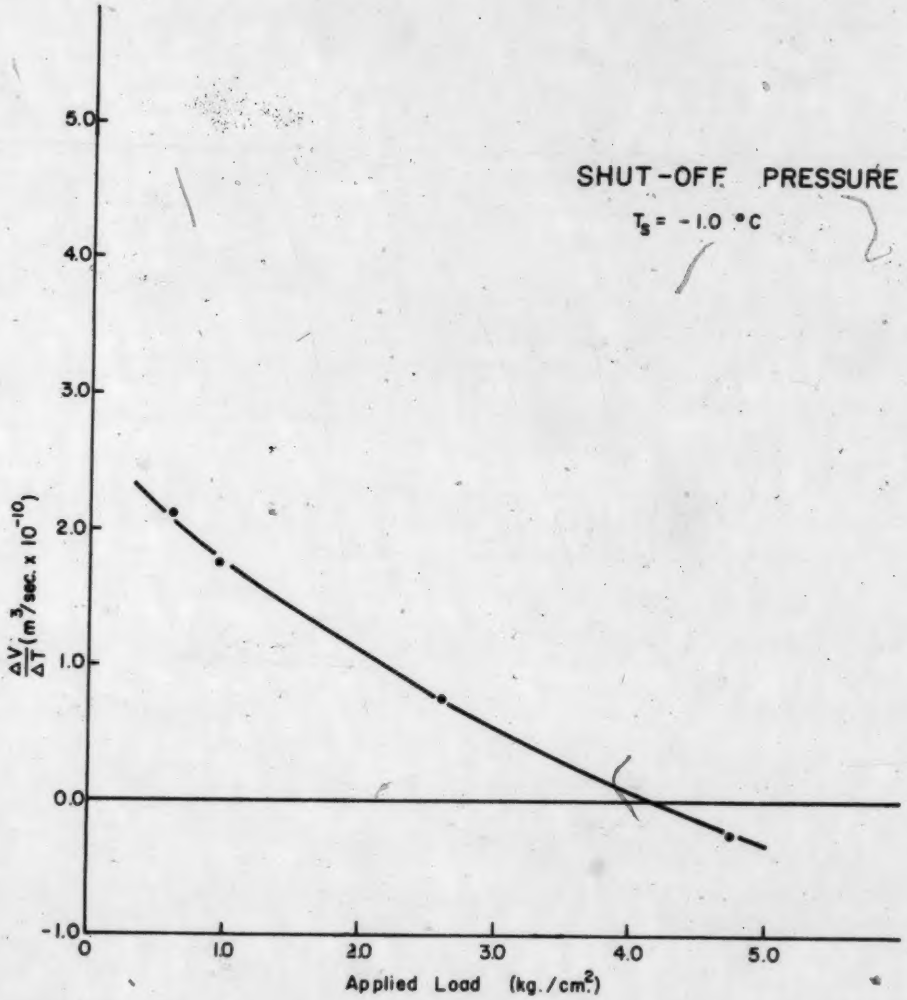
SHUT-OFF PRESSURE
T_s = -1.0 °C
5.0
4.0
3.0
2.0
1.0
0.0
-1.0
0
1.0
2.0
3.0
4.0
5.0
Applied Load (kg./cm.^{2})
$\frac{\Delta V}{\Delta T}$ (m^3/sec. x 10^{-10})

Fig. A.21

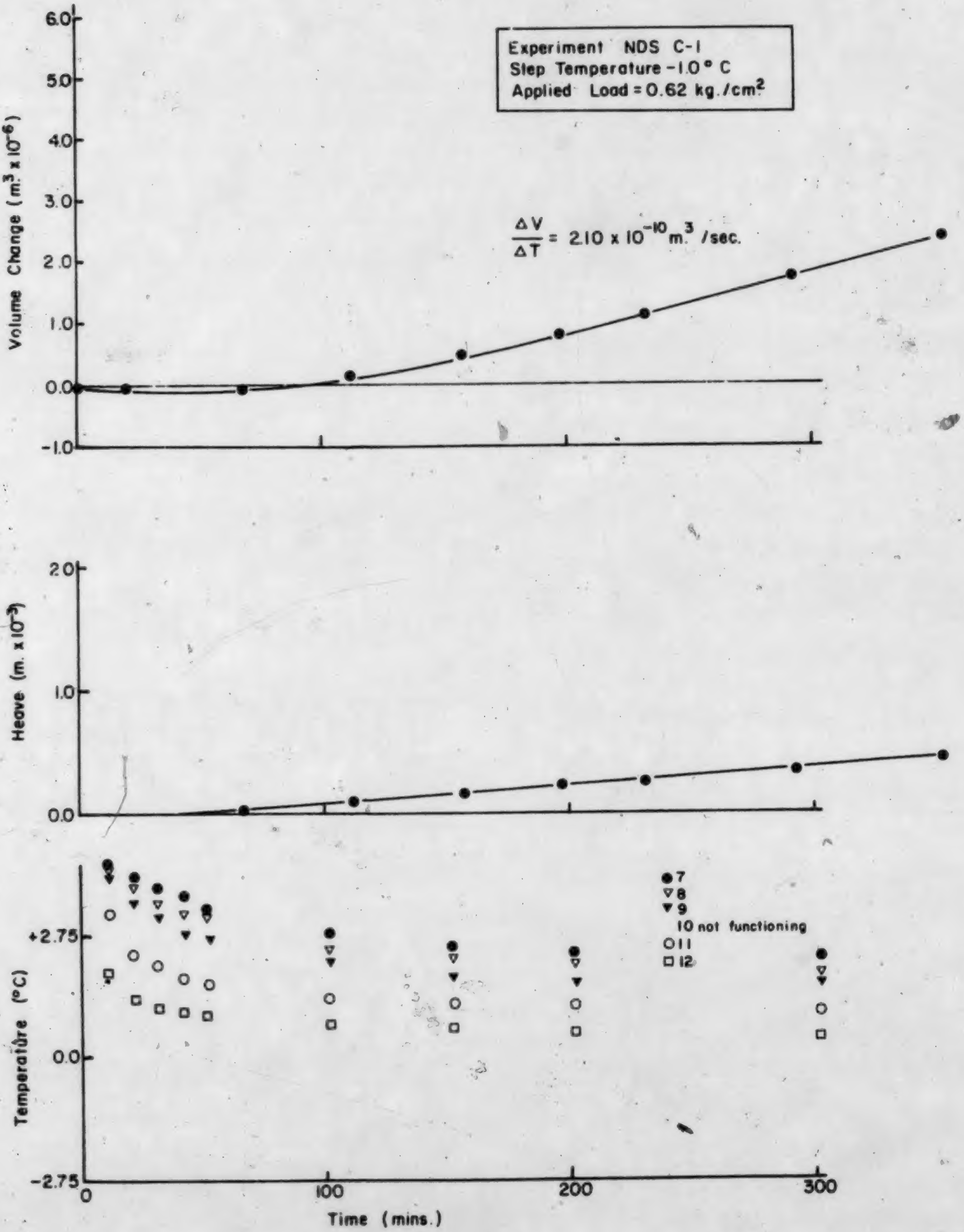
Experiment NDS C-1
Step Temperature -1.0° C
Applied Load = 0.62 kg./cm²
$\frac{\Delta V}{\Delta T}$ = 2.10 x 10⁻¹⁰ m³ /sec.
Volume Change (m³ x 10⁻⁶)
6.0
5.0
4.0
3.0
2.0
1.0
0.0
-1.0
Heave (m. x 10⁻³)
2.0
1.0
0.0
Temperature (°C)
+2.75
0.0
-2.75
● 7
▽ 8
▼ 9
10 not functioning
○ 11
□ 12
0
100
200
300
Time (mins.)

Fig. A.22

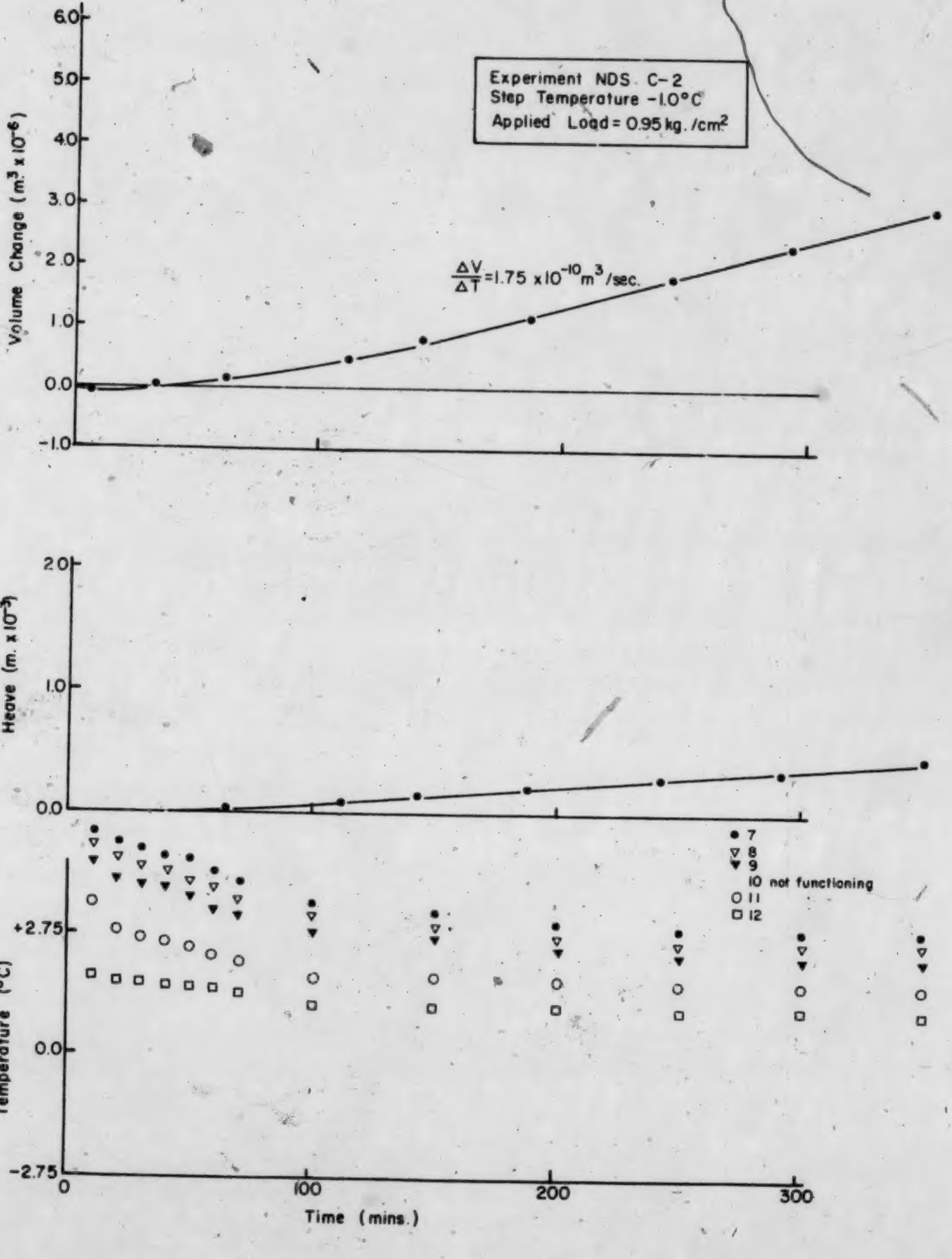
Experiment NDS. C-2
Step Temperature -1.0°C
Applied Load = 0.95 kg./cm²
Volume Change (m³ x 10⁻⁶)
6.0
5.0
4.0
3.0
2.0
1.0
0.0
-1.0
ΔV/ΔT = 1.75 x 10⁻¹⁰ m³/sec.
Heave (m. x 10⁻²)
2.0
1.0
0.0
Temperature (°C)
+2.75
0.0
-2.75
0
100
200
300
Time (mins.)
● 7
▽ 8
▼ 9
10 not functioning
○ 11
□ 12

Fig. A.23

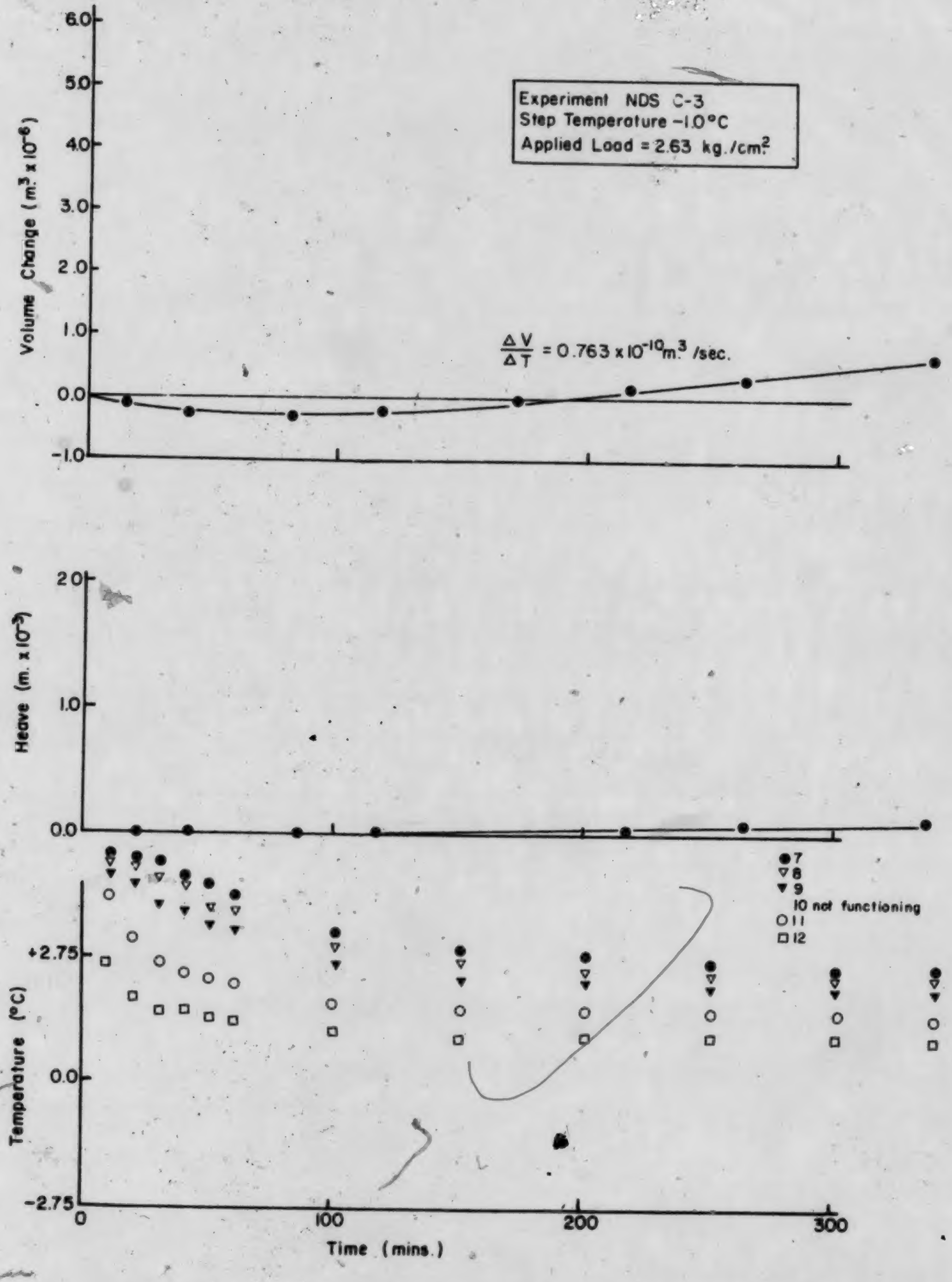
Experiment NDS C-3
Step Temperature -1.0°C
Applied Load = 2.63 kg./cm^2
Volume Change (m^3 x 10^{-6})
6.0
5.0
4.0
3.0
2.0
1.0
0.0
-1.0
$\frac{\Delta V}{\Delta T}$ = 0.763 x 10^{-10}m^3 /sec.
Heave (m. x 10^{-3})
2.0
1.0
0.0
Temperature (°C)
+2.75
0.0
-2.75
0
100
200
300
Time (mins.)
● 7
▽ 8
▼ 9
10 not functioning
○ 11
□ 12

Fig. A.24

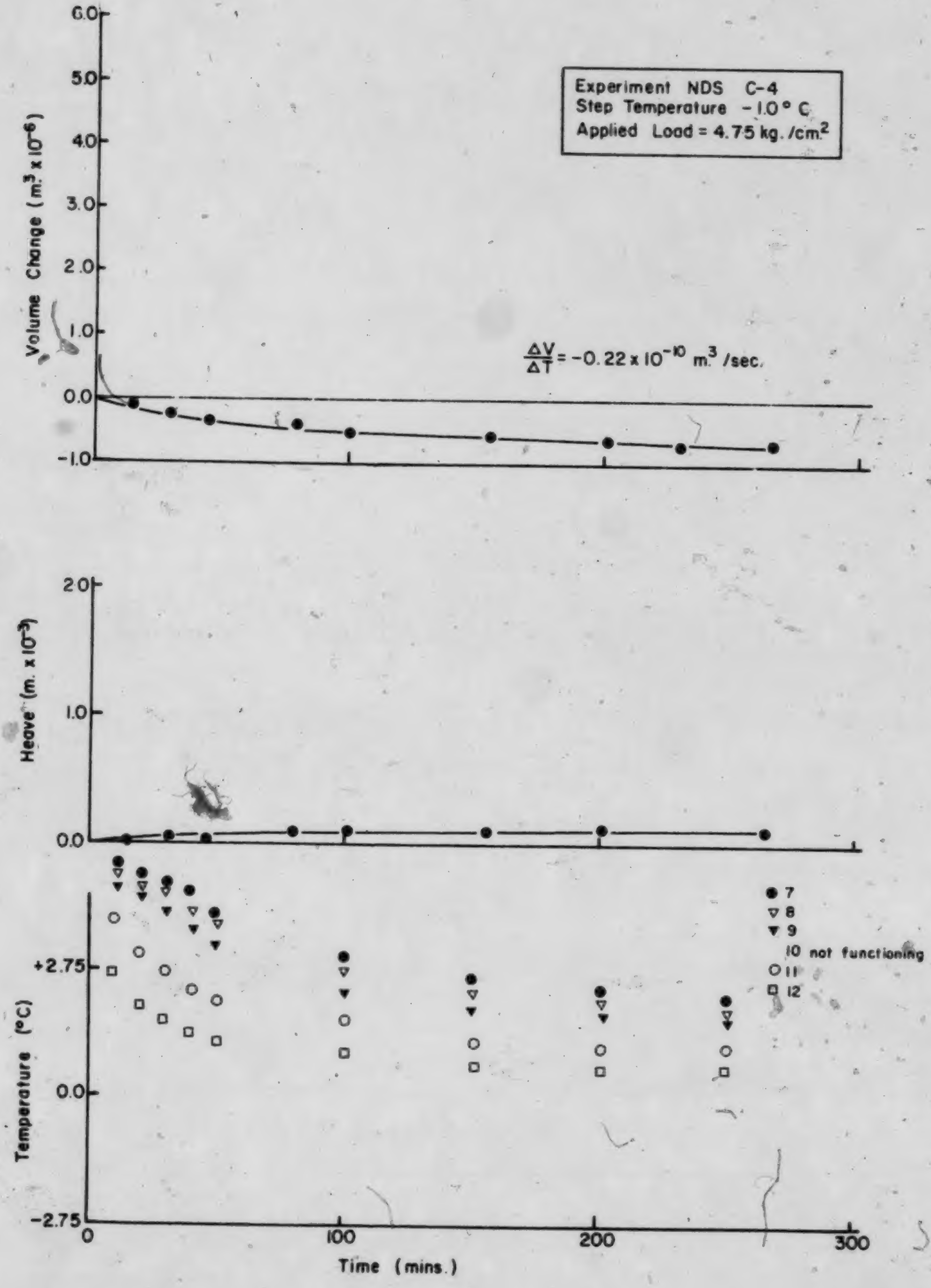
Experiment NDS C-4
Step Temperature -1.0° C
Applied Load = 4.75 kg./cm²
Volume Change (m³ x 10⁻⁶)
6.0
5.0
4.0
3.0
2.0
1.0
0.0
-1.0
ΔV/ΔT = -0.22 x 10⁻¹⁰ m³/sec.
Heave (m. x 10⁻³)
2.0
1.0
0.0
Temperature (°C)
+2.75
0.0
-2.75
0
100
200
300
Time (mins.)
● 7
▽ 8
▼ 9
10 not functioning
○ 11
□ 12

Fig. A.25

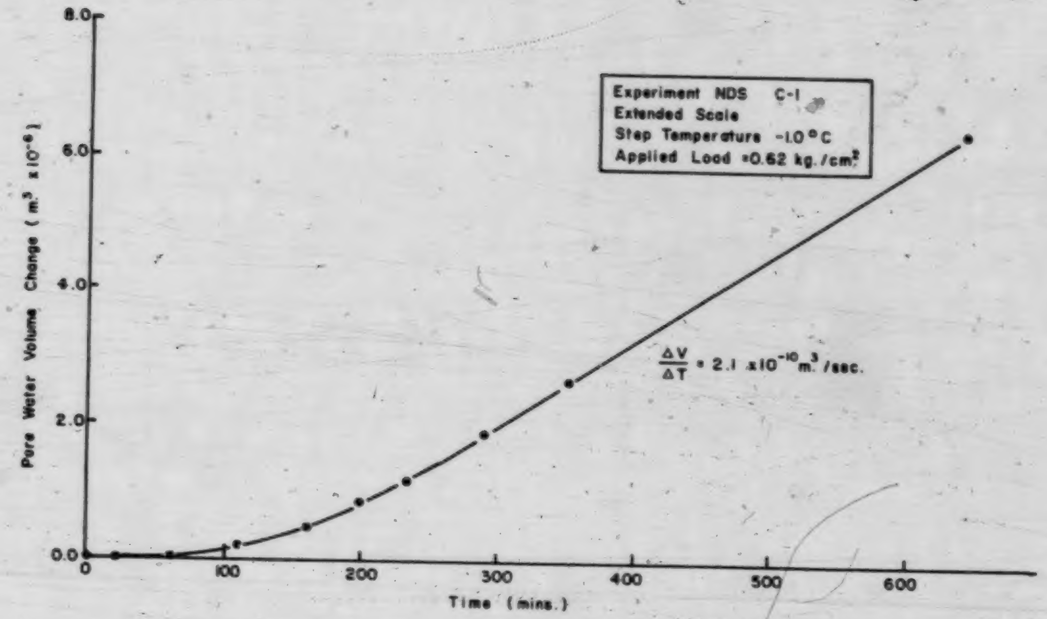

Fig. A.26

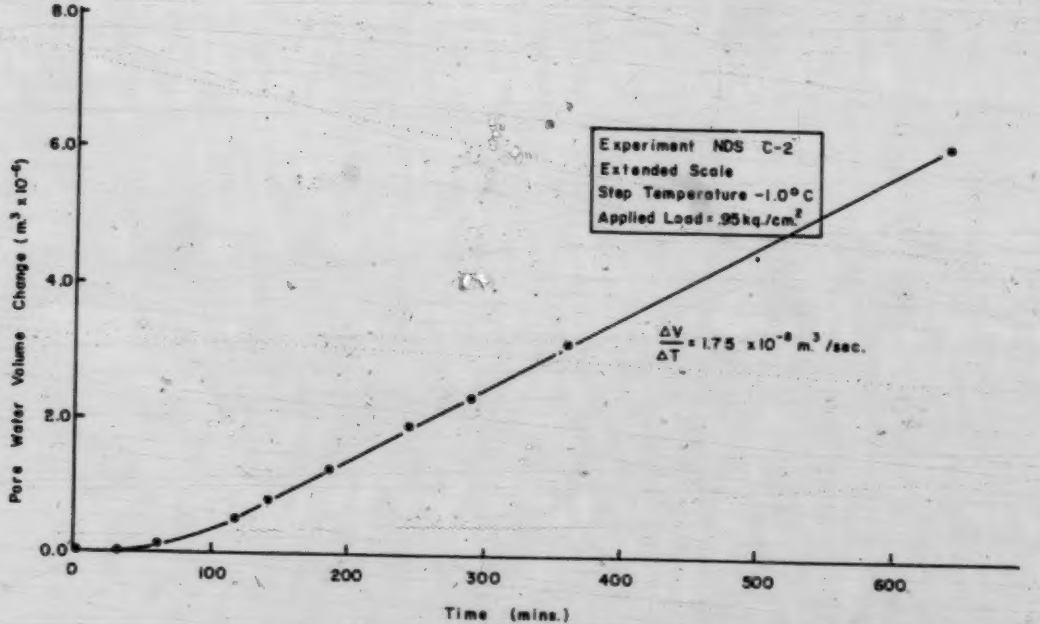

Fig. A.27

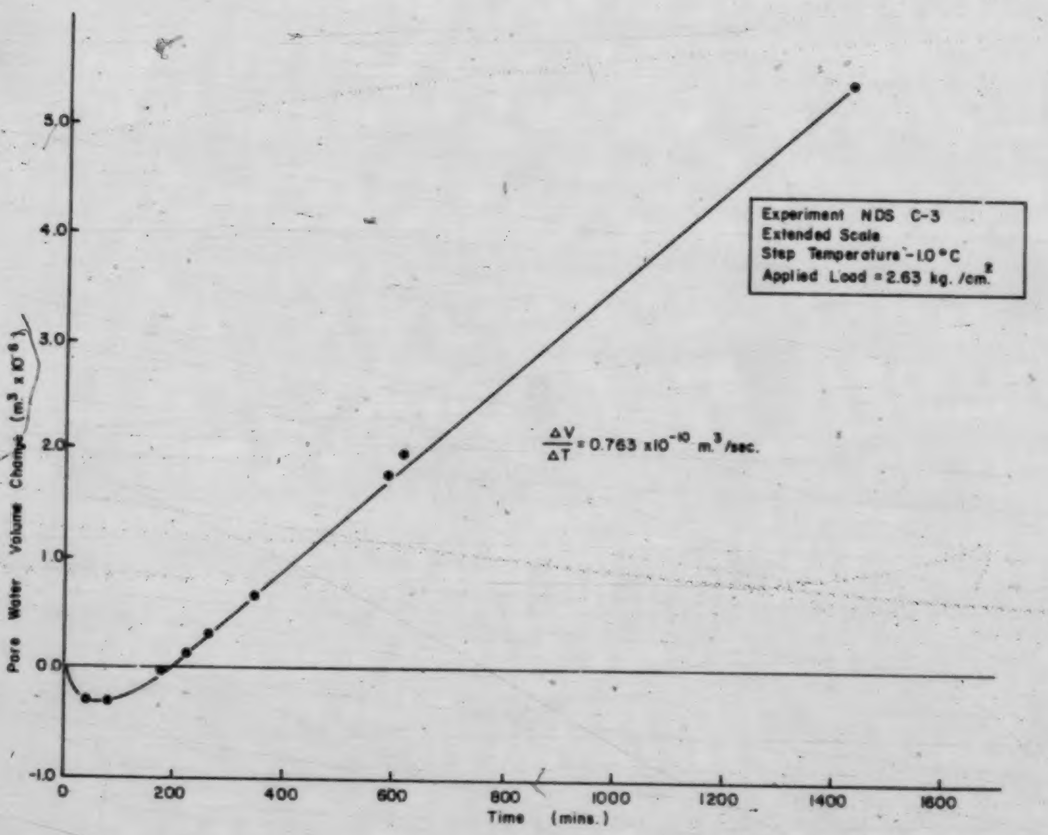
Experiment NDS C-3
Extended Scale
Step Temperature -1.0 °C
Applied Load = 2.63 kg. /cm.^{2}
$\frac{\Delta V}{\Delta T}$ = 0.763 x10^{-10} m.^{3}/sec.
Pore Water Volume Change (m^3 x 10^{-6})
5.0
4.0
3.0
2.0
1.0
0.0
-1.0
0
200
400
600
800
1000
1200
1400
1600
Time (mins.)

Fig. A.28

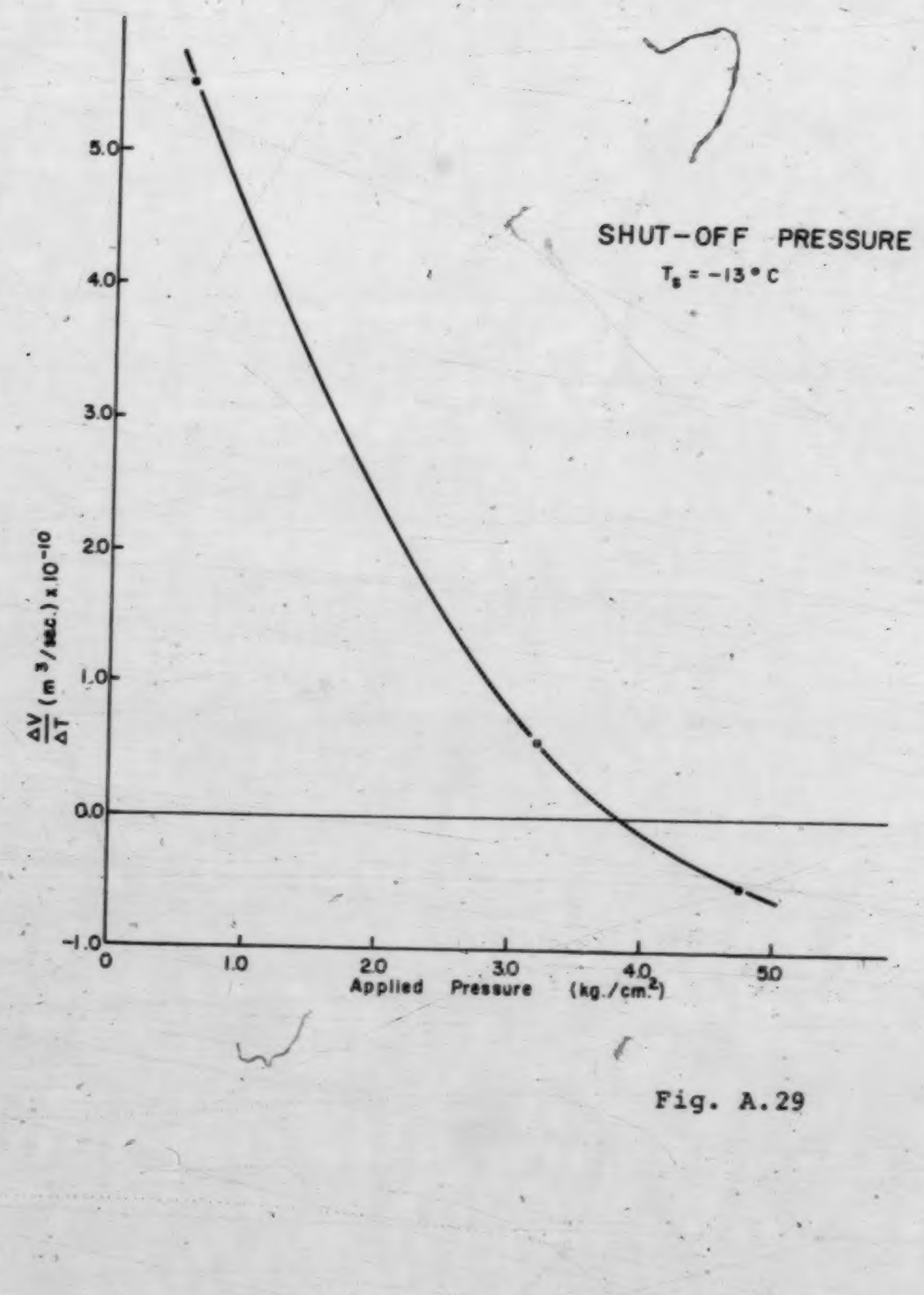
SHUT-OFF PRESSURE
$T_s = -13°C$
$\frac{\Delta V}{\Delta T}$ (m^3/sec.) x 10^{-10}
5.0
4.0
3.0
2.0
1.0
0.0
-1.0
0
1.0
2.0
3.0
4.0
5.0
Applied Pressure (kg./cm.^{2})

Fig. A.29

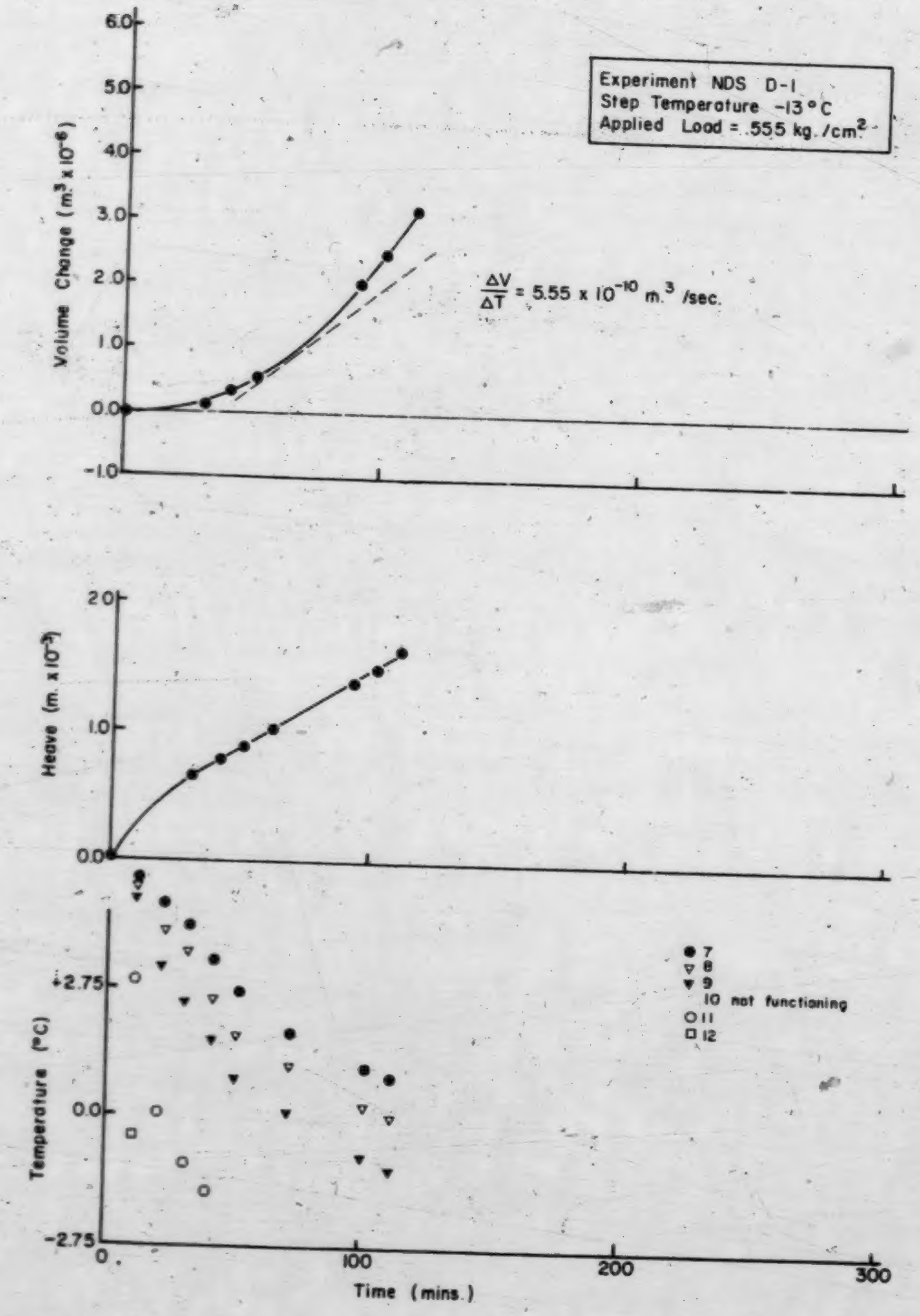
Experiment NDS D-1
Step Temperature -13 °C
Applied Load = .555 kg./cm.²
Volume Change (m.³ x 10⁻⁶)
6.0
5.0
4.0
3.0
2.0
1.0
0.0
-1.0
ΔV/ΔT = 5.55 x 10⁻¹⁰ m.³ /sec.
Heave (m. x 10⁻²)
2.0
1.0
0.0
Temperature (°C)
+2.75
0.0
-2.75
● 7
▽ 8
▼ 9
10 not functioning
○ 11
□ 12
0
100
200
300
Time (mins.)

Fig. A.30

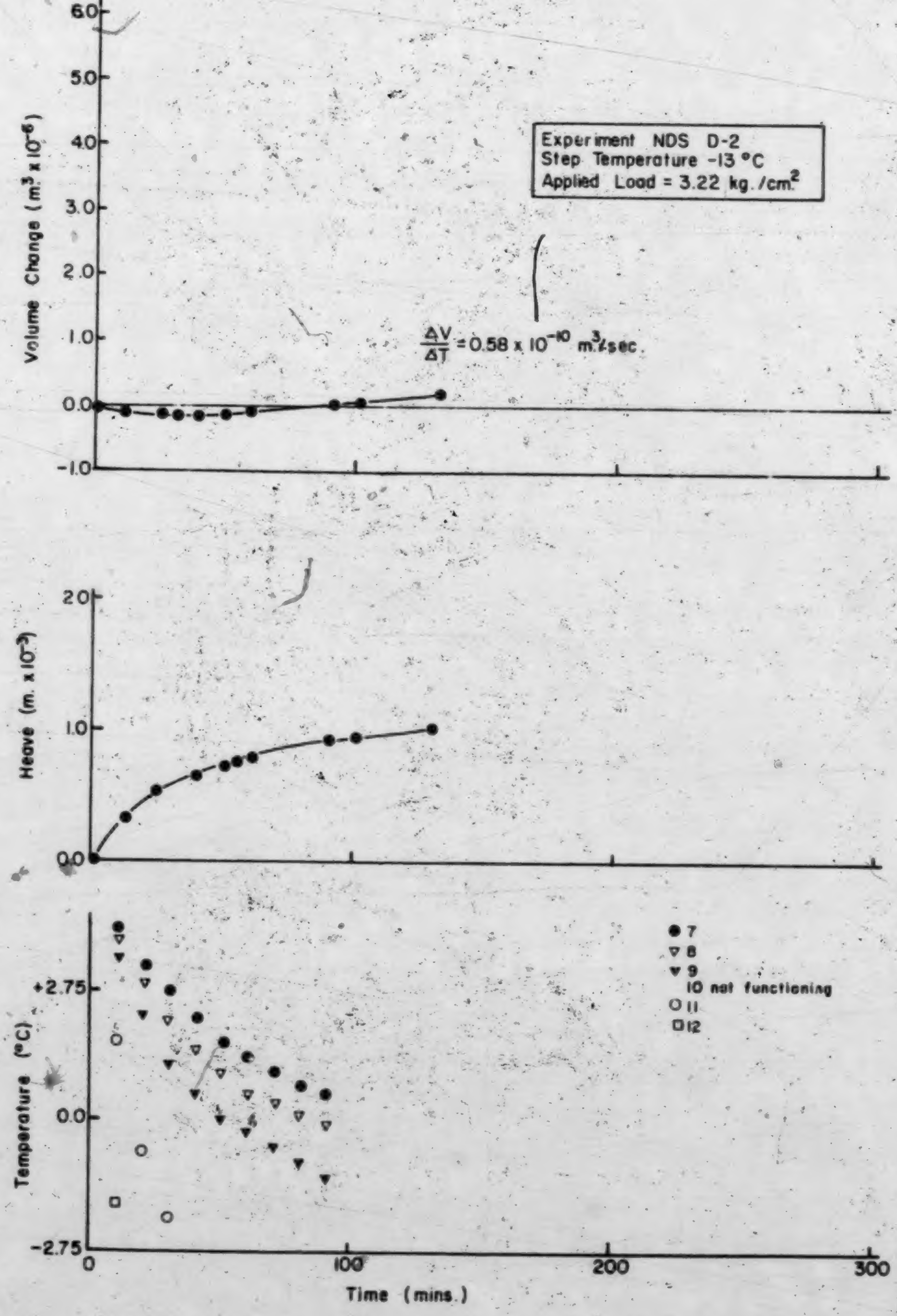
6.0
5.0
4.0
3.0
2.0
1.0
0.0
-1.0
Volume Change (m³ x 10⁻⁶)
Experiment NDS D-2
Step Temperature -13 °C
Applied Load = 3.22 kg./cm²
ΔV/ΔT = 0.58 x 10⁻¹⁰ m³/sec.
2.0
1.0
0.0
Heave (m. x 10⁻³)
+2.75
0.0
-2.75
Temperature (°C)
● 7
▽ 8
▼ 9
10 not functioning
○ 11
□ 12
0
100
200
300
Time (mins.)

Fig. A.31

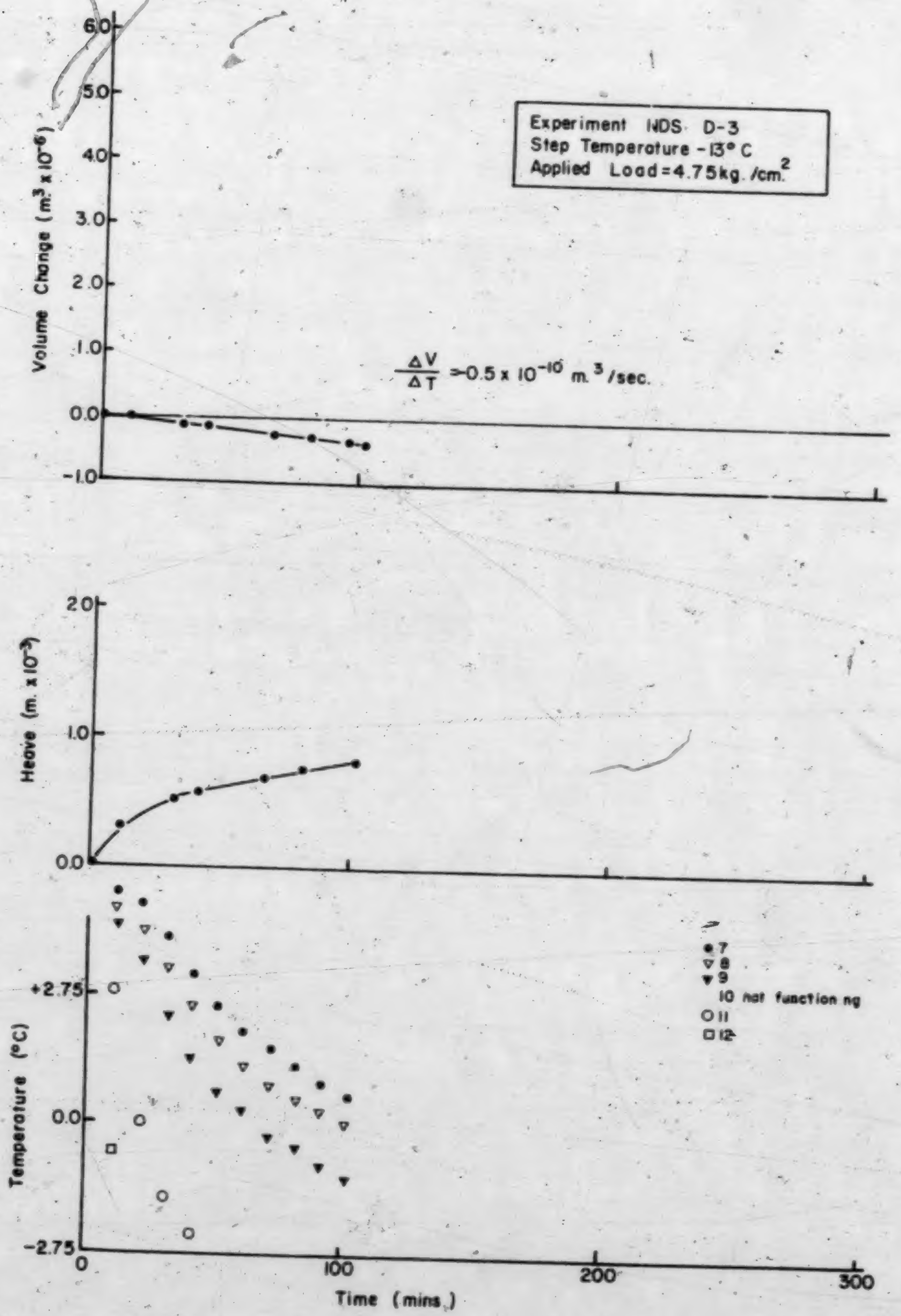
Experiment NDS D-3
Step Temperature -13° C
Applied Load=4.75kg. /cm^2
Volume Change (m^3 x 10^{-6})
6.0
5.0
4.0
3.0
2.0
1.0
0.0
-1.0
$\frac{\Delta V}{\Delta T}$ =-0.5 x 10^{-10} m.^{3}/sec.
Heave (m. x 10^{-3})
2.0
1.0
0.0
Temperature (°C)
+2.75
0.0
-2.75
0
100
200
300
Time (mins.)
● 7
▽ 8
▼ 9
10 not function ng
○ 11
□ 12

Fig. A.32

APPENDIX B

PROGRAM LISTING AND SAMPLE OUTPUT

```
      REAL U(200),UNEXT(200)
      COMMON P,Q,R,TCT,TCF,W,GAMD
    1 READ(5,2) TCT,TCF,P,Q,H,TS,TI,W
    2 FORMAT(8F10.0)
      WRITE(6,83) TCT,TCF,H
   83 FORMAT('1',//' THERMAL CONDUCTIVITY IN THAWED SOIL IS',F10.5/
     *' THERMAL CONDUCTIVITY IN THE FROZEN SOIL IS,',F10.5,' CAL/SEC-CM-
     *DEG.C.'/' THE HEIGHT OF SOIL CONSIDERED IS,',F8.2,' CM')
      WRITE(6,91) TS,TI,W
   91 FORMAT(' ','THE CONSTANT SURFACE TEMP IS',F10.5/'THE INITIAL
     *GROUND TEMPERATURE IS',F10.5/'THE WATER CONTENT IS',F10.5)
      R=ALOG(100.-P)
      CALL PLOTUF(P,Q,R)
      II=0
      N=20
      DX=H/N
      GAMD=2.7/(1.+W*2.7)
      CCF=TCF
      IF(TCT.GT.TCF)    CCF=TCT
      DT=GAMD*DX*DX*(0.2+0.5*W)/(2.2*CCF)
      DT0=0.2*DT
      DTF=DT
      WRITE(6,42) DT,DX
   42 FORMAT('0','THE TIME STEP IS',F10.3,' SEC.    DX IS',F8.3,' CM.'//
     */)
      DO 3 I=1,N
    3 U(I)=TI
      TIME=0.
      TOL=0.02
    4 U(N+1)=U(N-1)
   63 BET=DT/(DX*DX)
      DO 5 I=1,N
      T=U(I)
      TP=U(I+1)
      IF(I.EQ.1)    GO TO 6
      TM=U(I-1)
      GO TO 7
    6 TM=TS
    7 A=2.*BET/(CO(T)*(1./TC(TP) + 1./TC(T)))
      IF(I.GT.1)    GO TO 44
      B=2.*BET*TC(TM)/CO(T)
      GO TO 45
   44 B=2.*BET/(CO(T)*(1./TC(T) + 1./TC(TM)))
   45 AB=A+B
      IF(AB.LT.1.)    GO TO 46
      WRITE(6,47) I
   47 FORMAT('0','  THE',I3,'TH NODE IS UNSTABLE, AND THE TIME STEP WILL
     1 BE HALVED...')
      DT=DT/2.0
      GO TO 4
   46 E=79.6*W*GAMD/CO(T)
      D=A*TP+(1.-A-B)*T+B*TM+E*WU(T)
C-----COMMENCE THE ITERATION TO FIND U(I,J+1)...
C-----LET THE INITIAL APPROXIMATION BE U(I,J)...
      KOUNT=0
      SOL=T
    8 STORE=SOL
      F=SOL-D+E*WU(SOL)
      IF(SOL.LT.0.)    GO TO 15
      IF(T.LT.0.)    GO TO 50
      FDASH=1.
      GO TO 16
   50 FDASH=1. + E*(WU(SOL)-WU(T))/(SOL-T)
      GO TO 16
   15 FDASH=1.+E*Q*EXP(Q*SOL+R)/100.
   16 SOL=SOL-F/FDASH
      DIFF=ABS(SOL-STORE)
      KOUNT=KOUNT+1
      IF(KOUNT.LT.20)    GO TO 9
      SOL=0.5*(SOL+STORE)
      GO TO 11
    9 IF(DIFF.GT.TOL)    GO TO 8
   11 UNEXT(I)=SOL
    5 CONTINUE
      TIME=TIME+DT
      HOURS=TIME/3600.
      SQHR=SQRT(HOURS)
      DO 12 I=1,N
   12 U(I)=UNEXT(I)
      IF(II.LT.100) GO TO 70
      II=II-100
      WRITE(6,13)TIME,HOURS,SQHR,(U(I),I=1,N)
   13 FORMAT(' ','TIME=',F12.1,'  HOURS=',F10.2,'  ROOT TIME=',F10.3/
     1(10F10.4))
      GO TO 18
   70 II=II+1
   18 IF(U(10).LT.0)    STOP
      GO TO 4
      END
      REAL FUNCTION TC(T)
C-----THIS FUNCTION EVALUATES THE CONDUCTIVITY AS A FUNCTION OF
C-----TEMPERATURE....
C-----*******************************************
      COMMON P,Q,R,TCT,TCF,W,GAMD
      IF(T.LT.0.)    GO TO 1
      WU=1.
      GO TO 2
    1 WU=(P+EXP(Q*T+R))/100.
    2 TC=TCF+WU*(TCT-TCF)
      RETURN
      END
      REAL FUNCTION CO(T)
C-----THIS FUNCTION EVALUATES THE APPARENT VOLUMETRIC SPECIFIC HEAT
C-----OF THE SOIL...
C-----***********************************************
      COMMON P,Q,R,TCT,TCF,W,GAMD
      IF(T.LT.0.)    GO TO 1
      WU=1.
      GO TO 2
    1 WU=(P+EXP(Q*T+R))/100.
    2 CO=GAMD*(0.2+0.5*W*(1.+WU))
      RETURN
      END
      REAL FUNCTION WU(T)
C-----THIS FUNCTION EVALUATES THE UNFROZEN MOISTURE CONTENT OF THE SOIL
C-----AT THE TEMPERATURE ''T'' ......
C-----*****************************************************
      COMMON P,Q,R,TCT,TCF,W,GAMD
      IF(T.LT.0.)    GO TO 1
      WU=1.
      GO TO 2
    1 WU=(P+EXP(Q*T+R))/100.
    2 RETURN
      END
      SUBROUTINE PLOTUF(P,Q,R)
C-----THE SUBROUTINE PLOTS THE UNFROZEN MOISTURE CONTENT AGAINST TEMPERATURE
      INTEGER LINE(100),AST,DOT,BL
      BL=1077952576
      AST=1547714624
      DOT=1262501952
      WRITE(6,1)
 1    FORMAT('0','PLOT OF THE UNFROZEN MOISTURE CONTENT AGAINST TEMP.'/
     1' TEMP.')
      DO 2 I=1,60
 2    LINE(I)=DOT
      WRITE(6,3) (LINE(I),I=1,60)
 3    FORMAT(' ',9X,'0',24X,'50',23X,'100',10X,'PERCENT M.C.'/60A1)
      TEMP=-0.25
 6    UFMC=P+EXP(Q*TEMP+R)
      LL=UFMC/2.+10.
      DO 4 I=1,60
 4    LINE(I)=BL
      LINE(10)=DOT
      LINE(LL)=AST
      WRITE(6,5)TEMP,(LINE(I),I=10,60),UFMC
 5    FORMAT(' ',F6.1,3X,51A1,10X,F10.2)
      TEMP=TEMP-0.25
      IF(TEMP.GE.-5.00)  GO TO 6
      RETURN
      END
END OF FILE
```

```
1

 THERMAL CONDUCTIVITY IN THAWED SOIL IS   0.00289
 THERMAL CONDUCTIVITY IN THE FROZEN SOIL IS,   0.00496 CAL/SEC-CM-DEG.C.
 THE HEIGHT OF SOIL CONSIDERED IS,    6.00 CM
 THE CONSTANT SURFACE TEMP IS  -5.00000
THE INITIAL      GROUND TEMPERATURE IS   3.44000
THE WATER CONTENT IS  35.53000
0PLOT OF THE UNFROZEN MOISTURE CONTENT AGAINST TEMP.
 TEMP.
          0                         50                        100         PERCENT M.C.
**************************************************************
   -0.3   .                                           *                       86.73
   -0.5   .                                      *                            76.39
   -0.8   .                                  *                                68.34
   -1.0   .                               *                                   62.07
   -1.3   .                            *                                      57.19
   -1.5   .                          *                                        53.39
   -1.8   .                         *                                         50.43
   -2.0   .                        *                                          48.12
   -2.3   .                       *                                           46.32
   -2.5   .                      *                                            44.93
   -2.8   .                     *                                             43.08
   -3.0   .                     *                                             42.99
   -3.3   .                     *                                             42.33
   -3.5   .                    *                                              41.81
   -3.8   .                    *                                              41.41
   -4.0   .                    *                                              41.10
   -4.3   .                    *                                              40.86
   -4.5   .                    *                                              40.67
   -4.8   .                    *                                              40.52
   -5.0   .                    *                                              40.40
0THE TIME STEP IS     4.127 SEC.    DX IS   0.300 CM.



 TIME=       416.9  HOURS=      0.12  ROOT TIME=     0.340
   -3.6559   -0.7951   -0.0078    0.7382    1.3690    1.8912    2.3123    2.6421    2.8920    3.0750
    3.2044    3.2926    3.3505    3.3872    3.4096    3.4228    3.4302    3.4342    3.4361    3.4366
 TIME=       833.7  HOURS=      0.23  ROOT TIME=     0.481
   -4.0925   -2.2630   -0.4119    0.1097    0.6135    1.0670    1.4717    1.8288    2.1395    2.4055
    2.6294    2.8143    2.9640    3.0828    3.1746    3.2436    3.2933    3.3266    3.3457    3.3519
 TIME=      1250.5  HOURS=      0.35  ROOT TIME=     0.589
   -4.2391   -2.7115   -1.2006   -0.1249    0.2671    0.6469    1.0032    1.3339    1.6371    1.9113
    2.1557    2.3699    2.5545    2.7104    2.8388    2.9413    3.0191    3.0738    3.1061    3.1168
 TIME=      1667.4  HOURS=      0.46  ROOT TIME=     0.681
   -4.3466   -3.0360   -1.7300   -0.5079   -0.0092    0.3314    0.6621    0.9763    1.2692    1.5381
    1.7812    1.9980    2.1884    2.3524    2.4904    2.6027    2.6896    2.7515    2.7885    2.8009
 TIME=      2084.2  HOURS=      0.58  ROOT TIME=     0.761
   -4.4140   -3.2391   -2.0676   -0.9392   -0.1356    0.1668    0.4619    0.7411    1.0033    1.2473
    1.4717    1.6754    1.8573    2.0164    2.1521    2.2637    2.3508    2.4132    2.4507    2.4632
 TIME=      2501.1  HOURS=      0.69  ROOT TIME=     0.834
   -4.4657   -3.3949   -2.3265   -1.2826   -0.3852   -0.0090    0.2537    0.5096    0.7541    0.9836
    1.1955    1.3880    1.5599    1.7103    1.8385    1.9441    2.0267    2.0859    2.1215    2.1334
 TIME=      2917.9  HOURS=      0.81  ROOT TIME=     0.900
   -4.5059   -3.5158   -2.5273   -1.5539   -0.6599   -0.0902    0.1409    0.3659    0.5797    0.7809
    0.9681    1.1397    1.2945    1.4312    1.5487    1.6461    1.7227    1.7777    1.8109    1.8220
 TIME=      3334.8  HOURS=      0.93  ROOT TIME=     0.962
   -4.5381   -3.6128   -2.6886   -1.7747   -0.9105   -0.2469   -0.0016    0.2021    0.3995    0.5862
    0.7593    0.9171    1.0587    1.1831    1.2898    1.3780    1.4472    1.4970    1.5271    1.5371



 TIME=      3751.6  HOURS=      1.04  ROOT TIME=     1.021
   -4.5651   -3.6939   -2.8237   -1.9613   -1.1330   -0.4317   -0.0459    0.1236    0.2882    0.4447
    0.5918    0.7278    0.8514    0.9612    1.0561    1.1351    1.1973    1.2422    1.2694    1.2784
 TIME=      4168.4  HOURS=      1.16  ROOT TIME=     1.076
   -4.5881   -3.7631   -2.9387   -2.1202   -1.3257   -0.6153   -0.1409    0.0164    0.1688    0.3114
    0.4438    0.5651    0.6745    0.7712    0.8545    0.9237    0.9782    1.0174    1.0411    1.0491
 TIME=      4585.1  HOURS=      1.27  ROOT TIME=     1.129
   -4.6078   -3.8224   -3.0376   -2.2573   -1.4951   -0.7933   -0.2658   -0.0197    0.0992    0.2142
    0.3236    0.4257    0.5193    0.6029    0.6756    0.7363    0.7843    0.8190    0.8399    0.8469
 TIME=      5001.7  HOURS=      1.39  ROOT TIME=     1.179
   -4.6252   -3.8747   -3.1245   -2.3782   -1.6460   -0.9585   -0.3966   -0.0756    0.0302    0.1318
    0.2269    0.3147    0.3945    0.4656    0.5271    0.5784    0.6190    0.6483    0.6660    0.6719
 TIME=      5418.3  HOURS=      1.51  ROOT TIME=     1.227
   -4.6406   -3.9210   -3.2016   -2.4855   -1.7804   -1.1094   -0.5321   -0.1571   -0.0082    0.0706
    0.1468    0.2189    0.2855    0.3456    0.3981    0.4421    0.4770    0.5022    0.5175    0.5227
 TIME=      5834.9  HOURS=      1.62  ROOT TIME=     1.273
   -4.6544   -3.9623   -3.2705   -2.5814   -1.9013   -1.2480   -0.6666   -0.2468   -0.0406    0.0263
    0.0901    0.1496    0.2041    0.2530    0.2955    0.3313    0.3596    0.3801    0.3926    0.3968
END OF FILE
```